

CHARACTERIZATION OF N-ISOPROPYL
ACRYLAMIDE BASED POLYMERS FOR PH
SENSING AND
METAL ION BINDING

By

LEAH R. OXENFORD

Bachelor of Science in Chemistry

University of Northern Colorado

Greeley, Colorado

2004

Submitted to the Faculty of the
Graduate College of the
Oklahoma State University
in partial fulfillment of
the requirements for
the Degree of
MASTER OF SCIENCE
December, 2006

CHARACTERIZATION OF N-ISOPROPYL ACRYLAMIDE-CO-
METHACRYLIC ACID POLYMERS FOR PH AND
METAL SENSING

Thesis Approved:

Barry Lavine

Thesis Adviser

Stacy Benson

Nicholas Materer

Ziad El-Rassi

A. Gordon Emslie

Dean of the Graduate College

ACKNOWLEDGEMENTS

I would like to thank Dr. Barry Lavine for his role as my research advisor and for his support of my research; wherein his influence has played a pivotal role in defining my goals and perspective. Through his leadership, I learned that not only is a solid foundation in chemistry required, but quality communication skills are also essential to being a successful chemist. I would like to thank my graduate advisory committee for their patience and constructive criticism that has led to the successful completion of these works. I extend my gratitude to Dr. Necati Kaval for his tireless efforts in shaping my skills in analytical methodologies and my understanding of polymer swelling phenomenon. A special thanks goes out to my dear friends and colleagues in the graduate program at Oklahoma State University. I would like to extend my gratitude to Nikhil Mirjankar, Esla Subashi, and Kim Pham for their friendship and encouragement. Furthermore, I will always be grateful to Dane Scott, the eternal optimist; he was always there when I needed a friend, a confidant, and a new perspective.

TABLE OF CONTENTS

Chapter	Page
I. BACKGROUND AND THEORY.....	1
1.0 Introduction.....	1
1.1 Polymers of N-isopropylacrylamide.....	4
1.2 Polymer Swelling.....	9
1.3 pH Sensing Applications.....	12
II. EXPERIMENTAL.....	15
2.0 Introduction.....	15
2.1 Optical Transduction Mechanism Based on Polymer Swelling....	16
2.2 Polyvinyl Alcohol Immobilization - Membrane Description.....	19
2.3 Instrumentation.....	30
2.4 Defining Experimental Controls for Membrane Composition.....	36
2.5 Contribution of NIPA to Total Swelling Due to pH.....	39
2.6 Buffer Systems for pH Profiling.....	40
2.7 Synthesis of N-isopropyl Acrylamide Co-Polymers.....	44
2.8 Effect of Ionizable Co-Monomers on NIPA.....	50
III. OPTICAL PH SENSING USING NIPA BASED POLYMERS.....	54
3.0 Introduction.....	54
3.1 pH Response Profiles.....	55
3.2 Kinetics of pH Response Kinetics.....	57
3.3 Reversibility.....	58
3.4 Ionic Strength Effects on Polymer Swelling.....	59
3.5 pH Profiles at Elevated Temperatures	63
3.6 Effects of Crosslinking on Polymer Swelling.....	65
3.7 Methacrylic Acid Composition.....	71
3.8 Increasing Alkyl Chain Length of Functional Comonomer.....	72
3.9 Basic Functional Comonomers.....	77
3.10 Conclusions	80

IV. ADSORPTION OF METAL IONS BY NIPA HYDROGELS.....	82
4.0 Introduction.....	82
4.1 Materials.....	83
4.2 Ion Profiling – Group 1 Metals.....	86
4.3 Ion Profiling – Transition Metals.....	93
4.4 Role of Carboxyl Groups in Transition Metal Ion Binding.....	96
V. CONCLUSIONS.....	103
REFERENCES.....	107
APPENDIX I.....	113
APPENDIX II.....	116
APPENDIX III.....	120

LIST OF FIGURES

CHAPTER II

Figure	Page
2.1 Schematic of an optically sensitive membrane for measuring the concentration of an analyte which triggers the volume phase transition of the NIPA polymer. Swelling of the polymer particles increases the size of the particles and reduces their refractive index.....	17
2.2 The effect of the hydrogel membrane with suspended polymer particles on the intensity of a transmitted light beam.....	18
2.3 Characterization of the distribution of polystyrene microspheres in a PVA membrane using turbidity. Inserted diagram indicates the membrane section that was sampled to assess particle uniformity.....	25
2.4 Overlay of PVA response plots for both ascending and descending pH profiles with low ionic strength citrate buffer test solutions.....	27
2.5 Ascending and descending temperature response profiles for 0.25% polystyrene microspheres in polyvinyl alcohol immobilization membrane...	28
2.6 Thermal transition profile for NK 1-60 in DI water.....	29
2.7 Signal contribution of polyvinyl alcohol immobilization membrane with increasing solution ionic strength (NaCl concentration).....	30
2.8 Custom-made black plastic membrane test segment holder.....	33
2.9 Ray-Trace Diagram of the Cary 6000i (provided by Varian Inc.).....	35
2.10 (left) Comparison of pH profiles for hydrogel membranes with increasing amounts of immobilized pH sensitive polymer particles. (right) Membrane absorbance values at pH = 4.0 with increasing percent composition of particles by mass (w/w).....	38
2.11 Linear correlation between polymer particle weight percent and the total absorbance change.....	39
2.12 The DI water baseline values increase linearly with increasing particle	

	percent composition.....	39
2.13	The pH profile of N-isopropylacrylamide polymer without methacrylic acid functionalization. Some air bubble interference was observed at pH = 3.0 and 3.4.....	40
2.14	High and Low Ionic Strength pH Profile Comparison of a NIPA co-MAA (10%) polymer.....	41
2.15	High ionic strength pH profile for NK 1-28 with citrate buffer data (pH = 3.0-4.0) substituted for the original chloroacetic acid buffer data.....	42
2.16	The Cary 6000i scan software screen capture of the comparison between the mixed and citrate buffer system total induced swelling of NK 1-60.....	43
2.17	NK 1-60 pH profile ionic strength comparison.....	44
2.18	The NK-60 microspheres were dielectrophoretically chained across the 60 μm interelectrode gap.....	51
2.19	Behavior of NK-60 NIPA particles in the presence of the electrodes during application of the sinusoidal waveform voltage a) high pH solution and b) low pH solution.....	52

CHAPTER III

Figure		Page
3.0	pH profile of NK 1-60 (Composition: 70% NIPA, 10%MAA, %NTBA, 10% MBA).....	56
3.1	(left) NK 1-60 (10%MAA) reversible pH response. (right) NK 1-119 (20% MAA) poor reversibility over the pH transition range.....	59
3.2	pH profiles for NK 1-28 at ionic strength conditions of 0.05, 0.10, 0.50, and 1.0 IS units.....	60
3.3	NK 1-60 ascending and descending pH profiles were collected at 35.0°C....	64
3.4	pH response profile comparison for NK 1-60 at 35°C and 23°C (room temperature.).....	65
3.5	SEM images for the characterization of particle morphology with increasing percent crosslinking: NK1-28 5%XL, NK 1-18 10%XL, NK1-143 15%XL.....	66

3.6	Change in pH response profile morphology with respect to increased crosslinking.....	67
3.7	SEM Photos of polymers of increasing MAA percent composition. (a)NK 1-127 25% MAA, (b) NK 1-119 20% MAA, (c) NK 1-124 15% MAA, (d) NK 1-60 10% MAA, (e) NK 1-64 5% MAA.....	69
3.8	pH response profile comparison of polymers prepared with increased amounts of functional monomer (MAA).....	69
3.9	(clockwise from the upper left sub-figure): 5% MAA content, 10% MAA content, 15% MAA content, 25% MAA content.....	70-71
3.10	Total Absorbance Change Comparison Based on Percent Methacrylic Acid (MAA) Composition.....	72
3.11	(a) NK 1-156 Acrylic Acid, (b) NK 1-60 Methacrylic Acid, (c) NK 1-146 Ethacrylic Acid, (d) NK 1-155 Propacrylic Acid.....	74
3.12	Comparison of the apparent pKa values of NIPA co-polymers with functional monomers of increasing side chain length.....	75
3.13	Ascending and descending pH response profiles and HH fit plots for functional monomer acids: (1 st row) Acrylic, (2 nd row) Methacrylic, (3 rd row) Ethylacrylic, (4 th row) Propylacrylic.....	76-77
3.14	SEM photos of the NK 2-03 (VBC functionalization) and NK 2-13 (post-synthetic modification of NK 2-03 to a dimethyl amine functionality (DMA)).....	78
3.15	NK 2-13 pH response profile with low ionic strength phosphate buffer. Note the hysteresis between the pH response profiles.....	79
3.16	Comparison of pre and post functionalization of NK 2-13 to dimethyl amine.....	80

CHAPTER IV

Figure	Page	
4.1	(left) NK 1-135 reversible pH response profile and (right) Henderson-Hasselbalch data modeling for NK 1-135 pH response profiles.....	83

4.2	Chemical structures of the two crown ethers used to functionalize the polyNIPA-MAA particles. (right) Dibenzo 18crown6. (left) Dibenzo 15crown5.....	84
4.3	(Left) Group 1 metals profiles for a NIPA co-polymer (NK 1-161) without any functional monomer present in the formulation. (Right): Comparison of metals response profiles for NK 1-135.....	87
4.4	Comparison of Group 1 Metal Profiles for NK 1-135 conjugated with Dibenzo18crown6.....	89
4.5	Comparison of transition metal response profiles for lead, cadmium, and copper for NK 1-135 NIPA-co-MAA (10%).....	90
4.6	Metal ion response profiles for Ca ²⁺ , K ⁺ , and Pb ²⁺ for NK 1-135.....	92
4.7	Metal ion response profiles obtained by SPR for alkali and alkaline earth metals.....	93
4.8	Comparison of Pb ²⁺ response profiles for NK 1-135 (10% MAA) and NK 1-161 (No MAA) over a concentration range of 10 ⁻⁰⁷ – 10 ⁻⁰¹ M Pb ²⁺	94
4.9	Pb ²⁺ response for NK 1-156 (10% acrylic acid) and NK 1-135 (10% MAA)..	95
4.10	pH Response profile for NK 1-135 (70% NIPA, 10% MAA, 10% NTBA, 10% MBA).....	97
4.11	Fe ²⁺ response profile comparison in DI water for NIPA-co-MAA (10%) and NK 1-161 (No MAA).....	98
4.12	Comparison of Fe ²⁺ responses for NK 1-135 (10% MAA) at pH = 3.75, 5.00, 6.00.....	99
4.13	Comparison of Fe ²⁺ Response profiles for NK 1-161 (No MAA) and NK 1-135 (10% MAA) in pH = 3.75 acetate buffer.....	100
4.14	(a) Metal ion chelation by adjacent carboxylic acid groups. (b) Metal ion chelation by adjacent amide groups. (see Rivas et al 2003).....	101

LIST OF TABLES

CHAPTER II

Table	Page
2.0 Characteristics of an Ideal Immobilization Polymer.....	20
2.1 Cary 6000i specifications selected from the Varian UV-VIS-NIR Cary 4000, 5000, and 6000i Preliminary Performance Data pdf file.....	34
2.2 Buffer Series Composition and Associated pH Range.....	41
2.3 Structure and Function of Polymer Formulation Components.....	46

CHAPTER III

3.0 Polymer Composition-Varied % Crosslinking.....	65
3.1 Polymer Composition – Increasing %MAA Content.....	68
3.2 Polymer Composition – Increased Fun. Monomer Hydrophobicity.....	74
3.3 pKa Values in Free Solution and for Polymerized Acrylic Acids.....	75

CHAPTER IV

4.0 Preparation of Metal Stock Solutions in DI Water.....	84
---	----

LIST OF ABBREVIATIONS

NIPA.....	n-isopropyl acrylamide
MAA.....	methacrylic acid
AA.....	acrylic acid
EAA.....	ethacrylic acid
PAA.....	propylacrylic acid
PVA.....	poly vinyl alcohol
UV-vis.....	Ultraviolet-visible region

Chapter 1

Background and Theory

1.0 Introduction

Microgels developed from N-isopropylacrylamide (NIPA) have attracted considerable attention (1-5) because of their ability to undergo a reversible volume phase transition at near physiological temperature (6-7). These gels, which are often prepared as monodispersed colloidal particles, undergo dramatic changes in size and water content over a narrow temperature range. The characterization of their unique properties is crucial to the advancement of our understanding of polymer swelling and to the discovery of new applications for these materials.

Our current understanding of polymer swelling and how its composition directly correlates to swelling behavior is inadequate. Additional work is needed to elucidate the relationships between monomer content and type and how they directly relate to the lower critical solution temperature of the polymer. The volume phase transition of N-isopropylacrylamide (NIPA) is of particular interest not only for the study of polymer swelling, but also for its application in chemical sensing as a transduction mechanism. Most studies on the volume phase transition behavior of NIPA (8-10) have focused on temperature as the experimental variable to investigate since this transition is triggered as the polymer approaches its lower critical solution temperature. However, the incorporation of a pH sensitive functional comonomer into polyNIPA imparts unique

properties to the polymer that allow the volume phase transition of the polymer to also be triggered by pH (11-12).

PolyNIPA, which has been extensively characterized in studies involving temperature-induced volume phase transitions, is relatively insensitive to changes in pH over the range of 3.0 – 7.0. However, more complex formulations of NIPA, which include the use of pH sensitive functional comonomers, provide new opportunities to better understand the structural variables that influence polymer swelling. The investigation of the polymer phase transition by temperature alone limits what information can be gained about the polymer. However, copolymerization of NIPA with pH sensitive functional comonomers such as methacrylic acid (MAA) would allow pH to be used as a variable to characterize the swelling of NIPA particles since the volume phase transition would also be initiated by pH. Changes in how the composition of the polymer affects the volume phase transition could be investigated as well by varying the amount of functional comonomer in the polymer formulation.

Another advantage of copolymerizing NIPA with a pH sensitive functional comonomer is the development of polymers suitable for sensor applications. The pH response observed for NIPA-co-MAA polymers is similar to that of colorimetric indicators, wherein changes in the polymer induced by H^+ or OH^- in solution occur over a narrow, well defined pH range. As with colorimetric indicators, the changes in the optical properties of the polymer can be monitored by conventional UV-Visible absorbance spectroscopy. Although the pH range spanned by the volume phase transition is limited, the response of the polymer is sensitive albeit over a narrow range defined by the composition of the formulation used to synthesize the polymer. Characterization of

several NIPA copolymers of acrylic acid, methacrylic acid, ethacrylic acid, and propacrylic acid reveal polymer pKa values in the pH range of 4.0 to 6.0. Because there is interest in measuring small pH changes in the physiological range 5 to 7.4, efforts were made to shift the pKa of the NIPA copolymer particles to 7 without compromising the reversibility and magnitude of the pH response.

Metal ion binding by NIPA copolymer particles was also investigated. Information related to the organization of the monomer within the polymer obtained in pH profiling experiments suggested that copolymers of NIPA could have ion exchange properties. Binding of transition, alkali and alkaline earth metals was studied to determine whether polymer swelling could serve as a transduction mechanism to measure the binding of metal ions by the polymer particles. The incorporation of crown ethers in NIPA copolymer particles was examined as an approach to impart selectivity to the polymer particles for ion exchange reactions involving specific metal ions.

There are many advantages in using polymers for sensing applications. As polymers are composed of repetitive monomers, the substitution of these monomer units and changes in their relative percent compositions can provide a nearly limitless reservoir of materials with customized properties. The ability to tailor the properties of materials that are readily prepared through free-radical photopolymerization is paramount to meeting the specific requirements of sensing materials. Using the volume phase transition of the polymer as an optical transduction mechanism ensures reversibility of the sensor response, as the phase transition is reversible and continuous for colloidal microgels (13-14). Also, the polymers can be coupled with existing technologies such as fiber optics for remote sensor applications.

1.1 Polymers of N-isopropylacrylamide

Polymers of NIPA have generated interest due to their unique swelling properties. In particular, polymers of NIPA undergo a volume phase transition that results in a 1000-fold total volume change as the polymer undergoes a transition from a collapsed state to a swollen state (15). The volume phase transition corresponds to a change in the organization of the polymer chains as they collapse from a coiled structure to a globular one (16). This reversible transition can occur with changes in temperature, pH, ionic strength, and solvent composition due to interactions within the polymer as well as between the polymer and the solvent. The synthesis of acrylamide polymers such as polyNIPA was first reported in 1968. Interest in the synthesis and characterization of these materials is still relevant today (17).

The volume phase transition of polyNIPA in aqueous media is of particular interest. PolyNIPA is a thermally responsive polymer that undergoes a volume phase transition at 35⁰C. The volume phase transition is governed by hydrophobic interactions between the polymer and the solvent system. At temperatures below the lower critical solution temperature, the polymer exists in a swollen state. The polymer is permeated by aqueous solvent resulting in increased hydrophilic character. As the temperature is increased, polyNIPA undergoes a transition to a shrunken state through increased hydrophobic interactions resulting in the expulsion of water from the polymer network. The inflection point of the transition profile is defined as the lower critical solution temperature (LCST), and is dependent on the microstructure of the macromolecule (18).

The LCST of NIPA can be shifted to lower temperatures by inclusion of increasingly hydrophobic co-monomers such as *N-t-butyl* acrylamide (19). The inclusion

of comonomers with ionizable functional groups, such as methacrylic acid, also has an effect on the LCST of the bulk polymer material. The temperature-dependent volume phase transition of NIPA has been thoroughly characterized with respect to polymerization conditions used as well as the pH and ionic strength of the solvent in contact with the polymer. However, the properties of co-polymers formed, when NIPA is polymerized in the presence of compatible acrylamide monomers remains an active area of research (20, 21).

Dispersion polymerization performed with more than one monomer unit in the reaction mixture is referred to as copolymerization (22). The incorporation of a secondary monomer into a polymer is referred to as functionalization or the use of a functional monomer. By definition, the purpose of the functional monomer is to impart new properties to the bulk material such as enhanced swelling or analyte specificity through the incorporation of ionizable functional groups into the polymer. Copolymerization allows synthetic chemists more versatility in creating materials with a wide variety of properties using a limited number of monomer species.

Acrylates are both a logical and popular choice for copolymerization with NIPA due to their compatibility. The incorporation of the carboxylic acid functional group into the polymer imparts additional properties to NIPA polymers, such as a volume phase transition based on changes in solution pH. Success in the functionalization of NIPA with basic functional monomers such as amines has also been reported (23, 24), and the pH phase transition is opposite to that observed for NIPA-co-MAA. The NIPA-co-amine functionalized polymers undergo a phase transition to the swollen state, as the amine groups are protonated at lower pH values. Deprotonation of the amines with increasing

pH results in a decrease in the total volume of the polymer particles. As these materials are functionalized with a basic functional monomer, their apparent pKa values are centered near pH = 8.5. Regardless of the type of functionalization, the distribution of the monomers within the co-polymer structure is crucial for understanding its response characteristics.

The distribution of the functional comonomer within the polymer is of particular interest to scientists, as the organization of the comonomer and crosslinker in the polymer impacts its material properties. For copolymerization, there are often more than two monomers present in the reaction mixture. The polymer formulation will often contain aliquots of the following for a typical particle synthesis: base monomer (typically NIPA), functional monomer (e.g., methacrylic acid), transition temperature modifying monomer (e.g., N, t-butylacrylamide), reaction initiator (dimethoxyphenylacetophenone), and crosslinking agent (e.g., N'N'-methylene-bis-acrylamide). The presence of more than one monomer in the formulation increases the complexity of predicting the monomer distribution in the polymer.

A polymerization study conducted by Fernandez-Barbero (25) reported that crosslinker was consumed more quickly than NIPA, indicating that polymer particles of NIPA probably do not have uniform composition. Small-angle neutron scattering experiments revealed that polymer particles of NIPA are in fact, heterogeneous in character with two distinct zones corresponding to a core region of high monomer density and a less dense shell region. The idea of core-shell particle morphology for NIPA-copolymers (26-29) as well as the results from a study by Tanaka and Li (30) suggest that hydrophobic crosslinking monomers tend to aggregate upon free radical polymerization,

as in the case of polyacrylamide derivative gels crosslinked with N'N'-methylene-bis-acrylamide (MBA). These inhomogeneities have been cited as responsible for the increased porosity of the polymer shell layer and for the polymer surface being compatible with an aqueous environment.

The idea that polyNIPA particles have heterogeneous crosslinker distributions based on solvent affinity raises questions about the distribution of other monomers present in the polymer. If each monomer partitions based solely on its hydrophilicity, then a functional comonomer containing a carboxylic acid group in the polymerization mixture would be found in the shell layer of the particle. The relative reactivity ratio may also play a role in the acrylate monomer being selectively isolated at or near the surface of the polymer particle.

When one monomer is present in greater amounts than another, longer chains containing the abundant monomer are observed with intermittent inclusion of the minor unit (22). This will be true if the relative reactivity ratio is the same for all of the monomers. For the NIPA copolymers discussed in the research described in this thesis, NIPA is the dominant monomer with only a small amount (approximately 10%) of functional comonomer such as methacrylic acid (MAA) present. Not only will MAA be selectively isolated in the shell region of the particle based on hydrophilicity, it could also be well separated from other MAA units within the shell if the relative reactivity ratios of all the monomers are approximately the same. Excess NIPA monomer will be polymerized into chains containing well-separated functional monomer units. However, the three-dimensional nature of the polymer matrix does allow for some of the MAA groups to be more closely oriented than observed for linear polymer chains. Therefore,

understanding the relationship between the attractive and repulsive forces that define the structure of the polymer is crucial to understanding how changes in polymer composition translate into changes in the properties of the polymer.

There are several intermolecular forces involved in defining the structural state of the polymer. Van der Waals forces, hydrogen bonding, hydrophobicity, and electrostatic repulsion each play a role in defining the structure of the polymer. Hydrophobicity, van der Waals forces, and hydrogen bonding act as restrictive forces that work to maintain the polymer in a collapsed state. Hydrophobic interactions reinforce the shrunken state of NIPA by decreasing the solubility of NIPA in water and its compatibility with the solvent. Similarly, van der Waals forces provide weak attractions between the instantaneous electron dipoles of the parallel polymer chains. Since these dispersion forces increase with molecular mass, they play a significant role in polymer stabilization. Hydrogen bonding also serves to stabilize the polymer configuration in an aqueous solvent.

Expansive forces are also at work within the polymer. The deprotonation of ionizable groups polymerized into NIPA, such as methacrylic acid, act as expansive forces that work to swell the polymer network. Osmotic pressure inequalities also contribute to swelling of NIPA, as water rushes into the polymer to reduce the osmotic pressure difference. Through this delicate balance of intra-polymer interactions, the state of the polymer is defined. As the phase transition is a competitive balance between the forces working to expand and retract the polymer matrix, understanding the role of each interaction is key to understanding polymer swelling.

1.2 Polymer Swelling

When a crosslinked polymer is placed in a suitable solvent, swelling occurs. For nonionic polymers, the degree of swelling that occurs is a result of two forces: solvation and retraction. Solvation causes the solvent to penetrate into the polymer and dilute the bulk polymer. As the chains in the crosslinked polymer network elongate, an elastic retractive force in opposition to the deformation is generated. Eventually, the polymer reaches equilibrium - the retractive forces due to crosslinking counterbalance the elongation of the polymer network due to solvation. The extent to which a polymer swells is determined by its affinity for the solvent. For ionic polymers, electrostatic repulsion between neighboring charged groups is another factor that contributes to swelling. The strength of this force is a function of the ionic strength and dielectric constant of the solution in contact with the polymer.

Polymer swelling is either ionic or nonionic. NIPA polymers are composed of polymerized N-isopropylacrylamide groups that are non-ionizable, and therefore, NIPA undergoes purely non-ionic swelling. The amount of swelling observed for nonionic polymers is dependent on the balance between the solvation and retractive forces of the polymer (31). Solvation is an entropically driven process based on solvent penetration into the polymer as a function of temperature. To counter the expansion of the polymer network with increased solvent content, retractive forces work against the deformation of the polymer structure (32). Equilibrium is reached because of a counterbalance of these two forces.

The incorporation of ionizable MAA groups into the polymer may add an ionic component to the total polymer swelling observed. For ionic swelling, polymer charge

density with respect to the surrounding solvent contributes to the total swelling change (33). The deprotonation of ionizable groups such as carboxylic acids results in electrostatic repulsion between neighboring charged groups. This force works to swell the polymer, yet is highly sensitive to the ionic strength of the surrounding solution. Increased ionic strength of the surrounding solution leads to the repression of ionic swelling, and thus, swelling observed at high ionic strength is due to non-ionic swelling processes.

Polymer swelling was first described by Flory and Rehner (34). They suggested that a change in the Helmholtz free energy of a polymer due to swelling could be expressed as the sum of two terms: a polymer-solvent mixing free energy term and an elastic free energy term. Later, Flory and Huggins developed an expression for polymer swelling; see equation 1-1 (31). The larger the value of q_m , the more swelling that will occur. V_o/v_e is the volume of the unit segment in the unswollen polymer and when this term is multiplied by i/V_u the effective charge density of the polymer is obtained.

$$q_m^{5/3} \cong \frac{\left(\frac{i}{2V_u\sqrt{S}}\right)^2 + \left(\frac{1-X_1}{2}\right)}{\frac{v_e}{V_o}} \quad (1-1)$$

where

q_m = equilibrium swelling ratio (final polymer volume over initial volume)

i = amount of charge on the polymer

V_u = molecular volume of polymer repeating unit

S = molar ionic strength of solution in contact with polymer

X_1 = polymer-solvent interaction parameter

V_1 = molar volume of the polymer

ν_e = effective number of chains in the network

V_0 = volume of unswollen polymer

The ionic strength of the surrounding solution plays an important role in the swelling of charged polymers. The degree of swelling decreases with increasing ionic strength due to the reciprocal relationship between S and q_m . The non-ionic swelling term in the Flory Huggins equation, $(1/2 - X_1)/\nu_1$, describes the interaction between the unit segments of the polymer and the solvent. When the non-ionic swelling term is divided by ν_e/V_0 , an expression for polymer swelling due to the interaction of the polymer with the solvent is given. Nonionic swelling for highly charged polymers in polar solvents is negligible, but is crucial in governing the thermodynamics of swelling for uncharged polymer such as polyacrylamides (25).

Several conclusions can be drawn from the relationships detailed in the Flory-Huggins equation. Increasing the amount of crosslinker within the polymer results in an increase in the effective number of chains (ν_e), and a subsequent decrease in total swelling (q_m). Ionic swelling can be viewed as an osmotic pressure effect that results

from a charge density difference between the bulk polymer and the surrounding solvent, wherein the solvent diffuses into the polymer to equalize the charge imbalance. The significance of the solvent interaction parameter (X_1) for charged polymers is that it can reduce the total swelling. When X_1 is greater than 0.5, the non-ionic swelling term is negative due to the hydrophobic repulsion between the polar solvent and the polymer backbone (32).

For nonionic polymers, X_1 governs the thermodynamics of swelling. Polyacrylamides such as N-isopropyl acrylamide (NIPA) exist in either the swollen or collapsed state. In the swollen state, the refractive index of these gels is closer to water due to their high water content. In the collapsed state, the refractive index is significantly higher than water due to the water being expelled from the polymer. Even in the collapsed state, 20% of polyNIPA is water (34, 35). The size of the particles is controlled by X_1 and the change in X_1 with temperature or pH for functionalized polyacrylamides is the driving force for the volume phase transition that occurs in these polymers (36).

1.3 pH Sensing Applications

Interest in developing polymer materials for pH sensing is motivated by the importance of pH in modern analytical chemistry. pH can be defined as the negative logarithmic of the concentration of hydrogen ions in solution. This relationship is given by equation 1-2.

$$\text{pH} = -\text{Log}([\text{H}^+]) \quad (1-2)$$

pH is used to assess the degree of acidity or basicity of an aqueous solution at a given temperature. The concept of activity was introduced to further refine the concept of pH.

Activity becomes important as the ionic strength of the solution is increased, and non-ideal conditions persist (i.e. solution is no longer infinitely dilute).

The theory of pH and equilibrium are interrelated with the Henderson Hasselbalch equation, which bridges the gap between pH and equilibrium, see equation 1-3.

$$\text{pH} = \text{pK}_a + \text{Log} ([\text{A}^-] / [\text{HA}]) \quad (1-3)$$

The pH of the solution is equal to the pKa of the acid when equal concentrations (activities) of acid and conjugate base are present in solution. The inflection point of the pH titration curve for the pH sensitive polymers investigated in the research described in this thesis is called the apparent pKa.

pH is one of the most common laboratory measurements made due to the fact that many chemical and biological reactions depend heavily on the control of pH. Because of this, many different methods exist for the measurement of pH, ranging from colorimetric indicators to glass and metal electrodes. The glass electrode is the most widely used method for measuring pH due to its Nernstian response, independence from redox interferences, short electrical potential balancing time, high reproducibility, and long lifetime (37). Due to the well-established nature of the glass electrode, it was used to prepare pH buffer solutions in the pH profiling experiments described in this thesis. Accurate and precise measurements of pH for the buffer solutions were critical for the investigation of the pH response properties of pH sensitive copolymers of NIPA.

Acrylamide polymers have been investigated as materials suitable for chemical sensing (38). The ease of polymerization and the wide range of functionalization possibilities make acrylamides such as NIPA an ideal starting material for the construction of different chemical sensing platforms. Recently, efforts have been made

to utilize the volume phase transition of NIPA as a transduction mechanism in chemical sensing for optical (swelling and refractive index changes), electrochemical (charge transfer), and gravimetric (gel mass) methods (39-41). Applications of these materials to real world problems include sensors, drug delivery systems, remediation sorbants, and immobilization scaffolding for biomolecules (42). Incorporation of even a small amount of a functional comonomer such as methacrylic acid allows NIPA based polymers to respond to a variety of environmental stimuli. The response of NIPA-co-MAA (10%) polymer particles to changes in pH as well as metal ion content was investigated in the research described in this thesis. It is the goal of these studies to gain an understanding of how changes in the composition of the formulation affect the observed properties of the polymer including its response to pH and its affinity to bind alkali and transition metal ions.

Chapter 2

Experimental

2.0 Introduction

Polymers of NIPA swell in response to changes in environmental stimuli, such as temperature and pH. Work has been reported in the literature on exploiting the volume phase transition that occurs in copolymers of NIPA as a transduction mechanism for chemical sensing. However, developing a method to reproducibly measure the swelling of crosslinked NIPA particles in aqueous media can be an onerous task due to the difficulty in preparing stable particle dispersions of NIPA. The investigation of polymer swelling through secondary polymer immobilization is a viable method to study swelling of polymer particles in aqueous media. In this chapter, the method used for polymer immobilization in the experiments described in this thesis is discussed at length.

Both the investigatory method used and the controls for interpreting the data require a degree of standardization to ensure that valid conclusions can be drawn from the swelling data. The use of an immobilization membrane for characterization of polymer swelling introduces several new facets into the measurement process that can confound the interpretation of the data. Therefore, a series of control experiments have been conducted to either address or eliminate interferences due to the design and materials used to prepare the immobilization membrane.

2.1 Optical Transduction Mechanism Based on Polymer Swelling

Copolymers of NIPA display significant changes in their optical properties when exposed to appropriate environmental stimuli. The ability of the polymer to swell and shrink, thereby changing its refractive index, is of value for the development of chemical sensors based on polymer swelling. The idea of placing a swellable polymer (suitably sensitized to a specific analyte) on a glass slide to serve as a sensing platform was initially investigated by Seitz and coworkers (43), but delamination of the polymer film from the glass substrate was a serious problem with this approach. T. Mononaga and M. Shibayama (44), Wei Xue and W. Hamley (45), and Elliot et al. (46) showed promising preliminary results that swelling of NIPA co-polymers could be used for chemical sensing. However, the approach of weighing polymer segments to quantify water uptake with swelling, or to measure the dimensions of a polymer segment following a swelling event, are not viable for remote sensing or even routine sensing applications.

It was also first proposed by Seitz (43, 47) that polymers could be synthesized by dispersion polymerization to form microspheres that could be immobilized in a hydrogel to yield a membrane whose swelling behavior could be monitored by turbidimetry. Using a similar approach, we have investigated and characterized the unique properties of swellable NIPA polymers that have been sensitized to pH through copolymerization of NIPA with a pH sensitive comonomer. The entrapment of these environmentally sensitive polymers within an optically transparent membrane is shown in Figure 2.1.

The transduction mechanism for chemical sensing is based on swelling of the polymer particles in response to changes in the concentration of the analyte in the sample, which is an aqueous solution in contact with the membrane. If the analyte is not present

in the sample, the polymer particles shown in Figure 2.1 are in a shrunken state. The refractive index of the particles (n_1) differs significantly from that of the hydrogel (n_2), which is why the membrane is turbid. When the appropriate analyte is present in the sample solution, a decrease occurs in the refractive index of the particles. This can be attributed to an increase in the water content of the particles due to swelling. The particles go from a shrunken state (n_1) to a swollen state (n_3), which approaches the refractive index of the hydrogel (n_2) with increasing concentration of analyte in the sample.

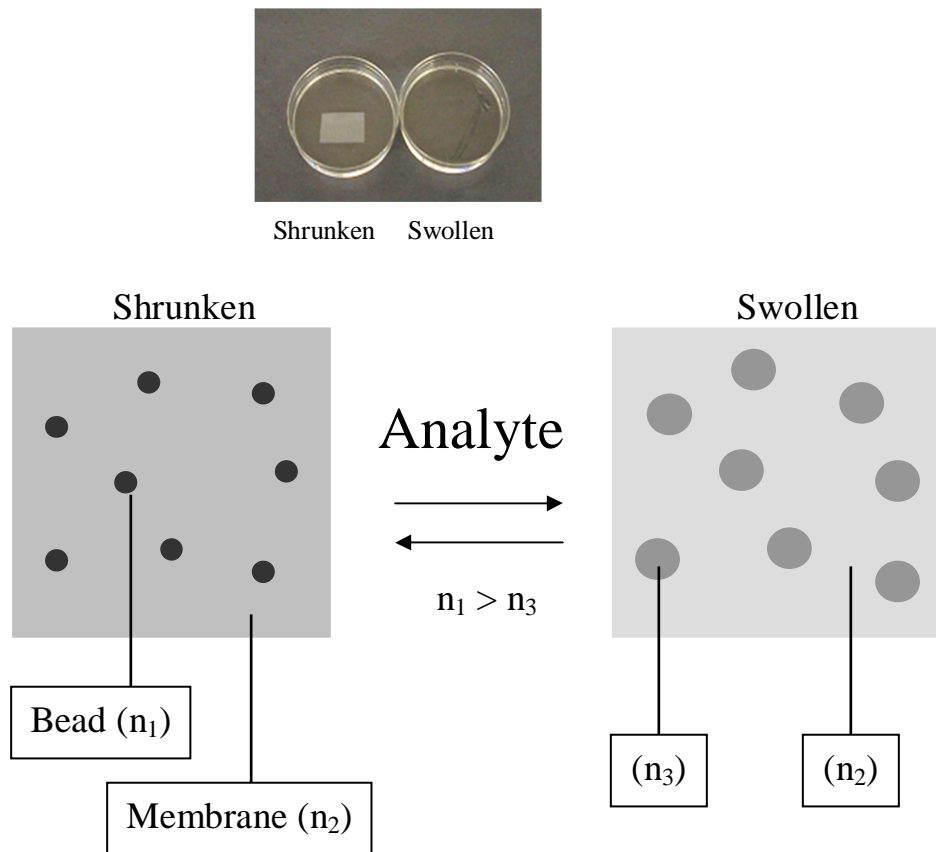


Figure 2.1: An optically sensitive membrane for measuring the concentration of an analyte, which triggers the volume phase transition of the NIPA polymer. Swelling increases the size and reduces the refractive index of the particles embedded in the membrane.

This leads to a decrease in the amount of light reflected by the particles (see equation 2-1). The membrane goes from turbid to clear in response to increasing analyte concentration, which can be monitored by measuring the change in turbidity or change in the intensity of the light reflected or scattered by the membrane (see Figure 2.2).

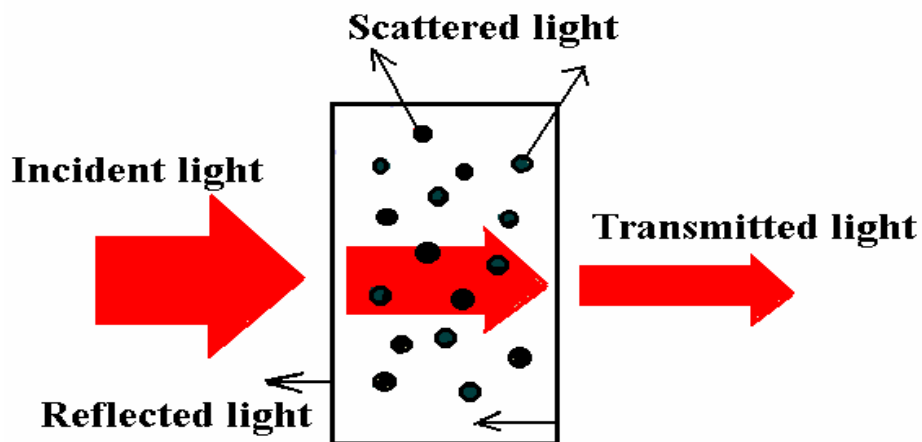


Figure 2.2: The effect of the hydrogel membrane with suspended polymer particles on the intensity of a transmitted light beam

Figure 2.2 illustrates the effect of the membrane on the intensity of a transmitted light beam. Reflection occurs at the phase boundaries as a result of refractive index differences between the membrane and its surroundings. Scattering is caused by the suspended particles and only occurs if the major dimension of the scattering particle is comparable to or larger than the wavelength of light and if its refractive index is different from the hydrogel. The amount of light reflected at the interface between two dissimilar phases depends on the difference in the refractive indices of the two phases.

For normal incidence:

$$R = (n_2 - n_1)^2 / (n_2 + n_1)^2 \quad (2-1)$$

where n_2 is the refractive index of the hydrogel and n_1 is the refractive index of the polymer particles. It is clear that reflectance increases as the difference in refractive index between the particles (n_1) and the hydrogel (n_2) increases.

Because the change in refractive index is the dominant effect for the NIPA particles studied, we can measure it as a change in membrane turbidity, which is easy to perform. Turbidity can be defined as the change in the intensity of light as it passes through the sample and obeys the relationship:

$$I_t = I_0 e^{-\tau b} \quad (2-2)$$

where I_t \equiv intensity of light passing through the sample, I_0 \equiv intensity of incident light, τ \equiv turbidity coefficient or turbidity, and b \equiv optical path length (cm). This equation, which is analogous to Beer's Law, defines the turbidity of the suspended particles in a medium. Thus, a conventional absorbance spectrometer can be used to measure polymer swelling when the polymer particles are immobilized in a hydrogel membrane.

2.2 Polyvinyl Alcohol Immobilization - Polymer Membrane Description

For the investigation of swelling, immobilization of the polymer microspheres is required to ensure reproducible measurements. Dispersion of polymer particles in an aqueous system is unstable, as it is prone to sedimentation over time. Therefore, a method to fix an array of polymer microspheres in the path of a light beam is needed such that light passing through a cuvette in an absorbance spectrometer strikes the same number of polymer particles in each measurement. Also, any problems created by particles in solution moving into and out of the path of the light beam would be eliminated. To overcome this problem, a secondary polymer was used to suspend the polymer particles in an array that remains relatively fixed during the turbidity

measurement as the membrane is mounted perpendicular to the beam from the light source of the instrument.

2.2.1 Properties of an Ideal Immobilization Polymer

An ideal immobilization membrane will have the following properties (Table 2.0).

Table 2.0: Characteristics of an Ideal Immobilization Polymer

Optical Transparency	The immobilization membrane should not significantly contribute to the measurement signal.
Chemically Inert	The immobilization membrane should not react with other solution component rendering a change in its optical properties over the course of the experiment.
Insoluble in Aqueous Medium	All polymer analyses will be conducted in aqueous media, so the immobilization membrane should not be soluble in DI water. Breakdown in DI water over time would reduce measurement reproducibility.
No Interference with the Polymer Swelling Event	An immobilization membrane composed of a rigid structure will reduce the total swelling potential of the polymer microspheres, and thus reduce the sensitivity and dynamic range of the measurement system.
Does not significantly reduce particle response time	The immobilization membrane needs to readily allow for the diffusion of the analyte so that response time of the particle swelling event is not negatively impacted.
Easy to work with / non-hazardous	The material used for the immobilization membrane should be non-toxic to the analyst, as well as to the system (potential for bio-applications). Moreover, the material used should be readily available and of a defined quality to ensure immobilization membrane standardization.

2.2.2 Properties of Polyvinyl Alcohol

Polyvinyl alcohol (PVA) possesses several attributes that make it a logical choice as an immobilization membrane. PVA is an odorless, non-hazardous substance that can be stored under typical laboratory conditions as it does not readily undergo hazardous polymerization. It is an optically transparent material that has already found applications in the life sciences as an immobilization medium for specimen preparation. PVA can also be crosslinked under controlled laboratory conditions to prepare reproducible hydrogel materials that are permeable to both water and hydrated ions. Therefore,

immobilization of environmentally sensitive polymer microspheres within a PVA membrane fixes the microspheres in a set orientation for the turbidity measurement, yet does not impair their accessibility to target analytes which can readily diffuse through the membrane. The immobilization of microspheres in the hydrogel also creates a material that can be readily adapted to chemical sensing, where as application of the polymer particles alone would prove problematic. However, it is crucial to prepare hydrogel membranes whose overall composition and polymer particle content is fixed in order for the membrane to be a viable sensing material. Therefore, a standardized procedure was developed to prepare these membranes.

2.2.3 Preparation of Polyvinyl Alcohol Membranes

- ***Membrane Preparation:***

Standardization of the preparation method for PVA membranes is vital for chemical sensing. Variations in the membrane's composition, thickness, or percent crosslinking can alter its properties. The introduction of an uncontrolled variable into the experimental testing could undermine or invalidate conclusions drawn when comparing different NIPA polymers. Therefore, a standardized procedure for the preparation of PVA membranes with 1% (w/w) polymer particle composition has been developed. This procedure can be divided into six distinct steps.

- ***Stock Solution Preparation:***

PVA was purchased from Sigma-Aldrich (Batch #032628MC Cat #: 3631154), and it was used as received. A 10% (w/w) solution was prepared in DI water, and 3-chlorophenol was added to prevent the growth of mold during storage. The amount of 3-chlorophenol added to the PVA stock solution yielded a 50ppm solution of the phenol. A

10% solution of glutaric dialdehyde (Sigma-Aldrich Batch #14727PA Cat #: 340855-25mL) was prepared by diluting 0.8848 g of the commercial stock solution (50% w/w in water) to 4.000 g using deionized (DI) water. The concentration of a stable polymer particle dispersion was determined by drying a 1.000 g aliquot of the dispersion until a constant mass was obtained and reporting the results as %mass (w/w). The concentration of the dispersion was adjusted by dilution or evaporation to the desired value, which was 2.5% (w/w) in methanol (unless otherwise noted on the vial inventory sheet).

- ***Preparation of Polymer Particle Dispersions:***

To ensure homogenous sampling, suspensions of the polymer particles were inverted for mixing, and sonicated for at least five minutes. Next, a 0.400 g sample of the suspension was placed in a tared vial and gravimetrically diluted to 1.0 g using deionized water. In an effort to remove methanol, the vial was placed under an airline for one hour while stirring to evaporate methanol until a mass approaching 0.40 g is attained.

- ***Glass Slide Membrane Mold Preparation:***

The casting mold used for the immobilization membrane consisted of glass microscope slides edged with Teflon tape as a spacer on each of the long edges of the slide. A second microscope slide was used as a cover to create a cast of uniform thickness (127 μm). With proper care and cleaning, the glass mold slides were reusable. To prepare slides for casting a PVA membrane, each set of slides was wiped clean with ethanol. Also, a glass Pasteur pipette was prepared, by breaking off its tip for the delivery of the polymerizing solution to the slides. This allowed a wide-bore opening to be formed that eased the aspiration of the viscous polymer solution.

- ***PVA Addition and Polymerization:***

Once the dispersion reaches its initial mass (0.400 grams) prior to dilution with DI water dilution by air stream drying, the vial contents were diluted to 2.00 g with the 10% PVA stock solution. The vial was allowed to stir for 8+ hours or overnight to ensure a homogeneous distribution of the particles in the PVA formulation. To polymerize the particle/PVA solution, 50 μL of the 10% glutaric dialdehyde (GDA) crosslinking solution was added and allowed to mix for an hour to ensure a homogenous mixture. Next, 25.0 μL of 4.0 M HCl was added to initiate the polymerization reaction between PVA and GDA crosslinker. The solution was stirred vigorously and sonicated to remove any bubbles. Complete polymerization of the sample occurred within 10 minutes, so membranes were cast immediately following sonication.

- ***Membrane Casting and Storage:***

The entire contents of the vial were transferred to the previously prepared Pasteur pipet and a thin bead of the solution was applied to each of the four previously prepared glass slide molds. Next, each glass cover slide was placed on top of a mold slide. This helped to spread the polymer solution bead allowing a uniform layer within the mold to form. Special care was taken in the application of the cover slide to prevent any air bubbles from forming at the cover slide/solution interface. Each covered slide pair was clipped with three medium portfolio clips on each edge and allowed to solidify. The membranes reach the desired consistency after one hour of curing. The clips were removed, and the glass slide pairs were placed in DI water to hydrate the membrane.

The membranes swell when hydrated, creating a gap between the cover slide and the mold slide. A razor blade was used to pry the glass slides apart, and the membrane

was removed from the mold slide by cutting the edges free of the spacer tape. Each polymer membrane was inspected for uniformity, and any obvious irregular segments were removed. The remaining membrane segments were stored in DI water in a sealed, labeled vial prior to use.

- ***Membrane Characterization:***

The membranes were removed from storage and placed in a recrystallization dish containing DI water. The membrane with the most uniform distribution of particles was selected for mounting. A small test segment was cut for insertion into the sample holder. The remaining portion of the membrane was returned to storage with the other membranes in DI water.

2.2.4 Polymer Membrane Uniformity

To ensure precision between membrane test segments, it is crucial for the polymer particles to be uniformly distributed in the hydrogel membrane. Since only a small sample segment is cut from the parent membrane for evaluation and testing, heterogeneity in the particle density could result in low measurement precision between test segments. The distribution of the polymer particles in the hydrogel membrane has been investigated to determine if modifications in the membrane casting process are required to ensure that polymer particles are homogeneously dispersed.

Polystyrene microspheres (diameter = 1.0 μm), which served as a surrogate for the swellable polymer particles, were cast into a PVA membrane (0.25% w/w) using the procedure described in this section of the thesis. The entire membrane was placed between two glass microscope slides, and absorbance measurements (700 nm) were taken every 5.0 mm along a 4.0 cm interior length. Figure 2.3 shows the section of the

membrane that was investigated and the turbidity (absorbance), which was measured at every 5.0 mm along this section of the membrane. (The section of the membrane sampled was from the central portion to avoid any edge effects.) The relative standard deviation between measurements taken across the membrane was less than 1.0%. These results show that it is possible to prepare hydrogel membranes containing polymer particles that are uniformly distributed throughout the membrane. Therefore, the current method used to disperse polymer particles in the hydrogel membrane was judged to be acceptable for the preparation of reproducible membrane segments.

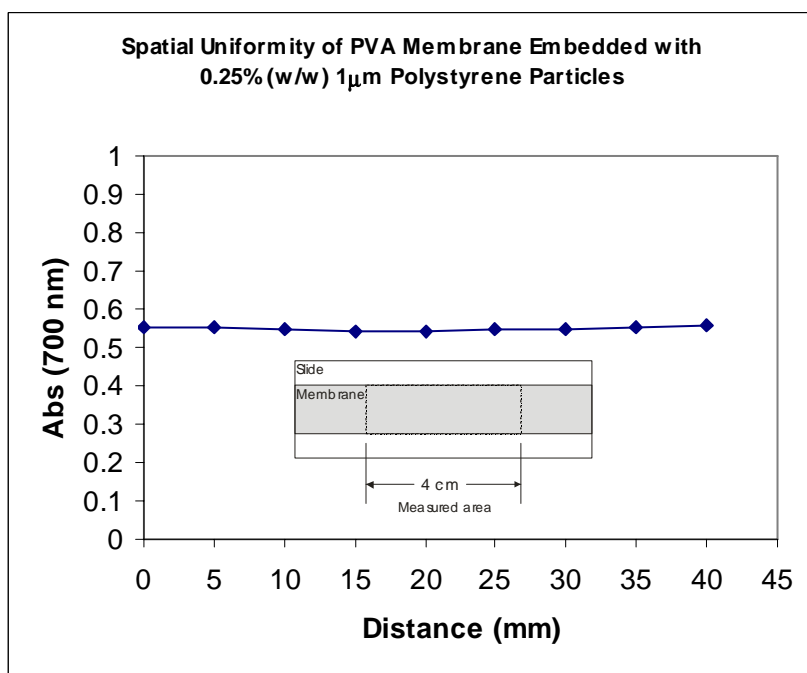


Figure 2.3: Characterization of the distribution of polystyrene microspheres in a PVA membrane using turbidity. Inserted diagram indicates the membrane section that was sampled to assess particle uniformity.

2.2.5 PVA Optical Effects due to pH, Temperature, and Ionic Strength

PVA is a suitable material for immobilization as it forms a three-dimensional matrix when crosslinked. The water content of a PVA membrane approaches 90% when it is fully hydrated, making it permeable to all hydrated ions. The ability of analytes in

the sample solution to diffuse quickly into the PVA membrane and to the polymer microspheres is crucial if polymer swelling is to be used as a transduction mechanism for chemical sensing. Furthermore, PVA as an embedding medium should not contribute significantly to changes in turbidity in response to changes in pH, temperature, and ionic strength.

PVA membranes prepared with 0.25% (w/w) polystyrene microspheres (see the study described in the previous section) were selected for investigating the effect that changes in the composition of the sample solution would have on the hydrogel itself. Polystyrene microspheres were chosen because they are insensitive to environmental stimuli such as pH or temperature. A test segment was cut from the parent membrane, and changes in its optical properties were evaluated as a function of pH, salt concentration, and temperature.

- ***PVA Measurement Contribution Due to pH:***

Low ionic strength citrate buffers ranging from pH = 3.0 to pH = 6.0 were prepared in 0.2 pH unit increments. The test membrane segment was mounted in the sample holder (see Figure 2.8), which is perpendicular to the light beam of the spectrophotometer. The membrane was challenged with citrate buffer starting at pH = 3.0 and progressing to pH = 6.0. A response curve for this same pH range (pH = 6.0 to pH = 3.0) but starting at high pH was also generated. The membrane was allowed to equilibrate in each buffer solution for five minutes prior to each turbidity measurement. Figure 2.4 shows the absorbance (turbidity) observed when the PVA membrane is exposed to solutions of pH increasing from 3 to 6 and then decreasing from 6 to 3.

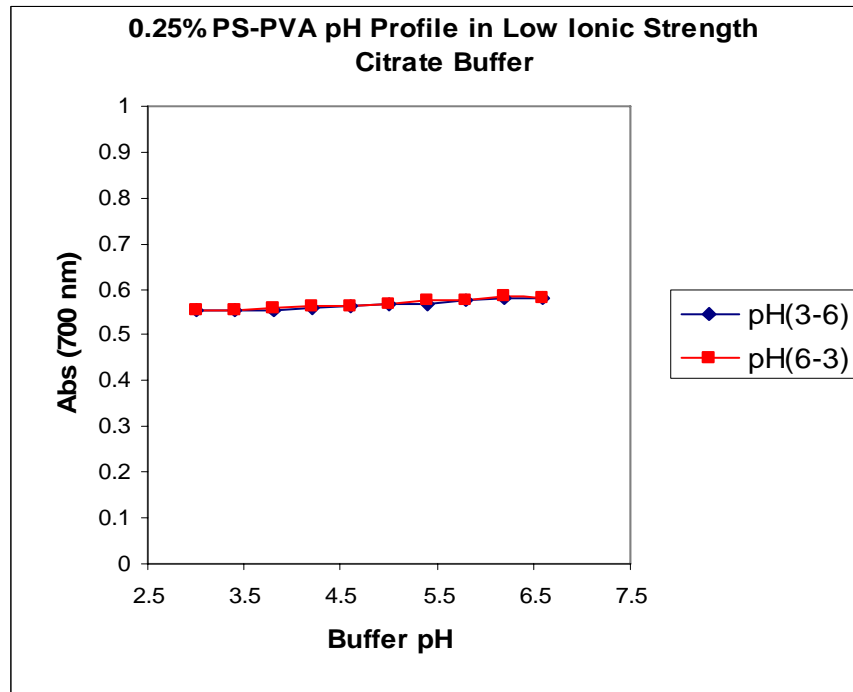


Figure 2.4: Overlay of PVA response plots for both ascending and descending pH profiles with low ionic strength citrate buffer test solutions.

Over the pH range (pH = 3.0 – 6.0) investigated, the membrane displayed a 0.0238 absorbance unit increase. This increase in turbidity is not significant in magnitude to the total turbidity change typically observed (which corresponds to 0.40 – 0.60 absorbance units) when pH sensitive polyNIPA particles are embedded in the hydrogel membrane. Clearly, the contribution of the PVA membrane to changes in turbidity with pH is an order of magnitude smaller than the changes in turbidity that occur with the pH sensitive polyNIPA particles. Furthermore, absorbance decreases with increasing pH for the pH sensitive polymer particles whereas absorbance increases for the PVA membrane with increasing pH of the buffer solution. Therefore, PVA is an acceptable membrane for measuring the swelling of pH sensitive polymer particles.

- ***PVA Measurement Contribution Due to Temperature:***

The contribution of the PVA membrane to turbidity with respect to temperature was also investigated. The PVA membrane containing 0.25% polystyrene (w/w) was placed in DI water, and the temperature of the solution was increased in five-degree increments every five minutes from 10° C to 60° C. (Polystyrene is not affected by temperature in the range investigated.) Figure 2.5 shows the change in turbidity with temperature for both ascending and descending temperature gradients. Over the temperature range investigated (10° C to 60° C), the total absorbance increase was 0.0830 for the PVA membrane.

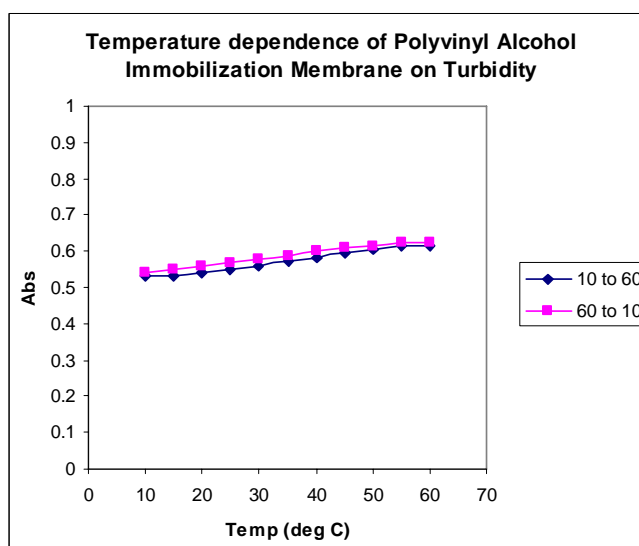


Figure 2.5: Ascending and descending temperature profiles for 0.25% polystyrene microspheres in a PVA membrane.

Polymer particles containing NIPA also undergo a volume phase transition at approximately 37° C where the particles go from a swollen state to a shrunken state due to a loss of water. This causes an increase in the turbidity of the membrane in which they are embedded. A typical temperature profile for polymer particles prepared from NIPA and MAA (NK 1-60) and embedded in a PVA membrane is shown in Figure 2.6. The

contribution of PVA to the change in turbidity (see Figure 2.5) is small and (to a first approximation) can be ignored in temperature studies involving copolymers of NIPA embedded in a PVA membrane.

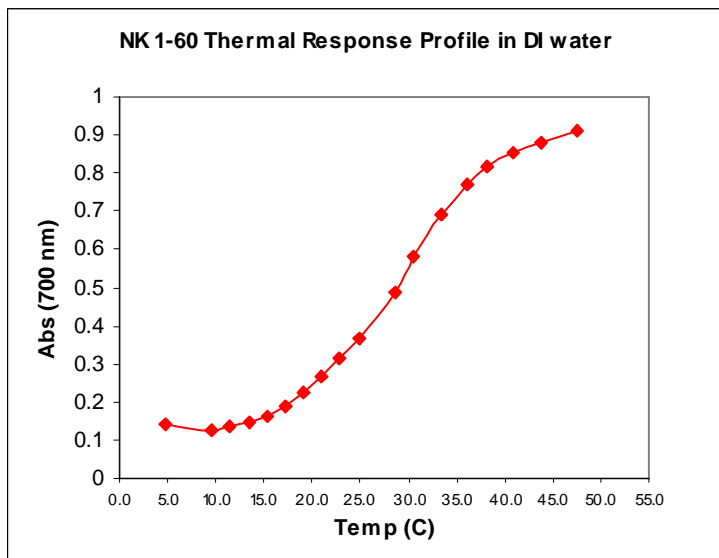


Figure 2.6: Thermal transition profile for NK 1-60 in DI water.

- ***PVA Measurement Contribution Due to Ionic Strength:***

The contribution of PVA to turbidity as a function of the ionic strength of the sample solution was also investigated. Solutions containing sodium chloride of increasing ionic strength were used to determine whether the optical properties of a PVA membrane would change. A PVA membrane with 0.25% polystyrene (w/w) was first placed in DI Water for purposes of equilibration. Next, the membrane was challenged with NaCl solution ranging from 1.0×10^{-7} M to 0.10 M NaCl. The membrane was allowed to equilibrate for 15 minutes between runs to ensure that equilibrium was reached. Figure 2.7 shows the change in absorbance (turbidity) as a function of the ionic strength of the sample solution in contact with the membrane. As there was no change in the turbidity of

the PVA membrane containing latex particles, one can conclude that the effect of ionic strength on polymer swelling can be investigated using turbidity data obtained from polymer particles that have been embedded in a PVA membrane since any changes in membrane turbidity will be solely attributable to the interactions of the polymer particles with the electrolyte.

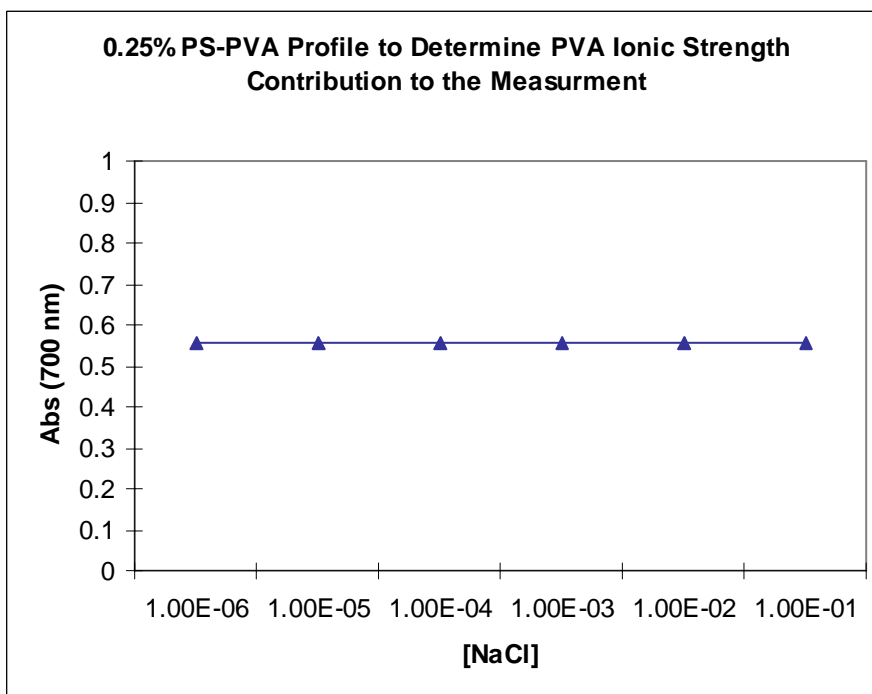


Figure 2.7: Signal contribution of polyvinyl alcohol immobilization membrane with increasing solution ionic strength (NaCl concentration).

2.3 Instrumentation

Turbidity (absorbance) measurements of the PVA membrane containing embedded polymer particles of NIPA were made using an ultraviolet-visible (UV-Visible) absorbance spectrophotometer. Although designs vary from one manufacturer to the next, the underlying components and their functions remain the same. By understanding the individual components that make up the UV-Visible absorbance

spectrophotometer, one can understand the advantages of using it to study polymer swelling. In this section, a brief discussion of an absorbance spectrophotometer, which can be used for turbidimetry, is given.

2.3.1 Components/Configuration of a UV-Vis Spectrophotometer

The major components of a UV-Vis absorbance spectrophotometer are the radiation source, monochromator, sample holder, photodetector, and database manager. The Cary 6000i (Varian Inc) was used for all of the polymer characterization experiments described in this thesis.

- ***Light Source***

It is important that a light source for a spectrometer emit a continuous spectrum of constant intensity over the ultraviolet and visible wavelength regions. Attenuation of the source output as it interacts with the sample is the basis of the absorbance measurement, wherein the attenuation of light is reported as an absorbance or the remaining signal is reported as the percent of light transmitted to the detector.

The Cary 6000i is equipped with a tungsten bulb as its continuous visible light source, and a deuterium lamp as its ultra-violet wavelength source. Absorbance (turbidity) measurements were obtained over the wavelength range of 350-700 nm with turbidity versus pH profiles reporting the absorbance at 700 nm and turbidity versus metal ion concentration profiles reporting the absorbance values at 500 nm (metals).

- ***Wavelength Selectors***

Fixing the wavelength of light that interacts with the sample is crucial for most spectrophotometric methods of analysis. This is usually achieved with a monochromator placed between the source and the sample to disperse the incident light

into its component wavelengths. For the turbidity measurements made in the studies described in this thesis, wavelength control was important. Polymer swelling was studied over the wavelength range of 350-700 nm, wherein pH profiles were constructed from absorbance (turbidity) data collected at 700 nm. The decision to use longer wavelengths for pH profiling of the polymer particles was made to address issues related to particle size. The polymer particles used are approximately 1.0 micron or less in diameter when swollen. As the wavelength of light striking the particles decrease, the measured absorbance will increase since the intensity of light scattered by the particles also increases. By measuring turbidity (absorbance) at longer wavelengths, the decrease in the refractive index of the particles, which is indicative of swelling, should be the dominant effect. However, if a short wavelength of light is used to monitor changes in swelling, there is concern that light scattering by the particles in the PVA membrane would attenuate the beam, biasing the absorbance towards higher values. For this reason as well as concern about absorption of light by the film, 700nm, which is a convenient wavelength to work with, was used to monitor polymer swelling.

- ***Sample Holders***

The purpose of the sample holder is to station the sample cuvet perpendicular to the light beam. This stationing must be reproducible. The Cary 6000i has a variety of accessories that facilitate this function depending on the application. These accessories include a standard dual cuvet stage, a six-unit cell changer (thermally controlled), a solid sample stage, and a flow cell setup. Despite the differences between these components, they each serve the same purpose of immobilizing the sample cuvet in the optical light path, as well as at a defined height within the light path for measurement reproducibility.

The six-unit cell changer with thermal control was used exclusively since it can regulate the temperature of the system and accommodate multiple samples. However, a few experiments were performed using a different experimental configuration and this was noted in the appropriate sections of this thesis. For any UV measurements ($\lambda < 350$ nm), a quartz cuvet is used because of its optical transparency. For profiling measurements collected within the visible region of the spectrum, disposable methacrylate cuvetts were used to house a black, custom-made polymer sample holder (see Figure 2.8).

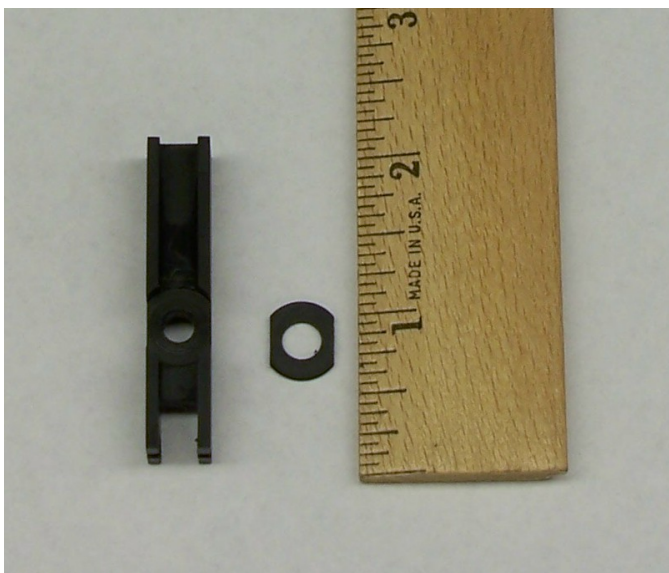


Figure 2.8: Custom-made black plastic membrane test segment holder.

The holder is made from black plastic to ensure that it will not contribute to any undue incident light reflections causing stray light bias. Furthermore, the black plastic is chemically inert to the sample solutions under investigation. Six identical polymer membrane holders were manufactured under the supervision of Mike Lucas of the Oklahoma State University Machine Shop. Due to the light attenuation that occurs from the membrane holder, a second matched holder is placed in the reference beam path.

To mount the polymer test membrane segment in the custom made sample holder, the membrane segment was placed in a Petri dish containing DI water. The segment was floated onto a microscope slide and smoothed to remove any wrinkles. The membrane was then attached to the inset piece of the sample holder by placing the piece on top of the membrane. This allowed the membrane to completely cover the opening of the inset piece and also to adhere to its plastic surface. After the membrane was again investigated for wrinkles or damage, the inset piece from the sample holder, which contained the membrane was snapped to the base unit of the sample holder. The complete sample holder (base unit and inset piece) is able to slide into a conventional UV-Visible cuvet, with the remaining space in the cuvet filled with DI water or the sample solution.

- **Detectors**

The purpose of the detector is to convert the intensity of the light beam into an electronic signal. The Cary 6000i is equipped with an Indium Gallium Arsenide detector for the near IR region and a photomultiplier tube for the UV-Vis region. A more detailed survey of the Cary 6000i specifications is provided in Table 2.1.

Table 2.1: Cary 6000i specifications selected from the Varian UV-VIS-NIR Cary 4000, 5000, and 6000i Preliminary Performance Data PDF file.

Component	Ultraviolet - Visible Spectrum	Near IR
Monochromator	Double out-of-plane Littrow monochromator	Double out-of-plane Littrow monochromator
Grating	Dual sided, 70x45mm, 1200 lines/mm blazed at 250nm,	Dual sided, 70x45mm, 600lines/mm blazed at 1000nm
Beam Splitting System	Chopper 30hz	Chopper 30hz
Detectors	R928 PMT	NIR: Cooled InGaAs Photodiode
Limiting Resolution	<0.05	<0.10
Wavelength Range (nm)	175-1800	175-1800
Wavelength Reproducibility (nm)	<0.005	<0.025
Wavelength Accuracy (nm)	Plus or Minus 0.10	Plus or Minus 0.20

- ***Database Manager***

The electronic signal from the detector must be converted into a domain that can be interpreted by the user. Modern instrumentation is designed to interface with computers allowing the spectral data to be compared, analyzed, and stored for long-term use. The Cary 6000i is equipped with a Dell personal computer that displays data through the Varian Cary software package. A typical turbidity spectrum for a polymer membrane is relatively featureless, with only a slight drift to higher absorbance values as the wavelength decreases. This allows the user to select among a large range of wavelengths for investigating polymer swelling.

2.3.2 Instrumental Setup for Polymer Characterization Measurements

Each of the optical and electronic components previously described in subsection 2.3.1 play a pivotal role in the reliable operation of a spectrophotometer. Figure 2.9 is a symbolic drawing of how each of the previously described components function together.

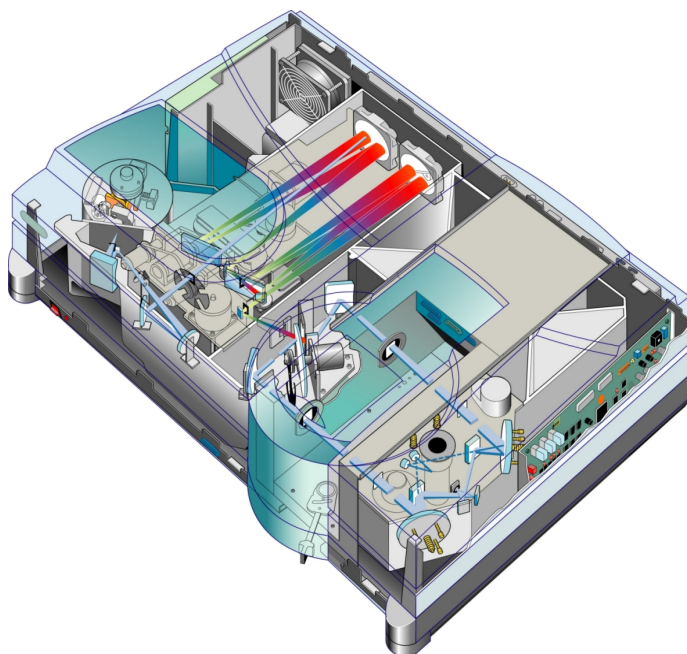


Figure 2.9: Ray-Trace Diagram of the Cary 6000i (provided by Varian Inc.)

The Cary 6000i is a double beam instrument, which allows for a reference cell to be monitored continuously in parallel to the sample cell. Instability in the light source of the instrument affects the intensity of both the reference and sample beams. For a single beam instrument, such fluctuations result in a lower signal to noise, raising the detection limits and lowering instrument specification levels such as sensitivity. In a true double beam geometry, the ratio of sample beam intensity to reference beam intensity is measured within a few milliseconds to reduce measurement noise arising from source instability, thereby improving detection limits and overall instrument specifications.

The ratio of sample and reference beam intensities requires that conditions for the cuvetts in both optical paths be roughly equivalent. Both light paths include a methacrylate cuvet containing a black plastic membrane sample holder. However, the reference cell contains DI water, while the sample cell contains a membrane in contact with the sample solution. As these solutions are of a dilute nature, the DI water in the reference cell was found to be an adequate match.

2.4 Defining Membrane Composition

Our early experiments in polymer swelling have shown that variability in the amount of polymer microspheres immobilized in the hydrogel membrane influences the magnitude of the swelling observed. Specifically, increasing the weight percent of polymer microspheres immobilized in the PVA membrane results in a larger change in membrane turbidity in response to environmental stimuli such as pH. For this reason, it was necessary to standardize the percent particle content of the hydrogel membrane to ensure a meaningful comparison of the results obtained using different hydrogel

membranes. Therefore, a study was undertaken to determine the weight percent of particles that would be optimum for membrane construction.

2.4.1 Experimental Setup / Methods

NK 1-60 polymer (70% NIPA, 10% MAA, 10% NTBA, and 10% MBA) was immobilized in PVA to yield membranes with the following percentage compositions: 0.25%, 0.5%, 1.0%, and 2.0% particle (w/w). A pH profile of each hydrogel membrane was collected at pH 3, 4, 5, 6, and 7 using low ionic strength citrate buffer (see appendix for information about the preparation of this buffer). The membrane test segments were exposed to buffer starting at pH = 3 and proceeding to pH = 7 with five minutes equilibration time for each buffer solution. The sample cell was rinsed three times with the next buffer solution prior to the start of the measurement cycle to ensure that buffer from the previous measurement step was not carried over to the next measurement cycle.

2.4.2 Data and Results

Spectral scans were collected over the wavelength range of 700-350nm, and pH profiles were developed using the absorbance values at 700nm for the turbidity of the membrane. Figure 2.10 depicts the change in turbidity for each of the four membranes versus increasing pH of the buffer solution in contact with the membrane. The percentage of swellable polymer particles in the membranes tested varied from 0.25% to 2.00%.

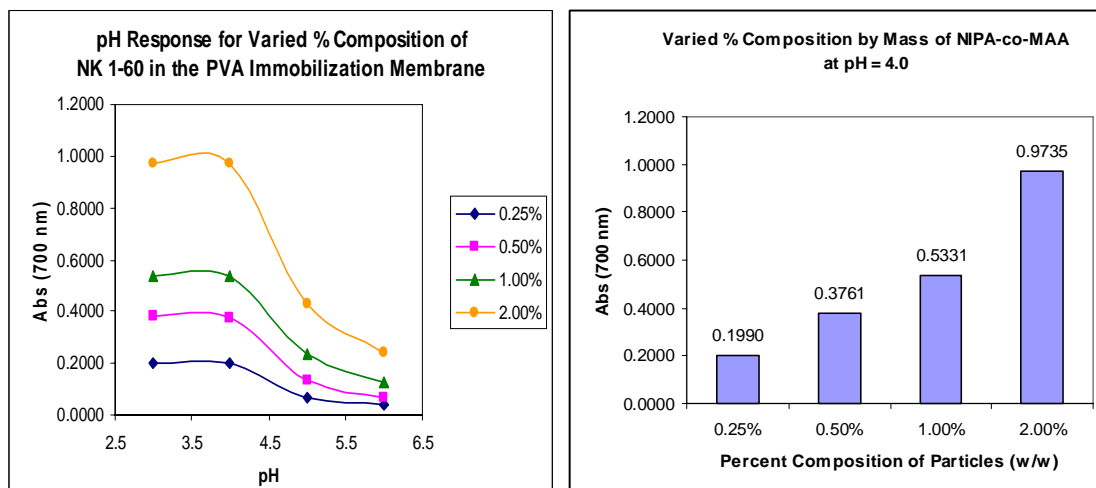


Figure 2.10: (left) pH profiles of hydrogel membranes with increasing amounts of immobilized pH sensitive polymer particles. (right) Membrane absorbance values at pH = 4.0 with increasing percent composition of particles by mass (w/w).

A plot of the total absorbance change between pH = 3.0 (shrunken state) and pH = 6.0 (swollen state) for each membrane tested versus the polymer particle weight percent yields a linear correlation shown in Figure 2.11. As the percentage of polymer particles in the hydrogel membrane increases, the larger the change is in total absorbance with increasing pH. However, the absorbance values recorded for the membranes in DI water also increase as the percentage of polymer particles in the hydrogel membrane increases, leading to higher absorbance values for the entire profile. The correlation between absorbance (turbidity) values for DI water versus the weight percent of swellable polymer particles in the hydrogel membrane is shown in Figure 2.12. From the data shown in Figures 2.10 – 2.12, the optimum weight percent of polymer particles in the membrane is approximately 1% as this allows for a measurable swelling response while not contributing a significant bias due to a high background.

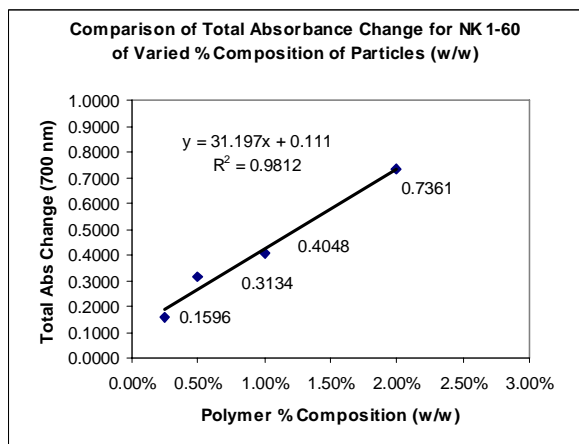


Figure 2.11: Linear correlation between polymer particle weight percent and the total absorbance change.

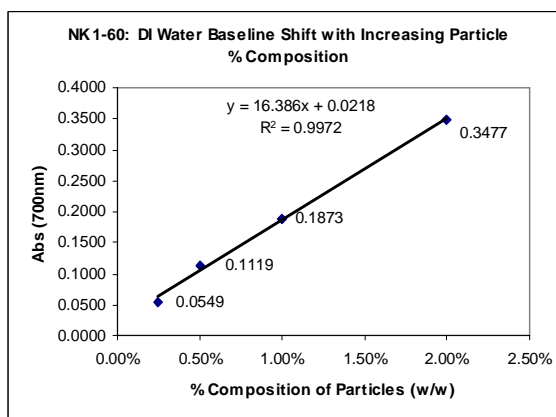


Figure 2.12: Turbidity of membrane in DI water increases linearly as the percent composition of particles in the membrane increases.

2.5 Contribution of NIPA to Total Swelling Due to pH

The swelling behavior of NIPA polymers prepared from formulations without functional co-monomer was investigated using buffered solutions of varying pH. Data were collected at 700 nm after each buffer was allowed to equilibrate with the membrane for 5 minutes. The data were plotted (see Figure 2.13) to determine whether polyNIPA itself swells in response to changes in the pH of the sample solution in contact with the membrane. Although the NIPA control test segment did not exhibit a measurable response over the pH range (3.0 to 6.6) investigated, there was a small positive drift.

During the course of this experiment, interference was encountered due to the formation of small micro bubbles on the membrane surface in the low pH solutions. However, we were able to correct this problem as the experiment proceeded.

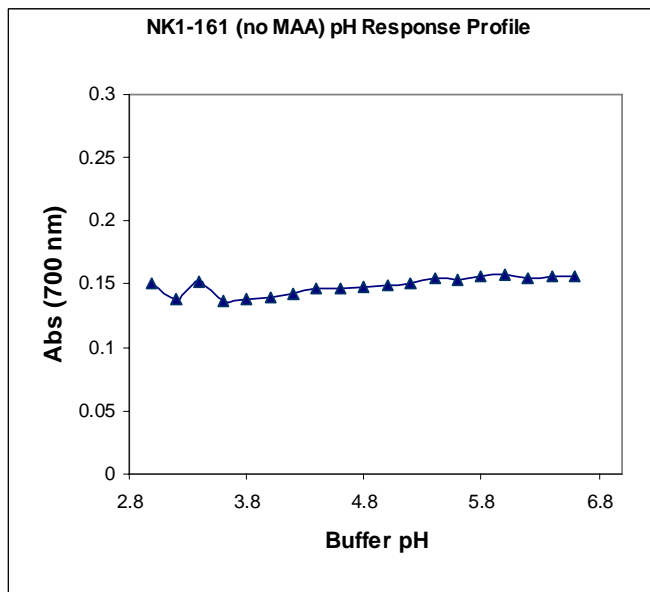


Figure 2.13: The pH profile of polyNIPA (without methacrylic acid comonomer). Interference was encountered due to the formation of small air bubbles on the surface of the membrane at pH = 3.0 and 3.4.

2.6 Buffer Systems for pH Profiling

pH profiling was initially performed using a buffer series composed of more than one type of buffer. The pH range investigated for many of the studies in this thesis was from 3-7 with the ionic strength of each buffer modified by adding known quantities of NaCl to an aliquot of the 0.1M buffer stock solution. Table 2.2 lists the buffers used and the pH range, which they encompass for the studies described in this thesis.

Table 2.2: Buffer Series Composition and Associated pH Range

Buffer	Start of pH Range	End of pH range
Chloroacetic Acid	3.0	3.8
Acetic Acid	4.0	5.4
2-Morpholinoethanesulfonic acid (MES)	5.6	6.6
Sodium Phosphate, Monobasic	6.8	8.0
Ammonium Chloride	8.2	10.0
Citric Acid	3.0	7.0

Using three different buffers over the pH range 3.0-7.0 proved to be problematic when the swelling behavior of the polymer particles was studied in high ionic strength (1.0 M) media. An unexplained anion effect occurred which caused a change in the transition temperature of the NIPA particles when the buffer was switched from chloroacetic acid to acetic acid resulting in a discontinuity in the pH profile (Figure 2.14).

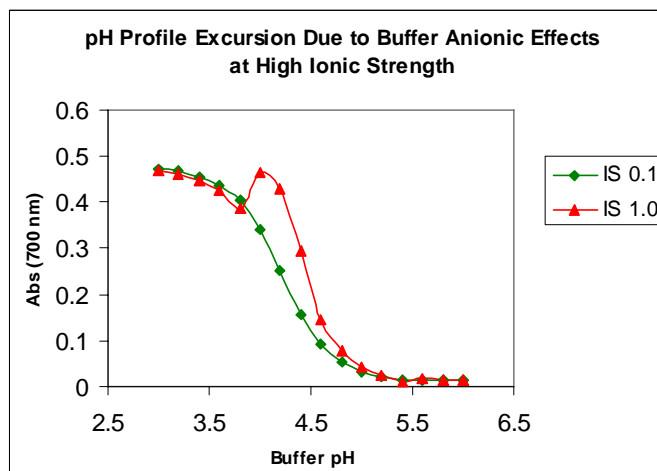


Figure 2.14: High and Low Ionic Strength pH Profile of a NIPA co-MAA (10%) polymer

When data from the corresponding citrate acid buffer was substituted for data from the chloroacetic acid portion of the pH profile (pH = 3.0-4.0, 1.0 M ionic strength), the profile shown in Figure 2.15 was obtained. The pH response profile was continuous over the entire pH range of 3.0-6.0. The seamless integration of the citrate buffer data

into the pH profile was indicative of the discontinuity in the high ionic strength profile being due to the chloroacetic acid buffer, and not the acetate buffer.

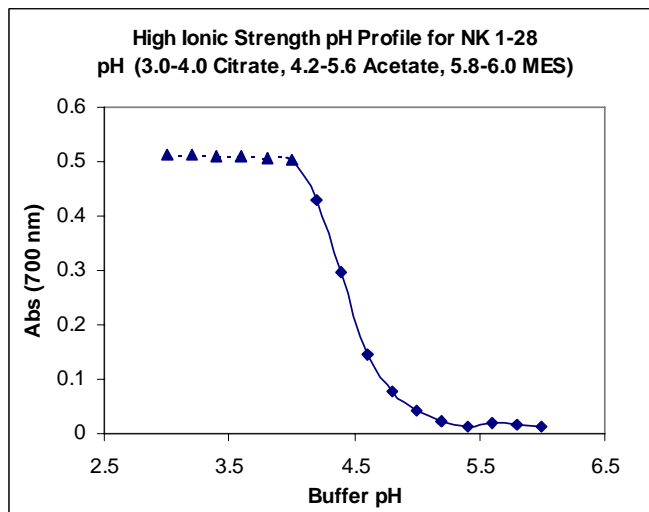


Figure 2.15: High ionic strength pH profile for NK 1-28 with citrate buffer data (pH = 3.0-4.0) substituted for the original chloroacetic acid buffer data.

Using a single buffer over the pH range 3.0-7.0 would resolve the high ionic strength pH profile discontinuity, which is why a citrate buffer was selected for most of the pH studies described in this thesis. Since the initial pH studies at low ionic strength were performed with a mixed buffer system, it was important to confirm the equivalency of the different buffer systems used. Otherwise, it would be necessary to repeat all of this work using the citrate buffer. Therefore, NK 1- 60 (70% NIPA, 10% MAA, 10%NTBA, and 10% MBA) was used to compare the two buffer systems. The test membrane segment was challenged with both pH = 3.0 and pH = 6.0 citrate buffer. After thorough rinsing, the membrane was then challenged with pH = 3.0 chloroacetic acid buffer and pH = 6.0 MES buffer. There were no significant differences in the total absorbance change observed for each buffer system (Figure 2.16).

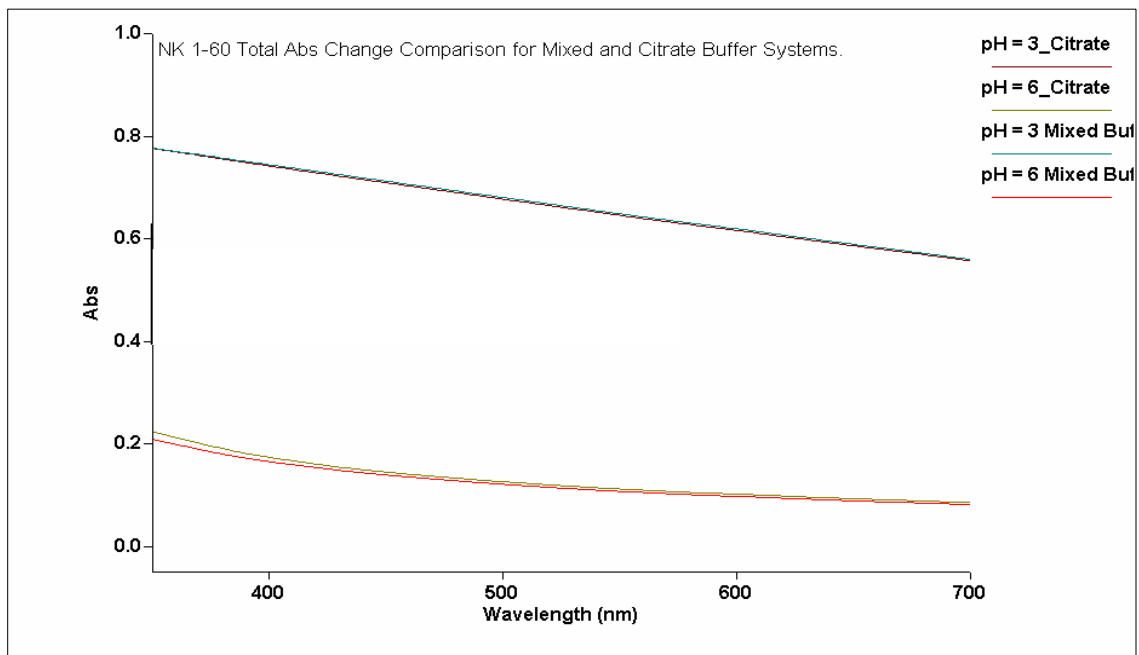


Figure 2.16: The Cary 6000i scan software screen capture of the mixed and citrate buffer induced swelling of NK 1-60.

Using a citrate buffer, pH response profiles at low and high ionic strength were also obtained for NK 1-60 (Figure 2.17). The discontinuity in the pH response curve for the chloroacetic acid/acetic acid buffer system was not observed when citrate buffer was used. Differences in the shape of the profiles shown in Figure 2.17 can be attributed to the effect of ionic strength on polymer swelling, not on the reagents used to prepare the buffer. All pH response profiles after 5.17.2005 were obtained from membranes that were exposed to citrate buffer over the pH range of 3.0-7.0. If higher pH was desired, buffers were prepared from sodium phosphate monobasic and ammonium chloride (Table 2.3).

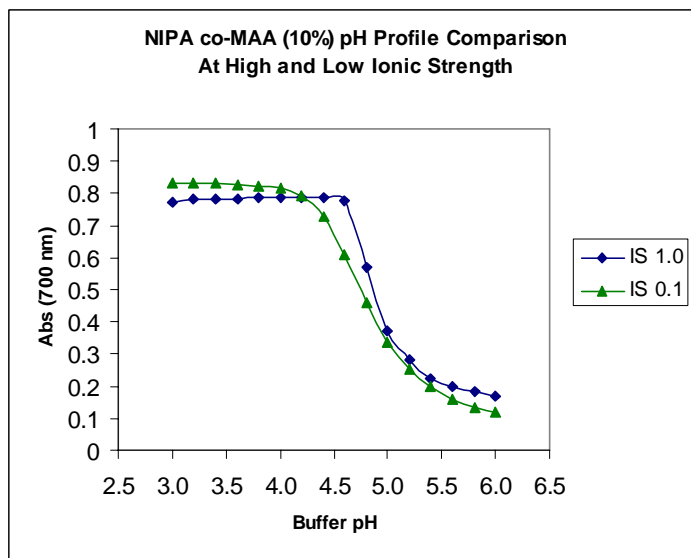


Figure 2.17: NK 1-60 pH profile at 0.1M and 1.0M ionic strength.

2.7 Synthesis of N-isopropyl Acrylamide Co-Polymers

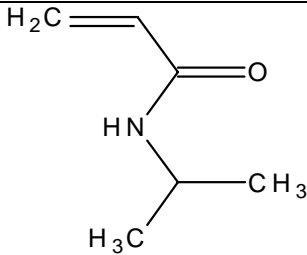
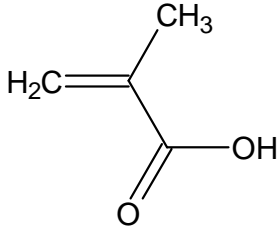
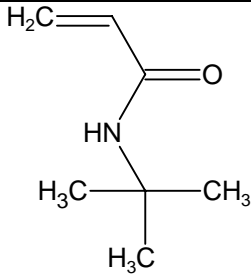
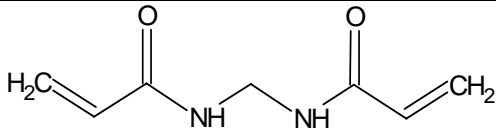
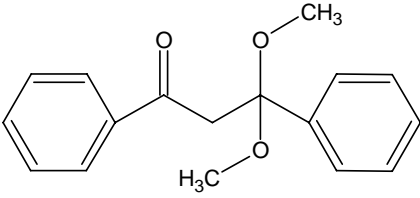
Polymers are large molecules comprised of many repeating subunits. Free radical polymerization is the most widely used method of chain polymerization and is used almost exclusively for the preparation of polymers. Free-radical polymerization can be performed in solutions, suspensions, dispersions, or emulsion. The polymer particles used in the studies described in this thesis were prepared by free-radical dispersion polymerization. This process is rapid, and conversion is high. The distinct character of this technique is that the dispersion is a continuous phase. A solvent is chosen that is a good solvent for the monomer but not for the polymer. Although both photo and thermal initiated radical polymerization processes are available, photo-initiated dispersion polymerization was the method of choice since pH sensitive monodispersed colloidal polymer particles of 0.5 -1.0 μm in diameter could be routinely prepared.

2.7.1 Polymerization Method and Co-Monomers

In dispersion polymerization, which is a variation of precipitation polymerization, the monomers, initiator, crosslinker, and solvent are placed in the reaction vessel at the same time, before initiation of the reaction. To perform photo polymerization, UV light is used to stimulate the generation of free radicals by the initiator. The advantage of using UV light to initiate this reaction, rather than temperature, is that stabilizer is not necessary. Because the reaction is run at room temperature, the NIPA polymer particles formed are in their swollen state, i.e., they contain a large amount of water and are therefore hydrophilic. Table 2.3 describes the role of each component in the formulation used to prepare pH sensitive NIPA based polymer particles.

The polymerization reactions used to prepare the pH sensitive particles were run under a nitrogen atmosphere with constant stirring for approximately 12 hours. The polymer particles were separated from the reaction mixture by centrifugation. The particles were stored for future use by suspending them in methanol with their concentration (g/mL) determined by gravimetric analysis.

Table 2.3: Structure and Function of Polymer Formulation Components:

Mixture Component:	Purpose:	Structure:
N-isopropyl Acrylamide (NIPA)	Base Monomer: Hydrophilic monomeric unit in the largest concentration in the polymerization solution. Selected based on thermal transition temperature and large following within literature due to swelling phenomenon.	
Methacrylic Acid (MAA)	Functional Monomer: Imparts pH sensitivity through the deprotonation of carboxylic acid functional group. Increase in the volume phase transition temperature is the dominant force in pH induced swelling events.	
N-Tert butyl acrylamide (NTBA)	Transition Temperature Adjuster: Hydrophobic monomer used to shift the volume phase transition temperature of NIPA closer to room temperature for swelling enhancement.	
N, N - Methelene Bisacrylamide (MBA)	Crosslinking Agent: Monomer used to connect forming polymer chains into a 3D matrix.	
Dimethoxy phenyl acetophenone (DMPA)	Free Radical Initiator: Absorption of light in the UV-visible wavelength range causes α cleavage to form benzoyl and benzoyl ketal radicals which subsequently initiate polymerization	
Acetonitrile	Solvent: 100mL solvent in which the polymerization occurs	CH ₃ CN

2.7.2 Particle Formation

In dispersion polymerization, colloidal polymer particles are formed. There is less mechanical stress induced in these particles as they swell compared to films of NIPA. Consequently, pH sensitive particles of NIPA have several advantages when compared to pH sensitive NIPA films including faster response times and enhanced sensitivity. The NIPA polymer particles have a diameter of 1.0 μm or less so the time required for an analyte to diffuse into the polymer and initiate swelling is reduced compared to a bulk polymer film. Furthermore, immobilized polymer particles in a hydrogel membrane swell in all three dimensions rather than in one or two.

The first step in dispersion polymerization is initiation, followed by propagation and nucleation. Although both photo and thermal initiated radical polymerization processes were available in our laboratory, photo-initiated dispersion polymerization was the method of choice. Through this method, pH sensitive monodispersed colloidal polymer particles of 0.5 -1.0 μm in diameter could be prepared reproducibly. Furthermore, the use of stabilizer was not required since the polymer particles formed at ambient temperature contained significant amounts of water.

To initiate the polymerization, the reaction mixture was exposed to intense UV-Visible radiation (350 nm), which caused the initiator to undergo fragmentation and form benzoyl and benzoyl ketal radicals which then react with the monomers and comonomers in solution leading to the propagation stage. This involves growth of the polymer chain by sequential addition of molecules of monomer to the active center. The time required for each monomer addition can be as short as a millisecond. Thus, a large number of monomer additions can occur within a few seconds.

As the polymer chains grow in size, they become more hydrophobic and subject to incorporation of crosslinker, which binds the chains. Once the polymer chains have passed a solubility threshold, they will precipitate out of solution. The solvent that is used in the reaction defines the solubility threshold and the size of the colloidal particles formed. As for the comonomer, e.g., methacrylic acid, it is more likely to be incorporated into the shell of the particles due to its hydrophilic character. Once the crosslinker has been consumed, the size of the particle approaches a constant value as the reaction terminates.

There are several stages of particle growth during the dispersion polymerization process. At the beginning, all of the components are in homogeneous solution. The commencement of polymerization is marked by the appearance of oligomers, which grow until they reach a critical chain length, at which point there is a phase separation. This phase separation results in the formation of particle nuclei, which have colloidal instability. The nucleation process takes place over a short period of time. Homocoagulation of the monomers or self-nucleation, results in the formation of even larger unstable species.

At the same time nuclei may also coalesce with oligomers. The growth of nuclei continues to propagate giving rise to mature particles. It has been suggested that for small particles, growth proceeds via capture of oligomers with termination in the particle; for large particles, initiation and growth both occur in the solvent phase leading to particle growth by the accretion of dead polymer. Particles that have grown to their final sizes remain suspended in the reaction mixture.

2.7.3 Materials

N-isopropylacrylamide (NIPA) and acetonitrile were obtained from Acros Chemicals (New Jersey, USA). Acrylic acid, methacrylic acid (MAA), N, N-methylenebisacrylamide (MBA), N, t-butyl acrylamide (NTBA), 2, 2-Dimethoxy-2-phenyl-acetophenone (DMPA), poly(vinyl alcohol) (Mwt 85,000 – 146,000, 98-99 % hydrolyzed), and glutaric dialdehyde (50 w % solution in water) were purchased from Aldrich Chemical Co. (Milwaukee, WI, USA). The glutaric dialdehyde was diluted to 10 % with DI water. Ethylacrylic acid and propylacrylic acid were obtained from the laboratory of Professor Richard Bunce at Oklahoma State University. All reagents and solvents were used as received.

2.7.4 Synthesis

Polymer microspheres were synthesized by free radical dispersion polymerization. In a typical synthesis, NIPA (14 mmol), MAA (2 mmol), MBA (2 mmol), NTBA (2 mmol), and DMPA (0.2 g) were transferred to a 500 ml 3-neck round bottom Pyrex flask and dissolved in 100 mL acetonitrile. The monomer solution was simultaneously sonicated using a Branson 1510 ultrasonicator and purged with dry nitrogen gas for 20 minutes in order to remove dissolved oxygen. The free radical photoreaction was performed at room temperature in a Rayonet photoreactor equipped with G4T5 type mercury lamps and a cooling fan. Since the UV cutoff of the Pyrex flask is less than 260 nm, monomer solution was radiated in the UV-A (315nm to 400nm) region. When a quartz flask was used which allowed radiation at shorter wavelengths to pass through, polymer particles were not produced probably due to photodegradation of reagents. After a 12-hour reaction period, a turbid polymer suspension was transferred

into two 50 mL polypropylene centrifuge tubes and centrifuged at 3000 RPM for 10 minutes. After separating the decant, particles were resuspended in 25 mL aliquots of 90/10 (v/v) mixture of methanol and glacial acetic acid, sonicated for 30 minutes and centrifuged at 3000 RPM for 10 minutes. This washing procedure was repeated four times in order to remove unreacted reagents. Finally, particles were washed three times with 25 mL aliquots of methanol, resuspended in a small amount of methanol and stored in glass vials until use.

2.8 Effect of Ionizable Co-Monomers on NIPA

Incorporating an ionizable co-monomer such as methacrylic acid into the NIPA polymer formulation dramatically changes the properties of the polymer particles formed. Polymer particles with higher surface charge density can be prepared through the introduction of ionizable groups such as amines, carboxylic acids, or thiols. The dispersion properties of the particles will also be enhanced. The structure of these particles may be pseudo-core/shell in nature with the ionizable functional group found at or near the surface of the particles. Evidence to support this hypothesis comes from an experiment performed in our laboratory in collaboration with Professor Bret Flanders (Department of Physics, Oklahoma State University).

The experiment involved the use of a dielectrophoretic cell to induce the spontaneous chaining together of 1 μ m-diameter polymer beads. Figure 2.18 depicts electrodes that are lithographically deposited on a glass substrate and used to induce the dielectrophoretic assembly of these chains. The chain spanning the 60 μ m electrode gap in this figure was grown by depositing a 10 μ l drop of the NK 1-60 particle dispersion over the gap and applying a 100-400 kHz sinusoidal waveform to the left electrode. The

formulation used to prepare the NK 1-60 particles consisted of NIPA (14 mmol), MAA (2 mmol), MBA (2 mmol), and NTBA (2 mmol).

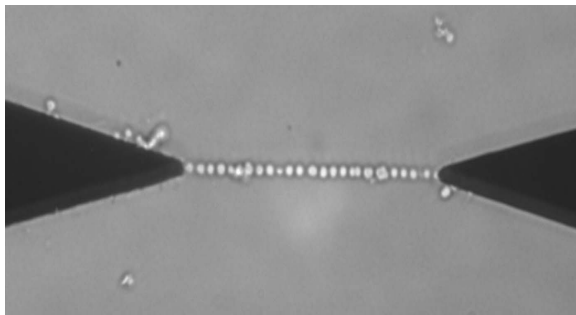


Figure 2.18: The NK 1-60 microspheres were dielectrophoretically chained across the 60µm interelectrode gap. Concentration of particles is greater than 0.01%.

The right electrode in the dielectrophoretic cell was grounded. The chain grows from the alternating electrode to the grounded electrode immediately (to the eye) after switching on the 18V_{RMS} voltage. This assembly process occurs because the geometry of the electrodes gives rise to electric field gradients in the inter-electrode region. The sense of the gradient defines the sense of the dielectrophoretic force on the particles (48, 49). Specifically, the dielectrophoretic force on a dipolar particle is approximated as $\mathbf{F} = (\boldsymbol{\mu} \cdot \nabla) \mathbf{E}$, where $\boldsymbol{\mu}$ is the dipole moment of a particle, \mathbf{E} is the applied field at the particle's position; boldface type denotes a vector-quantity (48). Provided that this force can overcome Brownian motion and any inter-particle repulsion, particle-field interactions draw the particles to the field maximum, which is located at the tip of the alternating electrode. Polarizable particles grow strongly dipolar under the field, and the close proximity of neighboring particles induces spontaneous chaining of particles along the inter-electrode line of electric field maxima (50).

In Figure 2.19, two snapshots of the NK1-60 particles are shown - one in high pH solution (pH > pKa of the polymer) and the other in low pH solution (pH < pKa of the

polymer). In high pH solution, the microspheres exist in a dispersed state even when a voltage gradient is applied because of the negative charge on the surface of the particles, which can be attributed to deprotonation of methacrylic acid. This causes electrostatic repulsion to occur which prevents the particles from chaining. In the low pH solution, chaining occurs when the voltage gradient is applied because the particle surface is uncharged, which is a direct result of methacrylic acid being protonated.

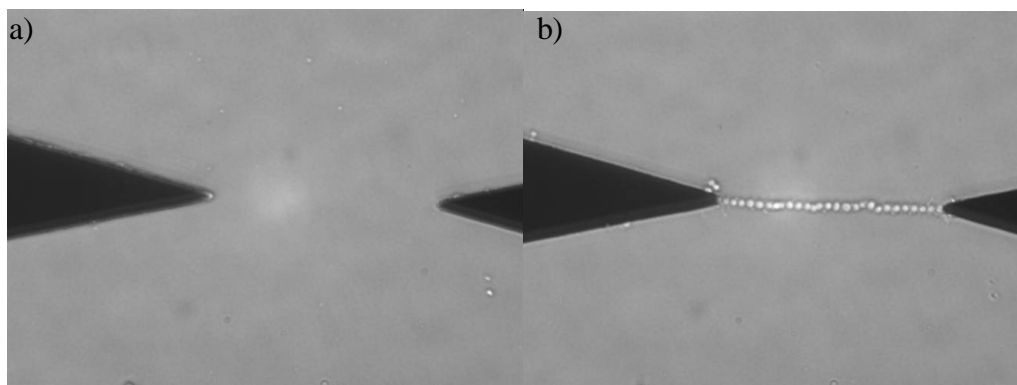


Figure 2.19: Behavior of NK 1-60 NIPA particles in the presence of the electrodes during application of the sinusoidal waveform voltage a) high pH solution and b) low pH solution

If the microscope slide were spotted with a low pH aqueous solution whose particle concentration is greater than 0.01% (w/w), the growth of several particle trees perpendicular to the tip of the electrode would occur, along with a multi-strand chain of particles between the electrodes (see Figure 2.18).

The dielectrophoretic experiment, which induces spontaneous chaining of the polymer microspheres, is sensitive to the surface charge of the polymer particles. By changing the frequency of the sinusoidal waveform used, polymer particles having a small surface charge can be chained. Because we can control the surface charge of the NK 1-60 particles by changing the pH of the solution in which they are dispersed, a small negative charge can be introduced onto the surface of these particles in a controlled

manner. This will allow us to explore the relationship between deprotonation of the methacrylic acid groups, which can be monitored using a dielectrophoretic cell, and the swelling of the polymer particles, which can be monitored as a function of pH using a hydrogel membrane.

The swelling of crosslinked cationic polymers, 0.200 μ m in diameter, was studied by A. Fernandez-Nieve and Vincent (11) who investigated polymer networks containing pH dependent ionizable groups. When charge was added to colloidal poly 2-vinylpyridine by adjusting the pH of the solvent, the microspheres remained in their collapsed state until the particle charge exceeded a critical value. In all likelihood, pH sensitive monomers located on the surface of the polymer were protonated first with the charge generated at these sites used to stabilize the polymer instead of initiating swelling in the solvent. Data from dielectrophoretic experiments involving NK 1-60 and related polymer particles could further elucidate the role of surface charge in polymer swelling and provide a better understanding of the shape of the pH profiles obtained in the experiments described in this thesis.

Chapter 3

Optical pH Sensing Using Colloidal Copolymers of N-Isopropylacrylamide

3.0 Introduction

pH sensing continues to be an active area of research. The determination of pH is one of the most important practical applications of direct potentiometry. Accurate and reliable pH measurements are crucial in a variety of applications. Both optical and electrochemical methods have been developed to measure pH.

Currently, there is interest in the development of polymer materials capable of responding to the physiologically relevant pHs between 5.0 and 7.4. The sharp coil-globule transition and phase separation of alkyl acrylamide polymers such as polyNIPA, which is triggered by temperature, can also be triggered by pH if NIPA is copolymerized with a pH sensitive monomer. Comonomers investigated as part of the research described in this thesis include acrylic acid, methacrylic acid, ethacrylic acid, propylacrylic acid, and vinyl benzyl chloride. The swelling and shrinking behavior of these NIPA copolymers in response to pH were studied as a function of the ionic strength and temperature of the solution in contact with the membrane, the percentage of crosslinker used to synthesize the polymer, and the amount, pKa, and hydrophobicity of the pH sensitive co-monomers in the polymer formulation.

Synthesizing polymer particles with reproducible swelling behavior from batch to batch is a challenging task when the polymer formulation consists of several monomers.

A variety of polymers can be prepared from the same monomer through variation in the relative amounts of each monomer. In the studies described in this chapter, judicious care was taken to control the composition of the polymer particles by fixing the reaction temperature and the total number of moles of each component used to ensure inter-batch compatibility. As a result, changes in the pH profile of the polymer particles and shifts in the inflection point of the pH response curves could be correlated to specific structural features of the polymer microspheres investigated.

3.1 pH Response Profiles

The response of the polymer particles to changes in the pH of the sample solution can be attributed to the volume phase transition. As the pH increases, the water content of the polymer particles increases through the deprotonation of the pH sensitive monomer, triggering the volume phase transition that is characterized by a decrease in the refractive index of the particles. Using absorbance spectrophotometry, a pH profile can be obtained by monitoring absorbance (turbidity) as a function of pH. Figure 3.0 shows a pH response profile of a NIPA co-polymer (70% NIPA, 10% MAA, 10% NTBA, and 10% MBA) functionalized using 10% methacrylic acid. At low pH (pH < 4.0), the polymer exists in a shrunken state. The turbidity measured by the spectrometer is large because the refractive index of the particles is higher than that of the PVA membrane. As the pH of the solution in contact with the membrane increases, the water content of the polymer also increases due to swelling induced by the deprotonation of methacrylic acid. The refractive index of the particles decreases as they swell and the refractive index value approaches that of the hydrogel membrane. The turbidity of the membrane continues to decrease as the water content of the polymer particles increases. Eventually, the

absorbance reaches a limiting value, which corresponds to complete deprotonation of methacrylic acid in the polymer.

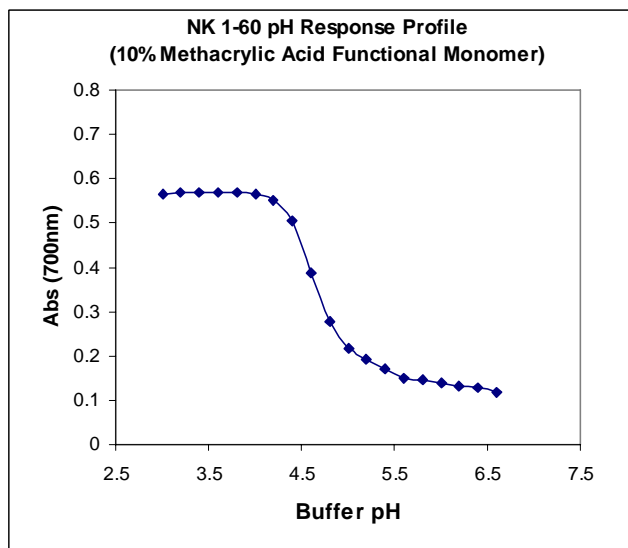


Figure 3.0: pH profile of NK 1-60 at 0.1M ionic strength.

The inflection point in the plot of absorbance (turbidity) versus pH is the apparent pKa of the polymer. At the inflection point, there are approximately equal amounts of protonated and deprotonated forms of the polymer. The term apparent pKa is used to refer to the point where the response is half-way between the response in excess base and excess acid because turbidity versus pH curves have not yet been described by theory in a manner that would allow us to know how to calculate the pKa from the observed data.

The degree to which the polymer swells can be correlated to the difference between the absorbance measured when methacrylic acid is fully protonated and when it is fully deprotonated. A larger change in turbidity between these two states corresponds to higher sensitivity of the proposed method for pH sensing. In addition to the total change in absorbance and the apparent pKa, the actual shape of the pH profile can also provide insight into swelling/shrinking behavior that is occurring. Using all three criteria,

a series of NIPA based polymers have been studied to assess their feasibility for physiological pH monitoring and to better understand the phenomenon of polymer swelling induced by a volume phase transition.

3.2 Kinetics of pH Response

For an analytical method to be both practical and amenable to automation, the response of the sensor to the physical or chemical changes being monitored must occur within a reasonable time frame. Therefore, the response kinetics of the NIPA-co-MAA polymer synthates were investigated to determine if the swelling response occurred fast enough to be a valid transduction mechanism for pH sensing. The Cary 6000i spectrometer, which was used to monitor turbidity changes, was fitted with a flow cell to allow for fresh sample solution presentation to the hydrogel membrane containing the NIPA particles. The flow was regulated with a peristaltic pump at a rate of 1.0 mL per minute. With continuous presentation of buffer, 90% of the pH response occurred within one minute. Therefore, a five-minute equilibration time was used in all pH sensor testing.

The rapid response of the membrane to the sample solution can be attributed to the porous nature of the immobilization membrane, the colloidal size and spherical shape of the NIPA particles, the presence of the pH sensitive comonomer at/near the particle's surface, and the thickness of the hydrogel membrane, which is approximately 127 μ m. Submicron sized gel particles will respond to external stimuli such as temperature or pH more quickly than bulk polymer films and as a result are more useful for chemical sensing.

3.3 Reversibility

Reversibility is important in chemical sensing. Materials that display reversible behavior in response to chemical stimuli have the advantage of being operational for long periods of time without the need for user intervention. Although one-time use materials such as test strips can also play a role in chemical analysis, they require the attention of a technician to run multiple samples or to perform routine analyses for an extended period of time.

Polymer swelling in pH sensitive copolymers of NIPA was investigated to assess whether the pH induced volume phase transition is reversible. For each polymer evaluated, the pH profile was collected in both ascending (pH = 3-7) and descending (pH = 7-3) order. Total swelling (difference between absorbance in the fully protonated and fully deprotonated states) was the same for both ascending and descending profiles. If the ascending and descending pH profiles were superimposable, the polymer was thought to display reversible swelling behavior. If the ascending and descending pH profiles were not superimposable, the polymer was thought to display nonreversible swelling behavior.

Figure 3.1 shows the ascending and descending pH profiles of two polymers. NK 1-60 (left) displays reversible swelling behavior, as its ascending and descending pH profiles are superimposable. NK-119 (right) does not display reversible swelling behavior, as its ascending and descending pH profiles are not superimposable. The difference in the swelling behavior can be attributed to the amount of methacrylic acid used in the polymer formulation and the ionic strength of the buffer solution in contact with the membrane. (This will be discussed at greater length in Sections 3.4 and 3.7 of

this chapter.) NK 1-60 contains 10% methacrylic acid and the ionic strength of the buffer solutions in contact with the membrane is 0.1M, whereas NK 1-119 contains 20% methacrylic acid and the ionic strength of the buffer solutions in contact with the membrane is 1.0 M.

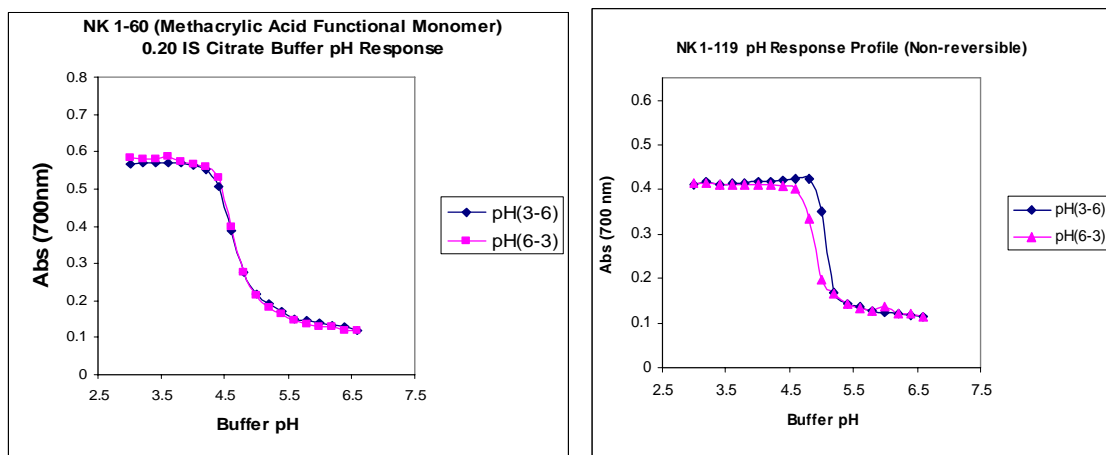


Figure 3.1: (Left) NK 1-60 (10%MAA) shows a reversible pH response in buffer solutions of 0.2M ionic strength. (Right) The pH response of NK 1-119 (20% MAA) is not fully reversible over the pH range investigated using 1.0M ionic strength buffers.

3.4 Ionic Strength Effects on Polymer Swelling

The Flory Huggins equation (see Chapter 1) describes polymer swelling in terms of ionic and nonionic contributions to this phenomenon. For ionic swelling, solution ionic strength is inversely proportional to the degree of swelling that occurs. This could be a major interferent for reliable sensing, as the sensitivity would be severely reduced in saline environments, such as the ocean or the human body. Since the pH sensitive copolymers of NIPA prepared by dispersion polymerization contain ionizable functional groups, the effect of solution ionic strength on their swelling was investigated.

pH response profiles of NIPA co-polymers were investigated in high and low ionic strength environments to better understand the implications of ionic strength on pH

sensing when swelling is used as the transduction mechanism. NK 1-28 (85%NIPA, 10%MAA, and 5%MBA) was selected for ionic strength testing because its pH profile was similar to the other pH sensitive NIPA based polymers that we prepared as part of this study. The polymer test segment was exposed to four citrate buffer systems of increasing ionic strength. Four pH profiles were collected at 0.05 M, 0.10 M, 0.50 M, and 1.0 M ionic strength over the pH range of 3.0 to 6.0 at 0.2 increments starting at pH = 3.0. Figure 3.2 shows the four pH profiles at the ionic strengths tested.

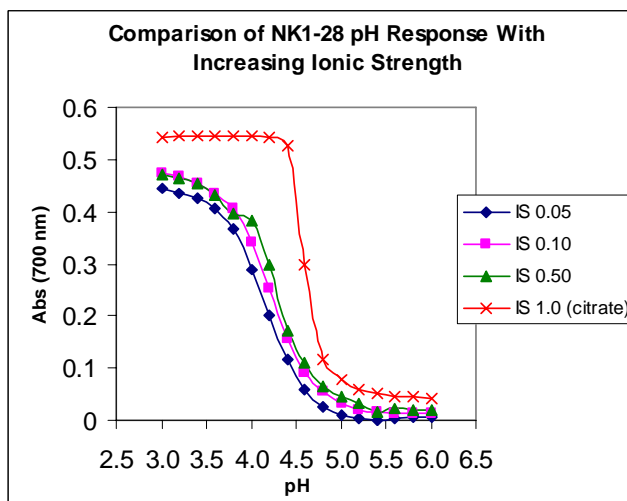


Figure 3.2: pH profiles of NK 1-28 at 0.05 M, 0.10 M, 0.50 M, and 1.0 M ionic strength.

For the pH profiles obtained at 0.05 M, 0.10 M, and 0.50 M ionic strength, there were no observable difference in the total swelling response, nor were there any significant differences in the overall shape or the inflection points of the pH profiles. Furthermore, the swelling behavior of the particles at 0.05 M, 0.10 M, and 0.50 M ionic strength was reversible. When the pH profile of NK1-28 was obtained at 1.0 M ionic strength, there was a significant change in its shape. Swelling occurred over a narrower pH range, and the apparent pKa of the polymer shifted to a higher value. Furthermore, the particles did not exhibit reversible swelling behavior, as the ascending and descending

pH profiles were not superimposable. However, the total swelling was the same. Similar results had been obtained with NK1-60 (see Figure 2.17) whose formulation differed from NK1-28 in the amount of crosslinker and NTBA used.

Polymer swelling usually does not occur in high ionic strength buffer solutions. This anomaly can be explained using the Flory-Huggins equation (see equation 3-1) where q_m is the swelling ratio, V_o is the volume of the unswollen polymer, v_e is the effective number of unit segments in the polymer network, i/V_u is the charge per network segment, S^* is the ionic strength, X_1 is the polymer-solvent interaction parameter, and v_1 is the molar volume of the polymer. According to the Flory Huggins equation, swelling has an ionic contribution and a nonionic contribution, which are separated by the addition operator. If the charge per polymer unit segment (i/V_u) is small, which we believe to be the case since the amount of MAA used to prepare the polymer particles is small, ionic swelling will not play a significant role. Under these circumstances, the observed swelling in the polymer particles (at least to a first approximation) is nonionic in nature and is therefore independent of the ionic strength of the buffer solution in contact with the membrane. For acrylamide gels, the polymer solvent interaction parameter is the central variable governing the thermodynamics of swelling.

$$q_m^{5/3} = \left(\frac{V_o}{v_e} \right) \left[\left(\frac{1}{4} \right) \left(\frac{i}{V_u} \right)^2 \left(\frac{1}{S^*} \right) + \frac{\left(\frac{1}{2} - X_1 \right)}{v_1} \right] \quad (3-1)$$

The change in the shape of the pH profile at 1.0 M ionic strength can be attributed to an osmotic pressure effect. When the charge density of a polymer is lower than that of the sample solution, water from the polymer will enter the sample solution to equalize the charge density in the two phases. The hydrated state of the polymer becomes destabilized, and the particles shrink. Methacrylic acid, which is the source of charge on the polymer, is distributed over a smaller chain length as the linear polymer chains undergo a conformational change from expanded coils to more compact ones. This causes an increase in the charge per polymer network segment term in the Flory-Huggins equation. The increase in the charge density of the polymer would explain the increase in the apparent pKa of the polymer particles, the irreversible swelling behavior of the particles, and why swelling occurs over a narrower pH range. This behavior cannot be attributed to suppression of the electrical double layer around the polymer chains in view of the similarities between the pH profiles obtained for NK 1-28 in 0.05, 0.10, and 0.50 M ionic strength buffer solutions.

The pH sensitive NIPA-co-MAA particles prepared in our laboratory may find application in a variety of environments since ionic strength does not affect their total swelling. However, the overall shape of the pH profile can be affected by ionic strength, since swelling occurs over a narrower pH region in very high ionic strength buffers. For this reason, the pH profile of NIPA-co-MAA polymer microspheres should be fully characterized using standards comparable to the samples being analyzed, as the ionic strength of the sample solution can alter the sensitivity of the swelling response in some cases, e.g., extremely high ionic strength solutions.

3.5 pH Profiles at Elevated Temperatures

The pH response of polyNIPA-MAA as a function of temperature was also investigated. Having the capability to measure pH at physiological temperatures (ca. 37⁰C) is crucial in many sensing applications, for example, gastric pH sensing or monitoring the progress of open-heart surgery where pH serves as a measure of tissue ischemia. If we are to use polyNIPA-MAA or other pH sensitive copolymers of NIPA in biomedical sensing applications, then understanding the effects of temperature on the pH response of the polyNIPA-MAA particles is important.

pH response profiles at physiological temperature were obtained in the same manner as ambient profiles. The temperature of the cell sample holder was controlled by a dedicated temperature control unit, with the temperature of the solution in the sample cell monitored by a probe to ensure reproducible thermal equilibration and accurate reporting of temperature. For each data point in Figure 3.3, the membrane was rinsed three times with buffer solution and allowed to equilibrate for 15 minutes prior to analysis by UV-Vis absorbance spectroscopy. Absorbance (turbidity) values, which were collected at 700 nm, were plotted against solution pH (see Figure 3.3) for NK 1-60 at 35⁰ C. Polymer swelling appeared to be reversible because the ascending and descending pH profiles shown in Figure 3.3 are superimposable.

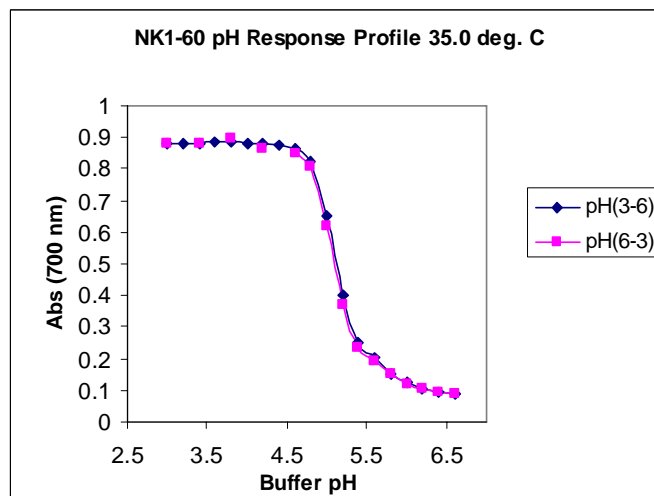


Figure 3.3: Ascending and descending pH profiles for NK 1-60 at 35° C.

In Figure 3.4, pH profiles at ambient temperature (23° C) and at 35° C for NK-60 are shown. Although higher temperature does not have a significant effect on the total swelling, there is an increase in the value of the apparent pKa of the polymer, and swelling occurs over a narrower pH range. At 35° C, the polymer solvent interaction parameter, which is a temperature dependent quantity, increases in value and the polymer particles in turn shrink in size. Methacrylic acid, which is the source of charge on the polymer, is being distributed over a smaller chain length as the temperature increases. The effect of temperature on the pH profile is similar to that of ionic strength (e.g., 1.0 M buffer solutions in contact with the polymer particles).

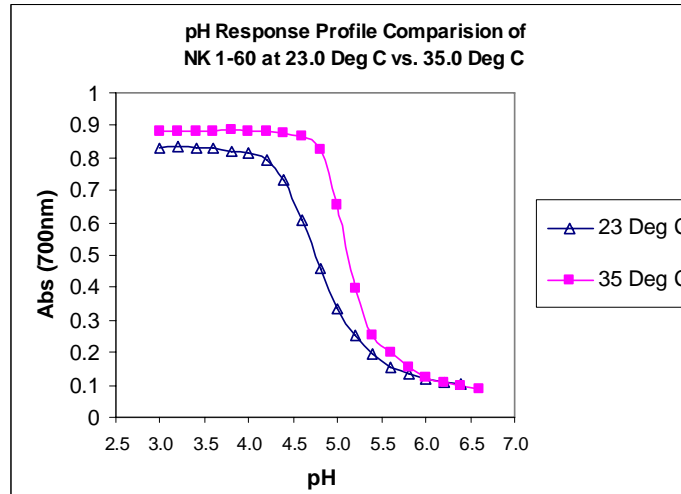


Figure 3.4: pH response profile comparison for NK 1-60 at 35° C and 23° C (room temperature.)

3.6 Effects of Crosslinking on Polymer Swelling

The effect of the crosslinker on the swelling properties of the polymer synthates was also investigated. Polymer microspheres were prepared with increasing amounts of crosslinker (5%, 10%, and 15%). Table 3.0 lists the composition of the formulation used to prepare these polymer particles. Although NK 1-143 has NTBA in its formulation whereas the other two polymers do not contain this compound, our experience has shown that pH induced swelling will not be affected by NTBA when it is present in small amounts (10% or less) in the formulation. (See Appendix III for further details).

Table 3.0: Polymer Composition-Variied % Crosslinking.

Component	NK 1-28	NK 1-18	NK 1-143	Function
% NIPA	85%	80%	65%	Monomer (1)
%MAA	10%	10%	10%	Monomer (2)
%NTBA	0%	0%	10%	Monomer (3)
%MBA	5%	10%	15%	Crosslinker

SEM photos were taken to characterize the particle morphology with respect to increasing amounts of crosslinking of the polymer chains. Figure 3.5 shows the SEM

images of NK 1-28, NK 1-18, and NK 1-143. The SEM images reveal that particle shape improves with increased crosslinking. NK 1-28 was prepared with 5% crosslinking; particle definition is poor and the material appears to be amorphous. Increasing the level of crosslinking to 10% resulted in improved particle definition, but the particles appear to exist as aggregates rather than monodispersed particles. With 15% crosslinking, the polymer can be characterized as monodispersed spherical particles whose diameter is less than 1 μm .

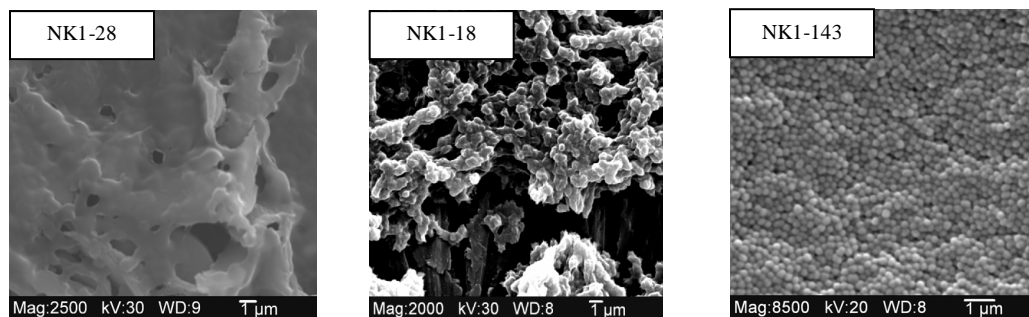


Figure 3.5: SEM images for characterization of particle morphology with increasing levels of crosslinking: NK1-28 5%XL, NK 1-18 10%XL, and NK1-143 15%XL

pH profiles were obtained for each polymer over the pH range of 3.0 to 6.4 in 0.2 pH increments at 25° C with five minutes for equilibration between each run of low ionic strength (0.20) buffer. The cuvet was rinsed three times with the next buffer in the series prior to the timed measurement to ensure that cross contamination between buffer solutions was minimized. Both ascending and descending profiles were obtained to determine the reversibility of swelling for the three polymers investigated. Figure 3.6 shows a comparison of the pH response profiles for polymers containing 5%, 10%, and 15% crosslinking.

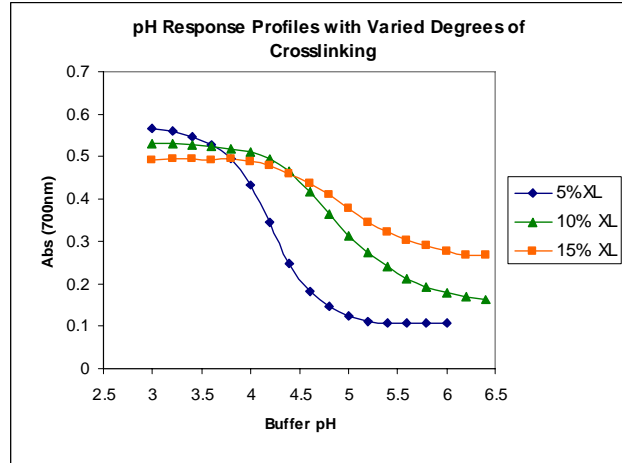


Figure 3.6: pH response profiles at 5%, 10%, and 15% crosslinking.

Increasing the level of crosslinking in NIPA-co-MAA particles resulted in a decrease in polymer swelling. The decrease in swelling with increased crosslinking can be attributed to increased structural rigidity, as the additional three-dimensional associations within the polymer physically resist swelling. This observation is supported by a study from Inomata (48). From the Flory Huggins Equation, higher crosslinking corresponds to a higher value of v_e , which is the effective number of chains in the polymer network. Since v_e is inversely proportional to swelling, higher levels of crosslinking should reduce total swelling. However, the use of low levels of crosslinking (5% or less) is not desirable, as the polymer is amorphous. This prevents it from being reproducibly dispersed in the hydrogel. Although higher levels of crosslinking favor the formation of uniform, monodispersed particles thereby yielding reproducible membrane dispersions, 15% crosslinking has the drawback that total swelling is suppressed limiting sensitivity. 10% crosslinking is a good compromise, as the magnitude of the pH response profile is indicative of high sensitivity, and particle morphology is suitable for reproducible membrane dispersions.

3.7 Methacrylic Acid Composition

The functional (pH sensitive) comonomer plays a crucial role in defining the response characteristics of the polymer particles. Acrylates are generally used as comonomers because of their compatibility with NIPA. They have a terminal carboxylic acid that contributes to polymer swelling when deprotonated. However, little work has been done to better understand how the increase in the percentage of functional comonomer in the formulation influences the overall response of the polymer.

To determine the optimal amount of functional comonomer, the pH response was determined for a series of NIPA-MAA copolymers that were prepared with increasing MAA content. The composition of these NIPA-MAA copolymer particles can be found in Table 3.1. SEM snapshots of these NIPA-MAA copolymer particles are shown in Figure 3.7. Each colloidal polymer is monodispersed. The particles are spherical in shape with a diameter less than 1.0 μm (dry). The pH profile of each polymer was obtained using the procedure described in Chapter 2. In Figure 3.8, the pH profile of each polymer is shown. The 5%, 10%, 15%, and 20% polyNIPA-MAA particles exhibited reversible swelling, as the ascending and descending pH profiles were superimposable in the 0.1 M ionic strength buffer, whereas the 25% polyNIPA-MAA particles exhibited irreversible swelling when using the same buffer solutions.

Table 3.1: Polymer Composition – Increasing %MAA Content

Component	NK 1-127	NK 1-119	NK 1-124	NK 1-60	NK 1-64	Function
% NIPA	55%	60%	65%	70%	75%	Monomer (1)
%MAA	25%	20%	15%	10%	5%	Monomer (2)
%NTBA	10%	10%	10%	10%	10%	Monomer (3)
%MBA	10%	10%	10%	10%	10%	Crosslinker

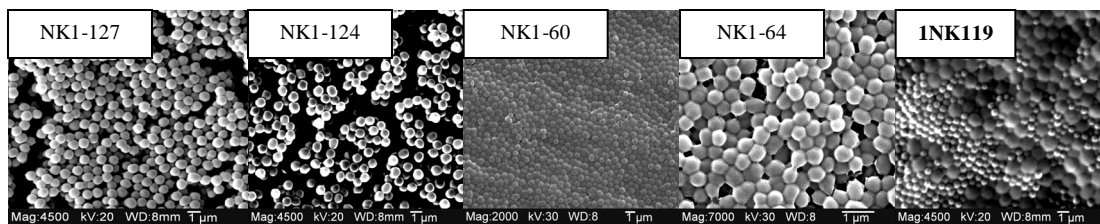


Figure 3.7: SEM snapshots of polymers with decreasing MAA content. (a) NK 1-127 25% MAA, (b) NK 1-119 20% MAA, (c) NK 1-124 15% MAA, (d) NK 1-60 10% MAA, (e) NK 1-64 5% MAA

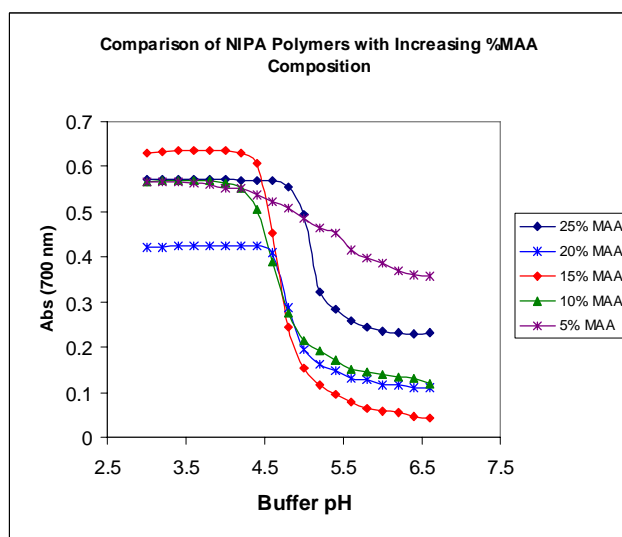


Figure 3.8: pH response profiles of polymers prepared with increasing amounts of MAA. The pH profile of each polymer was fitted to the Henderson-Hasselbalch (HH) equation.

Figure 3.9 shows a plot of the fractional concentration of the protonated and unprotonated form of each polymer as a function of pH at 700 nm. Equations 3-2 and 3-3 were used to compute the percentage of both the deprotonated and protonated forms of the polymer from the turbidity spectra (data points) where A^- is the deprotonated form of the polymer, Abs_{pH} is the absorbance (turbidity) of the membrane at a particular pH, Abs_{min} is the absorbance for the swollen form of the polymer, Abs_{max} is the absorbance for the unswollen form of the polymer, %HA is the percentage of the protonated form of the polymer, and % A^- is the percentage of the unprotonated form of the polymer. The

values from the Henderson Hasselbalch equation (solid line) were plotted in the same figure as the experimental data using the apparent pKa from the pH profile in the calculations. Polymer swelling for 5% MAA was adequately modeled using the Henderson-Hasselbalch equation. However, NIPA copolymers consisting of 10%, 15%, and 25% MAA did not obey the Henderson Hasselbalch equation. They exhibited a larger response over a narrower pH range. This behavior, which can be advantageous in monitoring situations, is due to the complex relationship between swelling and the charge on the polymer.

$$\% A^{-} = 100 \frac{(Abs_{pH} - Abs_{min})}{(Abs_{max} - Abs_{min})} \quad (3-2)$$

$$\% HA = 100 - \% A^{-} \quad (3-3)$$

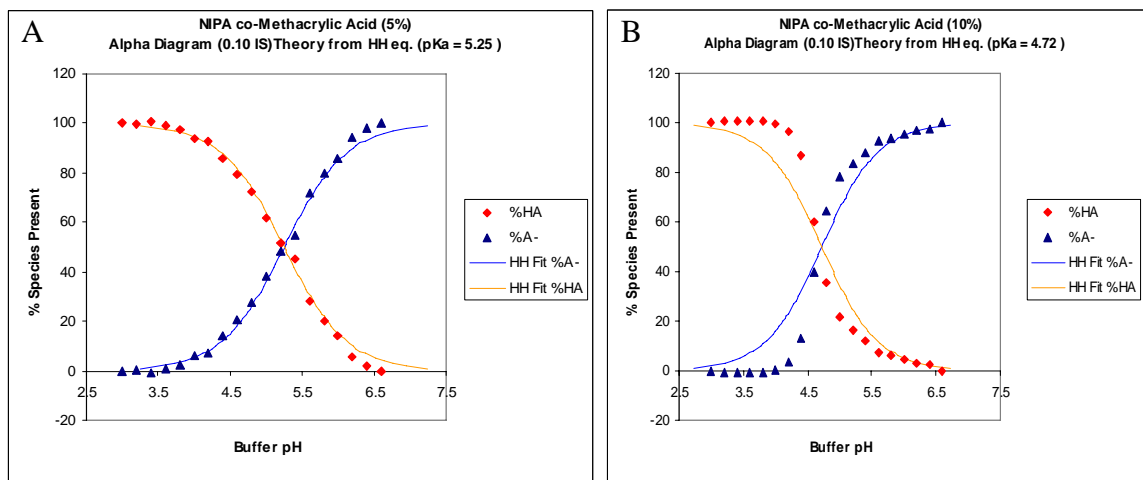


Figure 3.9: a) 5% MAA content, b) 10% MAA content, c) 15% MAA content, and d) 25% MAA content. (Continued on the following page.)

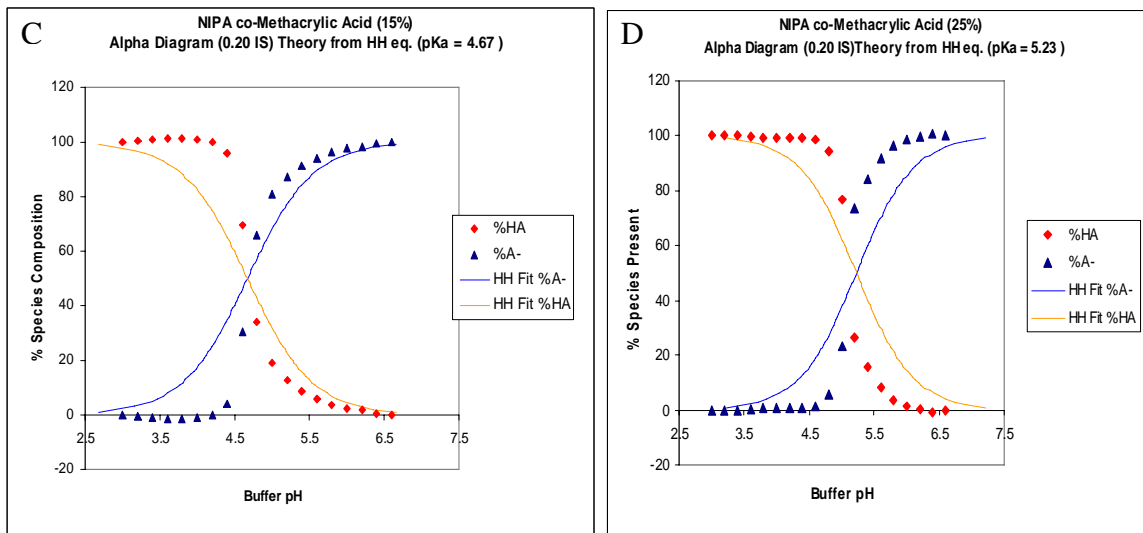


Figure 3.9: a) 5% MAA content, b) 10% MAA content, c) 15% MAA content, and d) 25% MAA content.

The change in swelling from reversible (10% and 15% MAA) to irreversible (25% MAA) and the shift in the apparent pKa of the polymer (see Figure 3.8) from 4.7 for 10% and 15% MAA (which corresponds to the pKa of the MAA monomer) to 5.1 for 25% MAA can be attributed to an increase in the charge density of the polymer. As for the total absorbance change (see Figure 3.10), the reduction in total swelling from 15% MAA to 25% MAA can be explained by charge screening which could be occurring on the polymer backbone. When the fraction of MAA molecules exceeds some threshold, counterions will condense on the polymer backbone, screening the free charges and effectively reducing the osmotic pressure. The role of ionic swelling in NK 1-127 could be significant due to the higher charge density of the polymer. This could explain the irreversible swelling behavior exhibited by NK 1-127.

The largest total absorbance change in the polymer series investigated occurs with 15% MAA. If only 5% MAA is used, the total absorbance (turbidity) change would be too small. By increasing the percent composition of MAA to 10% or 15%, there is a

dramatic increase in total swelling. However, a further increase in the amount of MAA copolymerized with NIPA could result in a reduction in swelling. Therefore, the optimum MAA composition probably lies between 10% and 15% MAA. For our studies, polymer particles with 10% MAA were used even though particles with 15% MAA exhibited more swelling because of the monodispersity and higher yields obtained for the 10% MAA particles.

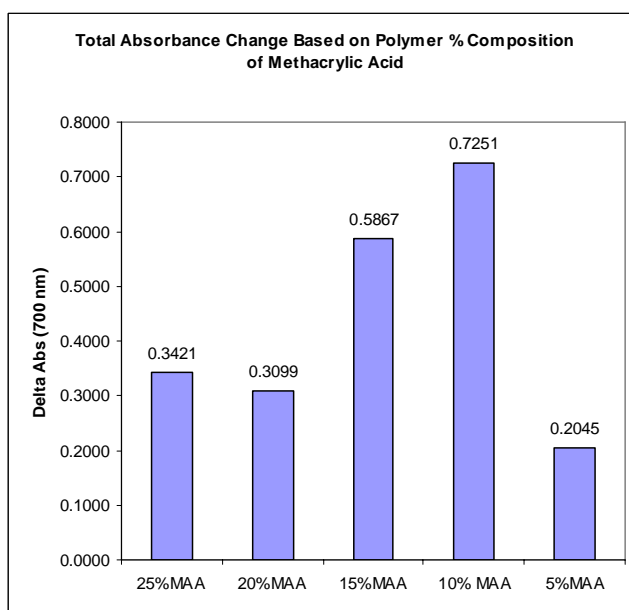


Figure 3.10: Comparison of Total Absorbance Change Based on Percentage of MAA.

3.8 Increasing Alkyl Chain Length of Functional Comonomer

The pH sensitive comonomer, although only a small fraction of the total formulation, imparts properties to the entire polymer. Comonomers with carboxylic acids, amines, amides, and phosphates have been investigated. Functional comonomers that are most often reported in the literature are from the acrylate family, wherein a terminal carboxylic acid is deprotonated as the pH increases. A series of closely related acrylates was investigated to determine if incorporating functional monomers with

increasing pKa values would translate into higher pKa values for the polymer synthates. Acrylates were selected because MAA is the functional comonomer incorporated into the majority of the polymers synthates investigated in the research described in this thesis. The acrylates under investigation were acrylic acid, methacrylic acid, ethacrylic acid, and propacrylic acid.

With the percent composition of functional monomer for each polymer batch fixed at 10%, a series of NIPA co-polymer particles were prepared for pH characterization. Table 3.2 is a summary of the composition of each polymer in the study, as well as its apparent pKa, total absorbance change at 700 nm, and the particle size based on SEM. Figure 3.11 shows SEM snapshots of each NIPA based polymer. Monodispersed spherical particles were generated in each synthesis. Each colloidal polymer was comprised of particles less than 1.0 μm in diameter. There was no relationship between particle diameter and the functional monomer side chain length.

pH profiles were obtained using the procedure discussed in Chapter 2. A comparison between the apparent pKa values of the polymers is shown in Figure 3.12. The acrylic acid functionalized particles have the lowest pKa of the polymers in this series and a shift in pKa of 1.5 units is observed over this functional monomer series. The increase in the apparent pKa of the polymer particles can be correlated to an increase in the alkyl side chain length and to the pKa of the free monomer (see Table 3.3). The pKa of acrylic and methacrylic acids were obtained from the literature whereas the pKa of EAA and PAA were determined by titration of the monomer with standardized NaOH. For acrylic and methacrylic acid, the apparent pKa of the polymer lies in close agreement

with the pKa of the corresponding free monomer. As for EAA and PAA, the apparent pKa of the polymer is larger than the pKa of the corresponding free monomer.

Table 3.2: Polymer Composition – Increased Fun. Monomer Hydrophobicity

Component	NK 1-156	NK 1-60	NK 1-146	NK 1-155
% NIPA	70%	70%	70%	70%
10% Comonomer	Acrylic	Methacrylic	Ethacrylic	Propacrylic
%NTBA	10%	10%	10%	10%
%MBA	10%	10%	10%	10%
Polymerization	photo	photo	photo	photo
Buffer System	0.20 IS Citrate	0.20 IS Citrate	0.20 IS Citrate	0.20 IS Citrate (3-7) Phosphate (7.2-8.0)
Apparent pKa	4.37	4.7	5.39	6.07
Total Abs Δ	0.328	0.4472	0.3661	0.3044
Particle Diameter	~350nm	~500nm	~850nm	~500nm

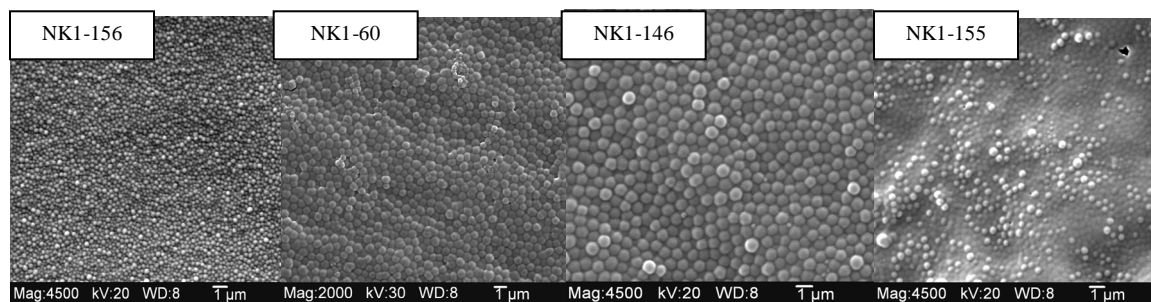


Figure 3.11: (a) NK 1-156 Acrylic Acid, (b) NK 1-60 Methacrylic Acid, (c) NK 1-146 Ethacrylic Acid, (d) NK 1-155 Propacrylic Acid.

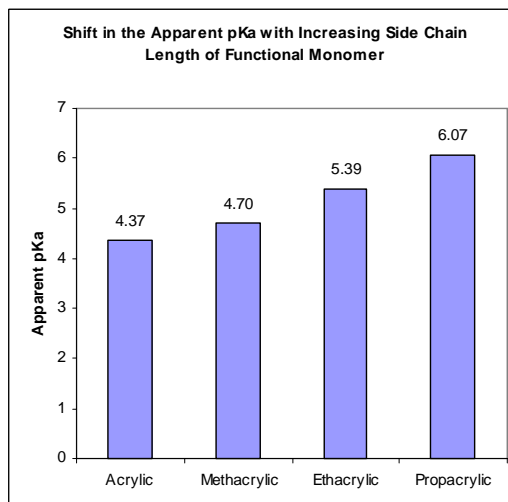


Figure 3.12: Comparison of the apparent pKa values of NIPA co-polymers with functional monomers of increasing side chain length.

Table 3.3: pKa Values in Free Solution and for Polymerized Acrylic Acids

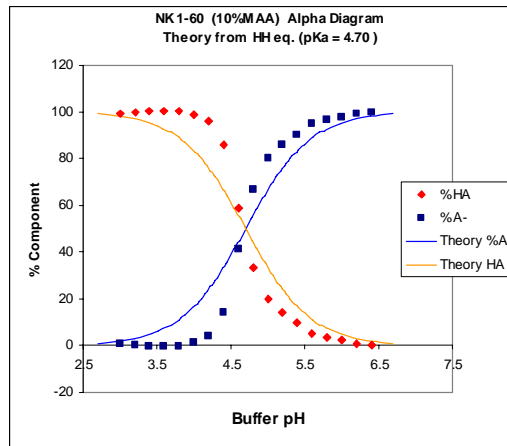
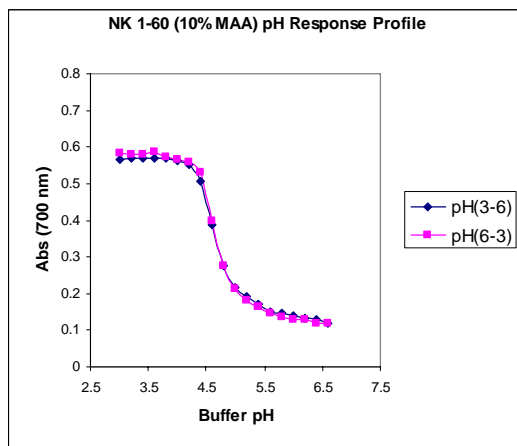
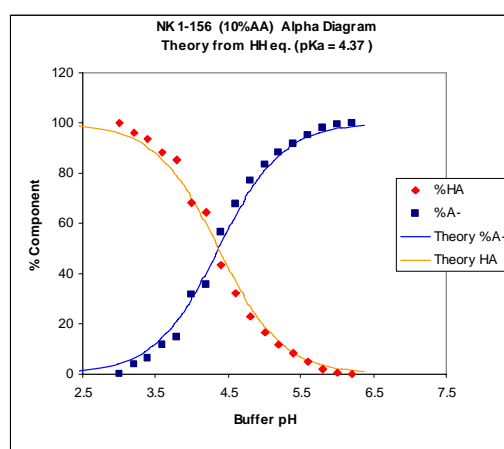
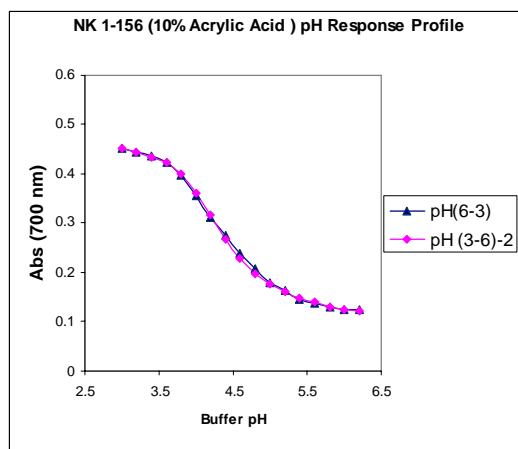
pKa Values	Acrylic Acid (AA)	Methacrylic Acid (MAA)	Ethacrylic Acid (EAA)	Propacrylic Acid (PAA)
# of Carbons in Side Chain	0	1	2	3
Free Solution	4.25*	4.65*	4.65**	4.84**
NIPA-co polymer (10%)	4.37	4.70	5.39	6.07

* Values obtained from the literature (see reference 49)

**Values determined by titration of monomer with NaOH, which was standardized using KHP.

The pH profile of each polymer synthate was fitted to the Henderson Hasselbalch equation in an effort to provide insight into the nature of the acid-base equilibrium of carboxylic acid groups in the particles as compared to their equilibrium in solution. Figure 3.13 shows ascending and descending pH profiles and the Henderson Hasselbalch fit of the titration data obtained for copolymers of NIPA containing 10% AA, MAA, EAA, and PAA. The titration data obtained for the NIPA-acrylic acid particles was well modeled by the Henderson Hasselbalch equation, and polymer swelling was reversible. For the colloidal polymers functionalized with MAA or EAA, polymer swelling was reversible but the particles showed a larger response over a narrower pH range than

predicted by the Henderson Hasselbalch equation. The incorporation of EAA into the NIPA polymer shifted the apparent pKa by nearly 0.5 units, but it did not affect the reversibility of the pH response. Although, incorporation of PAA into the NIPA polymer resulted in a further shift of the apparent pKa to 6.07, the pH response was not reversible as evidenced by the hysteresis observed in the ascending and descending pH response profiles. The irreversible swelling behavior exhibited by this polymer is a significant drawback, as difficulties will arise in obtaining reproducible and accurate measurements when using this material as the basis of a method for pH sensing.



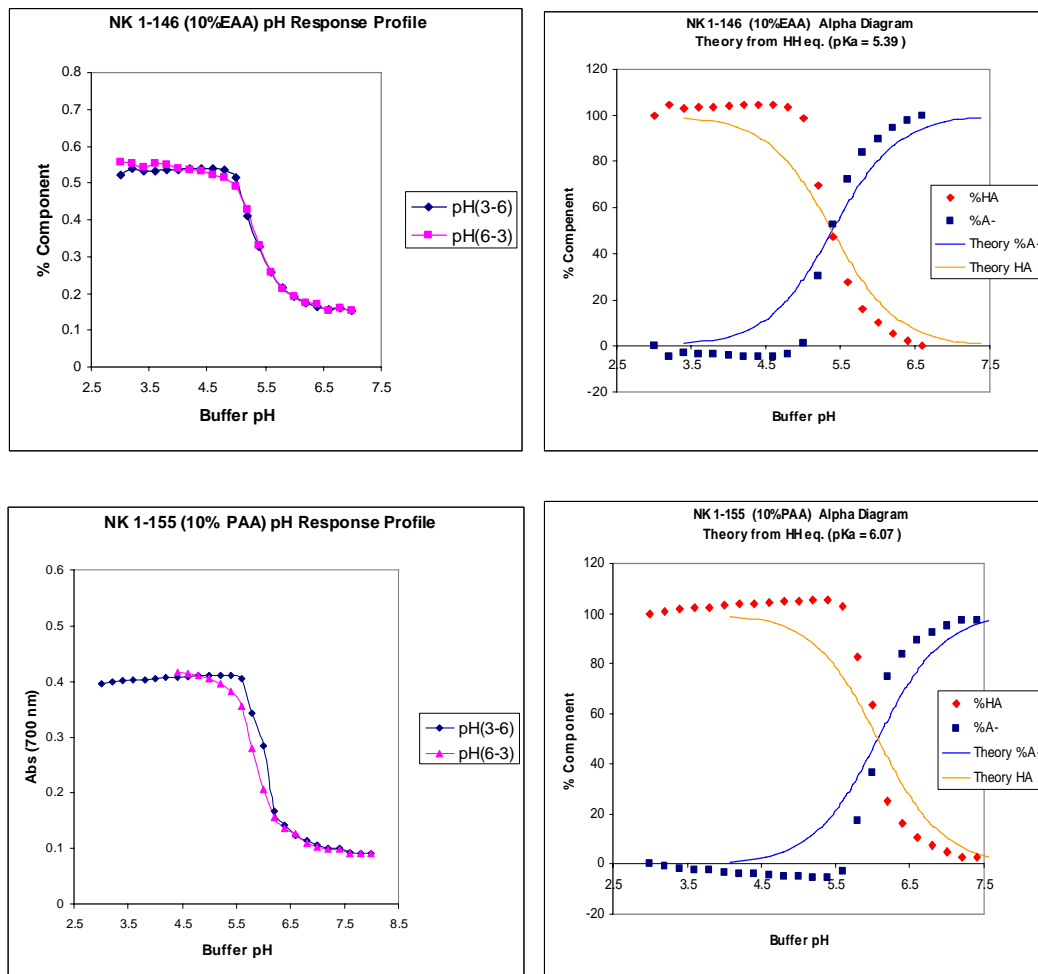


Figure 3.13: Ascending and descending pH response profiles and HH fit plots for functional monomer acids: (1st row) Acrylic, (2nd row) Methacrylic, (3rd row) Ethylacrylic, (4th row) Propacrylic.

3.9 Basic Functional Monomers

The polymerization of a basic comonomer with NIPA was also investigated as a potential route to prepare a pH sensitive polymer with an apparent pKa of 7.0. Comonomers that were investigated included 2-dimethylamino-ethyl-methacrylate, vinyl-imidazole, and vinyl-pyridine. Efforts were made to copolymerize each monomer in various formulations with the other co-monomers (NIPA, MBA, NTBA, etc.). Unfortunately, the polymer synthates that we prepared failed to respond to pH. This may have been due to the basic moiety of the comonomer losing its functionality due to the

manner in which it was incorporated in the polymer. For this reason, the co-monomer vinyl benzyl chloride was copolymerized with NIPA at 70⁰ C then derivatized with diethylamine to yield the corresponding amine. In this reaction diethylamine displaces the chloride from the chloromethyl group producing a tertiary amine. The derivatization reaction was carried out at room temperature for 3-4 days. SEM snapshots (see Figure 3.14) reveal that most of the polymer exists as an amorphous film.

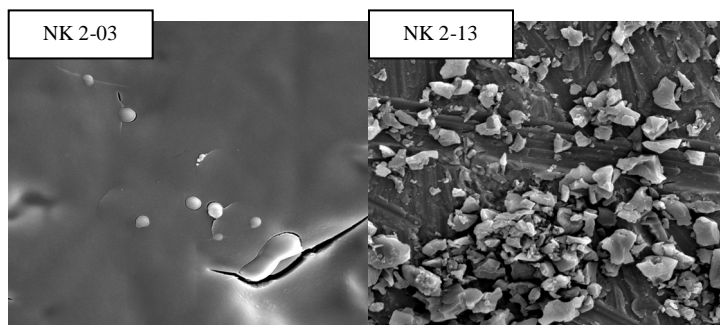


Figure 3.14: SEM photos of the NK 2-03 (VBC functionalization) and NK 2-13 (post-synthetic modification of NK 2-03 to a dimethyl amine functionality (DMA))

The pH response curve of the basic-functionalized polymer is similar to the curves obtained for the acrylate polymers discussed in the previous section. The polymer chunks which are embedded in a hydrogel membrane also swell and shrink in response to changes in pH and temperature. Unlike the acid-functionalized particles, the swelling/shrinking cycle is opposite to what has been previously discussed. At low pH (e.g., pH = 6.0) the polymer exists in the swollen state because the amine, which is fully protonated, has a net positive charge. When the pH is increased to a sufficiently high value (e.g., pH = 11), the polymer shrinks, as the amine is deprotonated with the net positive charge on the amine disappearing. An example of a pH response profile for a

polymer with the dimethyl amine functionality is shown in Figure 3.15. As the pH of the buffer solution is increased, the amine is deprotonated and the polymer shrinks.

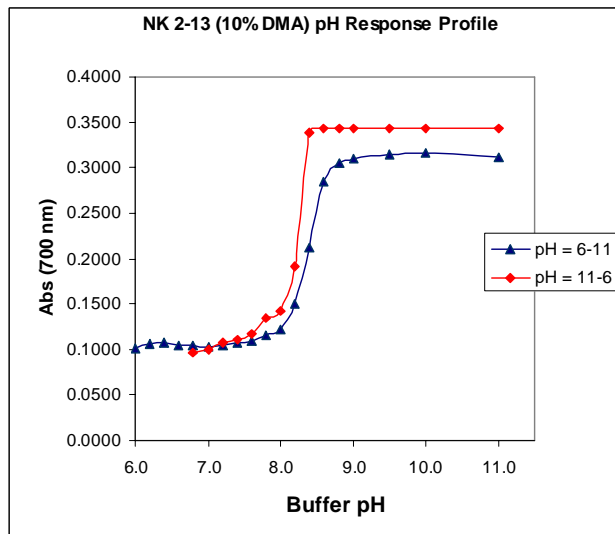


Figure 3.15: NK 2-13 pH response profile in low ionic strength phosphate buffer. Note the hysteresis with the ascending and descending pH response profiles.

The apparent pK_a of NK 2-13 is 8.4, which is outside of the physiological pH range of 5.0-7.4. However, this pK_a is consistent with what one would expect for an amine. Ascending and descending pH profiles were measured to determine if the pH response was reversible. Significant hysteresis is observed, which would preclude the use of this material in the proposed sensing applications. A comparison of the pH response profile of the original polymer, which was functionalized using vinyl benzyl chloride, (NK 2-03) to the derivatized VBC polymer which contains a dimethyl amine functionality (NK 2-13), shows that NK 2-03 does not respond to pH over the range investigated (pH = 6-10). The pH response of the control is consistent with the explanation that deprotonation of dimethylamine is responsible for the shrinking of NK 2-13 as it allows for the expulsion of water and the collapse of the polymer chains.

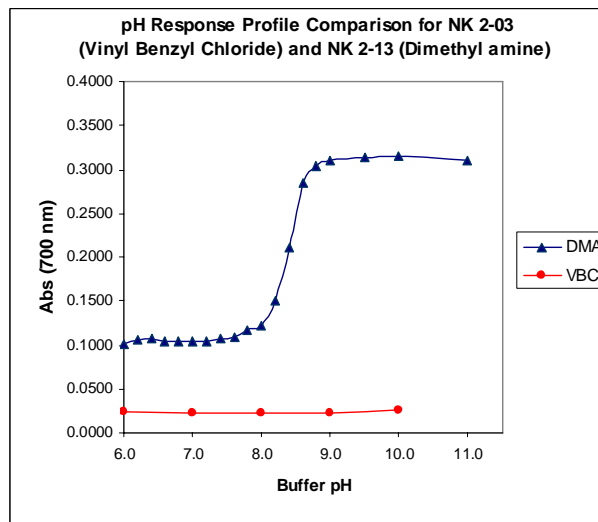


Figure 3.16. Comparison of NK 2-03 to NK 2-13 for pH sensing

3.10 Conclusions

Increasing the pKa of the polymer by increasing the pKa of the functional comonomer is a valid approach for developing pH sensitive polymers that respond in the physiological pH range 5.0 to 7.4. The pH response of the acrylate copolymers investigated in this study was usually reversible and as a rule was independent of the ionic strength of the buffer solutions used for the evaluation. Of the acrylate monomers investigated, polymers prepared from ethylacrylic acid and propylacrylic acid have pKa values that fall within the desired pH range. The pH profile of the polymer prepared from ethylacrylic acid did not exhibit hysteresis, which was not the case for the polymer prepared from propylacrylic acid. It may be possible to obtain a reversible pH response with polyNIPA-PAA if the amount of propylacrylic acid in the formulation is decreased. Alternatively, using a different pH sensitive comonomer with a pKa closer to 7.0 could prove to be beneficial. Small shifts in pKa within the physiological relevant interval could then be achieved by adjusting the amount of crosslinker or pH sensitive

comonomer in the polymer formulation. This would allow for fine-tuning within the desired pH range. However, copolymerizing NIPA with a basic comonomer was not successful as it yielded a polymer with a pH response that was not reversible. Furthermore, the overall swelling was substantially less than what had been observed with the other NIPA based polymers.

Chapter 4

Adsorption of Metal Ions by PolyNIPA Hydrogels

4.0 Introduction

Polymers prepared from N-isopropylacrylamide (NIPA) have received considerable attention in the scientific literature because of the large volume change, which these materials undergo in response to an external stimulus such as temperature or pH (52). PolyNIPA undergoes a transition from a swollen state to a shrunken state at 35⁰C. For this reason, polymers prepared from NIPA have been applied in thermo-sensitive drug delivery systems and separation processes. The reversible volume phase transition that NIPA based gels undergo also makes them an attractive material for removal of pollutants from the environment (53, 54).

Recently, polymers prepared from NIPA have been investigated as potential adsorbents for removal of metal ions in wastewater (55). However, little is known about the adsorption of metal ions by these polymers (56). Therefore, polymers and copolymers of NIPA were immobilized in a hydrogel membrane to study noncompetitive metal ion binding. We were particularly interested in studying the effects of metal ion binding on the swelling and shrinking behavior of NIPA and copolymers of NIPA. For this reason, the polymers, NK 1-135 (70% NIPA, 10%MAA, 10%NTBA, 10% MBA) and NK 1-161 (80% NIPA, 10%NTBA, and 10% MBA), were selected to investigate the metal ion binding properties of NIPA based polymers. NK 1-135 was prepared at the same

temperature and from the same formulation as NK 1-60, which is our prototype pH sensitive polymer. The entrapment of crown ethers (57, 58) in NK 1-135 as a means of integrating metal ion selectivity into the swelling response was also investigated as part of the research described in this thesis.

4.1 Materials

The pH response of NK 1-135, which was used as an adsorbent, has been characterized (see Figures 4.1). Metal ion stock solutions (10^{-1} M) were prepared by dissolving the appropriate amount of metal salt into DI water. Standards were prepared by serial dilution using distilled water. The concentration range investigated was 1.0×10^{-1} M to 1.0×10^{-7} M. The degree of hydration and the anion of the salt were taken into account when calculating the amount of salt required to prepare each solution. Metal ion salts were selected to ensure that counter ions present would not alter the solution pH, and not form precipitates or secondary complexes in the solution. Table 4.0 lists details about the preparation of each stock solution.

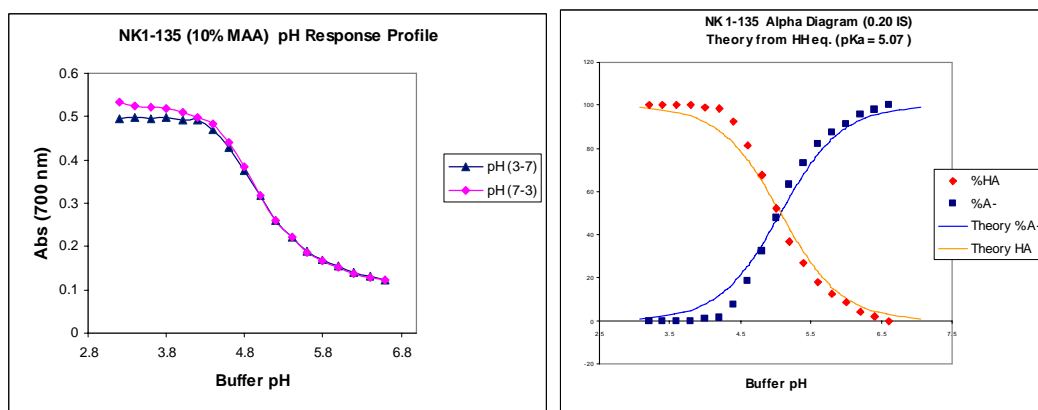


Figure 4.1: (left) NK 1-135 pH response profile and (right) fitting of the Henderson-Hasselbalch equation to the NK 1-135 pH response profiles.

Table 4.0: Preparation of Metal Stock Solutions in DI Water

Ion Name	Ion Symbol	Compound	Mass (g)	Volume (mL)
Cadmium (II)	Cd ²⁺	Cd(NO ₃) ₂ * 4H ₂ O	0.7710	25
Calcium	Ca ²⁺	CaCl ₂	1.1573	100
Cesium	Cs ⁺	CsNO ₃	0.9718	50
Copper (II)	Cu ²⁺	CuSO ₄ * 5H ₂ O	1.2446	50
Iron (II)	Fe ²⁺	FeSO ₄ * 7H ₂ O	1.3901	50
Lead (II)	Pb ²⁺	Pb(NO ₃) ₂	3.3120	100
Lithium	Li ⁺	LiCl	0.4223	100
Potassium	K ⁺	KCl	0.7456	100
Sodium	Na ⁺	NaCl	0.5844	100

NK 1-135 polymer particles were selected for functionalization using crown ethers in an effort to impart metal ion selectivity. The ability of NK 1-135 to shrink in acidic conditions and swell in alkaline conditions allows one to entrap crown ethers within the polymer. The crown ethers were selected based on ring coordination diameter, binding affinity, and availability. The crown ethers investigated were dibenzo18crown6 and dibenzo15crown5. Dibenzo18crown6 was selected to impart selectivity for K⁺ over other alkaline metal ions (59), whereas dibenzo15crown5 was chosen to impart lead (II) ion selectivity (60). Both compounds (i.e., crown ethers) were purchased from Aldrich and were used as received. The structures of dibenzo18crown6 and dibenzo15crown5 are shown in Figure 4.2.

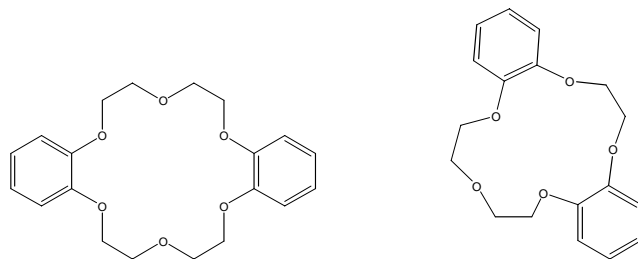


Figure 4.2: The two crown ethers used to functionalize the polyNIPA-MAA particles. (left) Dibenzo 15crown5, (right) Dibenzo 18crown6

The turbidimetry analysis was conducted via UV-Visible absorbance spectroscopy at 500 nm. To ensure that each polymer test strip began each experiment under the same conditions, it was necessary to shock the polymer with 0.10 M HCl and rinse it with copious amounts of water until a stable protonated baseline was achieved. Metal ion test solutions were introduced from lowest concentration to highest concentration and allowed to equilibrate for 15 minutes with the polymer test strip. The cuvet was then rinsed with the solution of the next highest concentration to ensure proper clean out and no carry-over contamination from the previous solution.

The entrapment of crown ethers within the polymer microspheres is based on the principle of ion exchange. When the NK 1-135 polymer microspheres are in an alkaline solution ($\text{pH} > 6$), the MAA functional monomer deprotonates resulting in a net negative charge on the particle. The crown ether forms a positively charged complex when dissolved in a solution with the targeted metal ion (61). These opposite charges attract one another, and the crown ether complex will diffuse into the polymer. Inducing the polymer to shrink state by a 1.0 M HCl titration will trap the complex in the polymer. A detailed description of the crown ether entrapment is provided below:

- ***Day One:***

A 7.5 mL KOH solution is prepared by dissolving three pellets of KOH in deionized water. The crown ether, which is added to the KOH solution, is allowed to dissolve by sonication/stirring for one hour to complete complexation. Concurrently, 1.0 mL of NK 1-135 polymer stock solution (5% w/w in methanol) is washed with 5.0 mL of deionized water, and is then pelleted by centrifugation at 10,000 rpm for 10 min. The supernatant is removed and the polymer pellet is resuspended in the KOH-crown ether solution

previously prepared. The suspension is allowed to stir over night to maximize the amount of crown ether complex that diffuses into the polymer.

- ***Day Two:***

After 24 hours, the solution is centrifuged at 10,000 rpm for 10 min, and the basic supernatant is discarded. The functionalized polymer pellet is acidified by suspension in 5.0 mL of 1.0 M HCl. Centrifugation is used to isolate the polymer, the acidic supernatant is removed, and the particles are washed with deionized water. A second deionized water wash is performed to eliminate the presence of any residual acid that would prematurely initiate PVA polymerization. This wash is also discarded to waste, and the pellet is saved for PVA immobilization.

The functionalized polymer pellet is resuspended in deionized water to yield a final solution mass of approximately 0.40 g. PVA (1.6 g) is added to this solution and allowed to stir overnight to achieve homogeneity. The following day, 50 μ L of GDA crosslinker and 25 μ L of 4.0 M HCl are added to the solution to polymerize the PVA around the functionalized particles. Test membranes are cut from the parent membrane and exposed to alkaline metal ion solutions of increasing concentration.

4.2 Ion Profiling – Group I Metals

NK 1-135 was profiled using the following metal ions: Li^+ , Na^+ , K^+ , Cs^+ , Ca^{2+} , Cu^{2+} , Pb^{2+} , Cd^{2+} . Also, a control denoted as NK 1-161 was used in an attempt to further elucidate the mechanism of interaction between the metal ions and polyNIPA-MAA. The composition of NK 1-161 (80% NIPA, 10% NTBA, and 10% MBA) is similar to NK 1-161 with the exception that methacrylic acid is not present in the polymer formulation.

Figure 4.3 shows the response profile of the polymer test strip for Li^+ , Na^+ , K^+ , and Cs^+ . The exposure of NK1-135 to each of these metals caused the particles to swell. By comparison, the exposure of NK 1-161 (No MAA) to the alkaline metal ions caused the polymer particles to shrink. The swelling response obtained for NK 1-135 (10% MAA) is less than the total absorbance change previously observed for pH (see Figure 4.1).

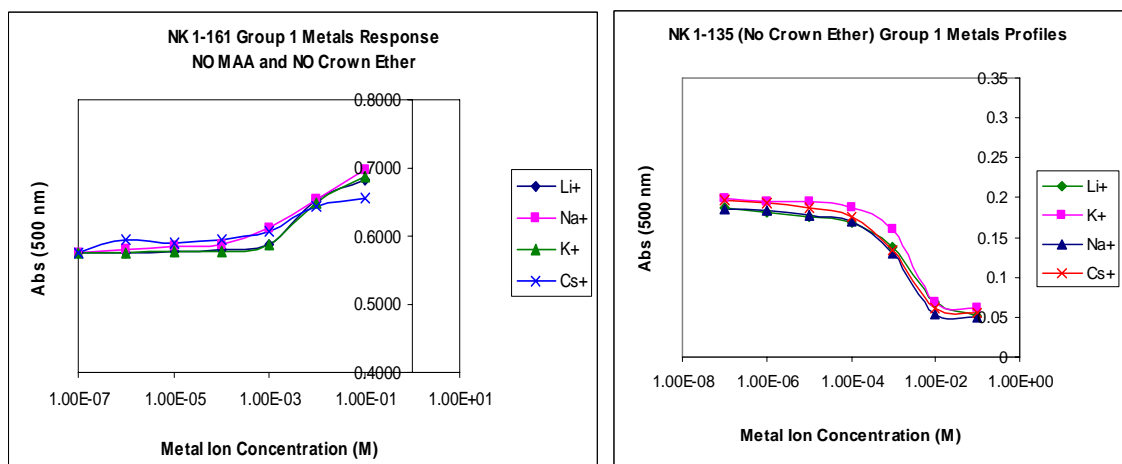


Figure 4.3: (Left) Group 1 metal ion profiles for NK 1-161 (no MAA). (Right): Group I metal ion profiles for NK 1-135 (10% MAA).

An ion exchange mechanism is likely responsible for the swelling. In these experiments, the PVA membrane is first shocked with HCl to ensure that all carboxylic acid groups of MAA are protonated. The membrane was then rinsed with copious amounts of water until a stable baseline in DI water is achieved. In this state, the NK 1-135 particles contain both protonated and deprotonated carboxylic acid groups, which would explain why the swelling response for the metal ions is depressed compared to pH since the polymer particles are always in a fully protonated state at the start of a pH titration.

As the concentration of the alkaline metal ions in the surrounding solution was increased, the positively charged monovalent cations displace protons from protonated carboxylic acid groups causing the polymer to swell. Metal ion binding by NK 1-135 particles occurs through ion pairing between the deprotonated methacrylic acid groups and the positively charged cationic species, which leads to an increase in the water content of the particles. The adsorbed ions act as fixed charges on the network chains, decreasing the value of the solvent interaction parameter (X_1) of the polymer. Each particle will therefore have increased compatibility with its aqueous solvent environment.

The lack of selectivity exhibited by NK 1-135 towards the alkaline metals can be attributed to the low level of crosslinking used, which allows the particles to swell. However, hydration occurs because of swelling, which decreases the density of the binding sites and their selectivity for the different metal ions. This phenomenon is well known among workers in the field of ion exchange chromatography [62].

In an effort to better understand the ion exchange processes occurring at the polymer particles and to impart potassium ion selectivity, dibenzo18crown6 was entrapped in NK 1-135 particles using the procedure described in Section 4.1. Dibenzo18crown6 selectively binds K^+ due to the optimal cavity size of the crown ether for K^+ . Other Group I metal ions are either too small (e.g., Li^+ or Na^+) or are too large to be retained by the cavity. The two benzo functional groups attached to the crown ether provide the macrocyclic ring with additional rigidity, thereby maintaining its planarity and optimal interaction distances between the coordinating oxygen atoms and K^+ . The conjugated polymer particles were embedded in a PVA membrane, and the hydrogel

membrane was exposed to solutions of Li^+ , Na^+ , K^+ , and Cs^+ . Figure 4.5 shows the response profile for each metal ion.

The ionophore (I) doped polymer particles can be modeled as a cation-exchange resin (63). Ion binding is accompanied by a release of protons from the carboxylic acid groups of the polymer (see equation 4-1). This introduces charged sites onto the polymer causing it to swell. The K^+ response is larger because protons are displaced from carboxylic acid groups that are conjugated with dibenzo18crown6 as well as from carboxylic acids that are not conjugated with the crown ether. For Li^+ , Na^+ , and Cs^+ , only protons from carboxylic acids that are not conjugated with the ionophore are displaced. Therefore, K^+ induced swelling occurs at a lower concentration than Li^+ , Na^+ or Cs^+ induced swelling. The failure to obtain a more selective response for K^+ is probably due to the small amount of ionophore entrapped in the polymer.

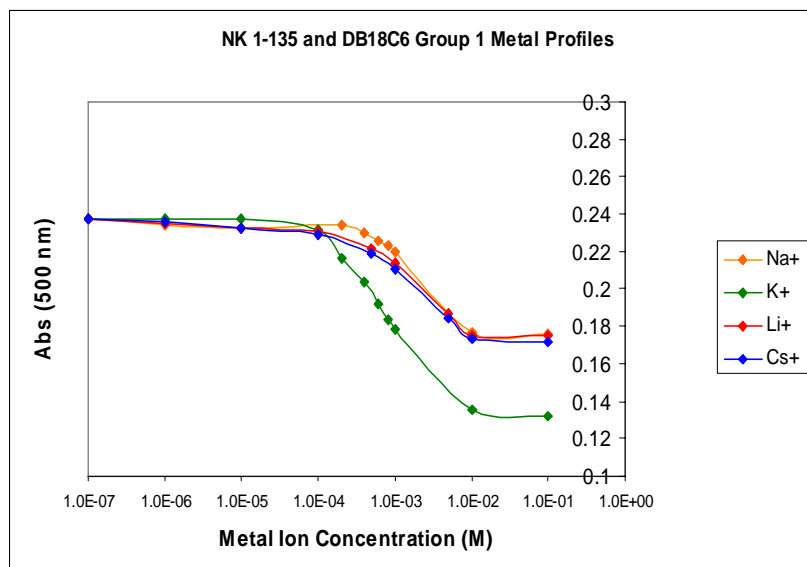
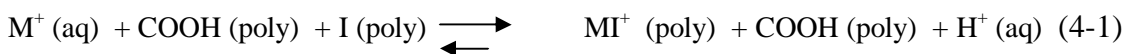


Figure 4.4. Metal ion Profiles of the alkaline metals for NK 1-135 conjugated with Dibenzo18crown6.



4.3 Ion Profiling - Transition Metals

Adsorption of transition metal ions by NIPA and copolymers of NIPA has also been investigated. NK 1-135 (10% MAA) was challenged with solutions of lead (II) nitrate, cadmium (II) nitrate, and copper (II) sulfate (1×10^{-7} M to 1.0×10^{-1} M). The metal ion profiles were obtained using the same procedure as those for the alkali group metals. The polymer was protonated with HCl, rinsed with deionized water until a stable baseline was achieved, and then challenged with solutions of the individual salts from lowest to highest concentration. Each metal ion solution was allowed to equilibrate for 15 minutes at 23° C before an absorbance measurement was made at 500 nm. Figure 4.6 shows the response of NK 1-135 to Pb^{2+} , Cd^{2+} , and Cu^{2+} . All three transition metal ions used to challenge the hydrogel membrane caused water to be expelled from the polymer particles. The increase in the turbidity of the membrane suggests that a different binding mechanism is at work for the transition metal ions.

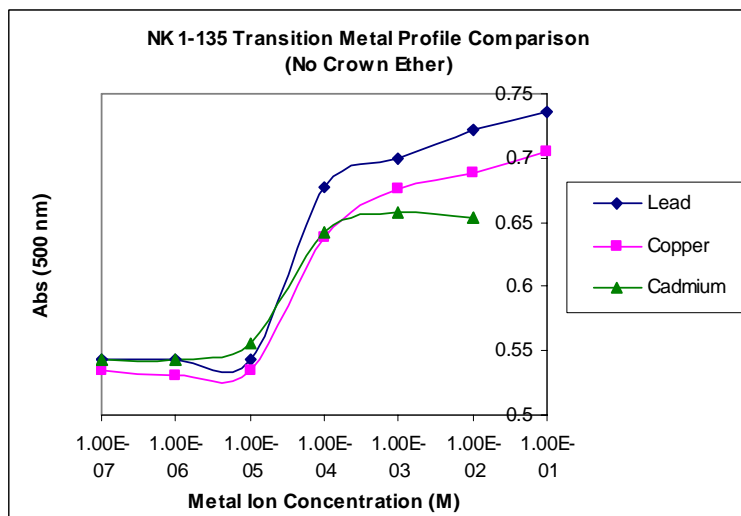


Figure 4.5: Transition metal ion response profiles of lead, cadmium, and copper for NK 1-135 NIPA-co-MAA (10%).

To better understand binding by the transition metal ions, the lead ionophore, dibenzo15crown5, was entrapped in NK 1-135 using the procedure described in Section 4.1. Because Pb^{2+} , Cu^{2+} , and Cd^{2+} form insoluble hydroxides, the ionophore was complexed with K^+ for particle entrapment. Entrapment of the crown ether in NK 1-135 polymer did not produce a selective response for Pb^{2+} or for any of the other transition metal ions investigated as neither the shape nor the magnitude of the response profile differed significantly from the response profiles obtained for NK 1-135 particles without dibenzo15crown5. It was anticipated that a cation complex would form between Pb^{2+} and the entrapped dibenzo15crown5. Ion binding (i.e., complexation) would be accompanied by a release of protons. This would introduce charge sites in the polymer and swelling would occur. However, there was no change in the response of the membrane to Pb^{2+} , Cd^{2+} and Cu^{2+} after entrapment of dibenzo15crown5 in the polymer. Since an increase in selectivity was observed for the alkaline metals after the entrapment of crown ether in the polymer, one can conclude that binding of the transition metals and the alkaline metals does not occur by the same mechanism.

The binding of alkali group metals to NK 1-135 occurs by ion pairing with the carboxylic acid groups. Nevertheless, the question of the charge of the ion cannot be ignored since the transition metal ions that cause the polymer to shrink have a charge of +2 whereas the alkali group metals have a charge of +1. For this reason, Ca^{2+} was selected to determine the role of charge on metal ion binding. Calcium has a 2^+ ionization state, but does not have the additional complication of partially filled d-orbitals as is the case with transition metals. The metal ion profile for Ca^{2+} was obtained for NK 1-135. Figure 4.7 shows the metal ion profiles for Ca^{2+} , K^+ , and Pb^{2+} .

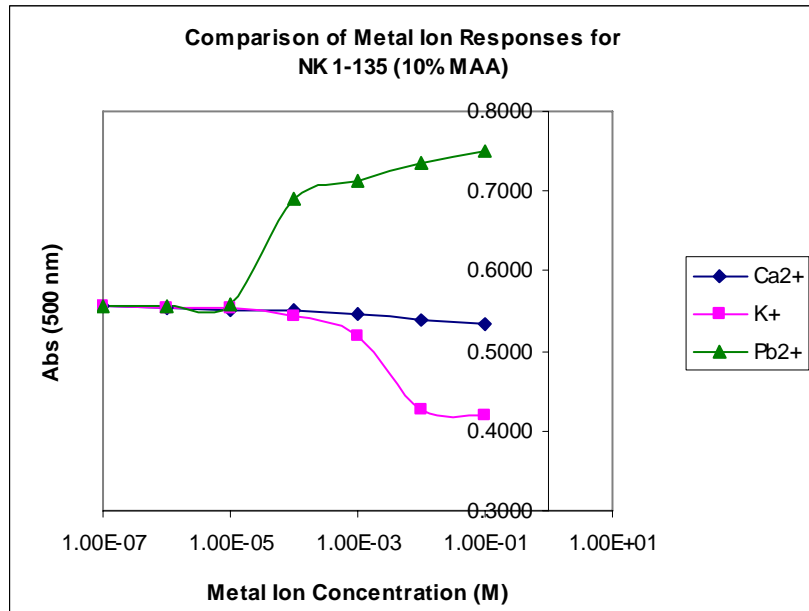


Figure 4.6: Metal ion profiles of Ca²⁺, K⁺, and Pb²⁺ for NK 1-135.

Ca²⁺ does not induce a response in the NK 1-135 particles over the concentration range investigated. If the binding mechanism were based solely on the charge of the ion, then Ca²⁺ would have induced a response similar to that observed for Cu²⁺, Cd²⁺, or Pb²⁺. Using surface plasmon resonance spectroscopy, which is a more sensitive technique than turbimetry to study polymer swelling, the swelling behavior of Ca²⁺ and several monovalent Group I metal ions was investigated. Figure 4-8 shows a plot of refractive index versus the log of the concentration of alkali and alkaline earth metals (10⁻⁷ M to 10⁻¹ M) obtained from SPR for the NK 1-135 particles that were spin coated onto a gold surface. The refractive index of the polymer particles was determined by fitting the SPR data to a 5-layer model (Layers 0, 1, 2, 3, and 4) with the diameter of the NK 1-135 particles defining the thickness of the third layer. As the concentration of Li⁺, Na⁺, K⁺, or Ca²⁺ in contact with the polymer particles increases, the refractive index of the particles

decreases due to an increase in the water content of the polymer. Clearly, the presence of these cations in the solution causes the polymer to swell.

Ca^{2+} response profile from turbimetry and SPR are consistent with an ion pairing mechanism. However, Ca^{2+} binding probably requires two carboxylic acid groups, whereas the binding of Li^+ , Na^+ , and K^+ only require one carboxylic acid group. As most MAA groups are well separated in NK 1-135, there are too few carboxylic acid groups involved in Ca^{2+} binding to stimulate polymer swelling to the same degree that occurs with the alkali metals.

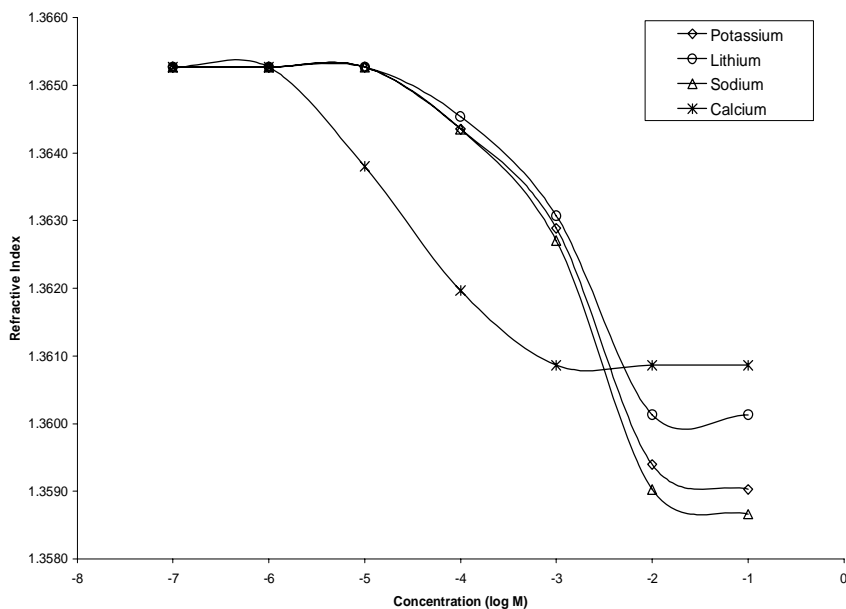


Figure 4.7: Metal ion response profiles obtained by SPR for alkali and alkaline earth metals

To better understand the binding of transition metal ions by NK 1-135, a NIPA polymer (NK 1-161) was prepared without MAA. The composition of the polymer was 80%NIPA, 10%NTBA, and 10%MBA. NK 1-161 was selected for metal ion profiling, as its formulation was similar to NK 1-135. The exclusion of methacrylic acid from the formulation ensures that carboxylic acids, which are involved in ion pairing for alkali and

alkaline earth metals, are not present in the polymer. Figure 4.9 shows metal ion profiles of lead with and without the presence of methacrylic acid in the colloidal particles.

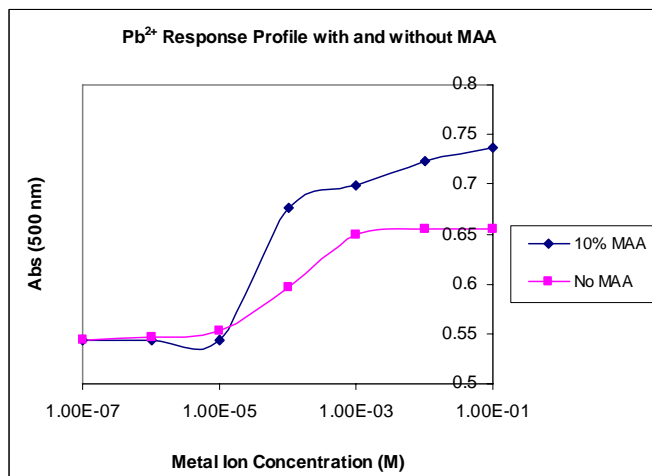


Figure 4.8: Pb^{2+} response profiles of NK 1-135 (10% MAA) and NK 1-161 (No MAA) over the concentration range of $10^{-7} - 10^{-1}$ M Pb^{2+}

Both polymers exhibit an increase in turbidity (absorbance) over the concentration range investigated. However, there is a marked difference in the total turbidity change that occurs. For NK 1-161, the total absorbance change is 0.1124 whereas the total absorbance change for NK 1-135 is 0.1933 over the concentration range investigated. Furthermore, the inflection point in the response curve of NK 1-161 occurs at a higher Pb^{2+} concentration: 1.0×10^{-4} M for NK 1-161 (0% MAA) versus 5.0×10^{-5} M for NK 1-135 (10% MAA). From this data, two conclusions can be drawn. First, the amide groups of NIPA probably play a role in the binding of transition metal ions by polyNIPA particles. Second, carboxylic acid groups promote the binding of transition metal ions in copolymers of NIPA and MAA.

In an effort to better understand the role of carboxylic acids in the binding of transition metal ions, NK 1-156 (10% acrylic acid) was selected for study. As the Pb^{2+} , Cu^{2+} , and Cd^{2+} profiles were similar in their shape and inflection point, reproducing the

entire series for NK 1-156 was unnecessary. Therefore, Pb^{2+} was selected as a test probe, and NK 1-156 was challenged with increasingly concentrated Pb^{2+} solutions. The Pb^{2+} response profile for NK 1-156 (10% acrylic acid) and NK 1-135 (10% MAA) is shown in Figure 4.9.

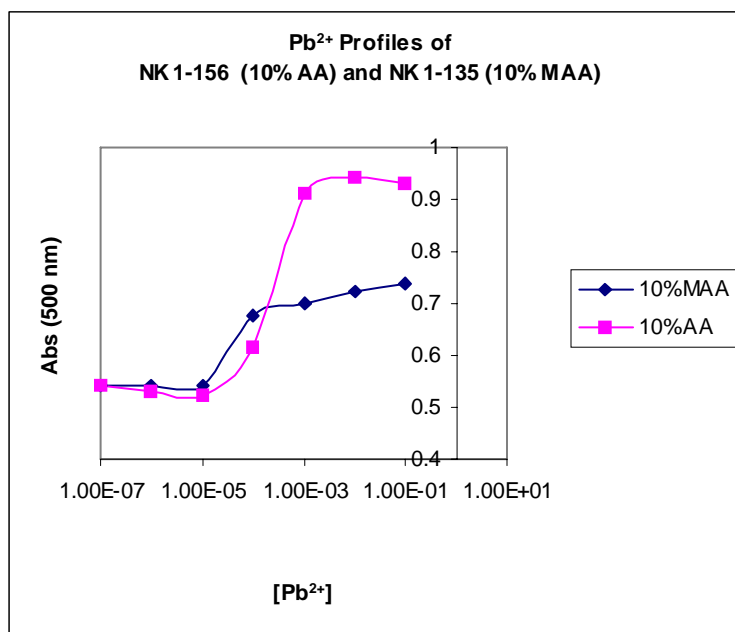


Figure 4.9: Pb^{2+} response profile for NK 1-156 (10% acrylic acid) and NK 1-135 (10% MAA)

The response of NK 1-156 (10% acrylic acid in its formulation) is approximately twice that of the response of NK 1-135 (10% methacrylic acid in its formulation) to Pb^{2+} . In all likelihood, the increase in the Pb^{2+} response can be attributed to the amount of acrylic acid present in the polymer. Previous work has suggested that methacrylic acid groups are located at or near the surface of the polymer particles (see Chapter 3). Based on the pH profile of NK 1-135 (see Figure 4.1), most of the carboxylic acid groups in this polymer are well separated since the polymer microspheres exhibit a larger response over a narrower pH range than that predicted by the Henderson Hasselbach equation. For the acrylic acid functionalized NIPA particles (NK 1-156), the Henderson Hasselbach

equation is obeyed (see Chapter 3). This combined with a higher Pb^{2+} response suggests that carboxylic acid groups in NK 1-156 (10% acrylic acid) are not as well separated, as are the carboxylic acid groups in NK 1-135 (methacrylic acid) because there are more carboxylic acid groups present in NK 1-156. We attribute this to acrylic acid being more reactive than methacrylic acid.

4.4 Role of Carboxyl Groups in Transition Metal Ion Binding

The role of the carboxylic acid group in the binding of transition metal ions was further investigated. Metal ion profiles for NK 1-135 were obtained when the particles were in a fully protonated ($\text{pH} < \text{apparent pKa}$), half protonated ($\text{pH} = \text{apparent pKa}$ of MAA), or fully deprotonated ($\text{pH} > \text{apparent pKa}$) state. As pH control is crucial for a study of this type, the pH response profile of NK 1-135 was reexamined to select the proper pH values for the buffer solutions used in the metal ion profiling experiments. Figure 4.10 is the pH response profile of NK 1-135. The apparent pKa of the polymer is 5.00 and the polymer is fully deprotonated at pH 6.00. Acetate buffer was selected to control pH in this range. Iron (II) sulfate was used in this study because Fe^{2+} has a binding constant of only 100 with the acetate ligand.

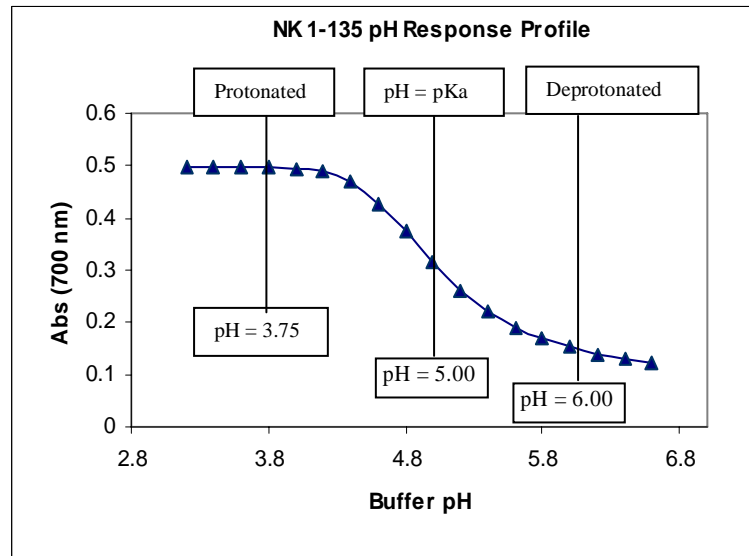


Figure 4.10: pH Response profile of NK 1-135 (70% NIPA, 10% MAA, 10% NTBA, 10% MBA).

Figure 4.11 shows the Fe^{2+} profile in DI water for NK 1-135 (10% MAA) and NK 1-161 (No MAA). An increase in turbidity, which was observed for both NK 1-135 (10% MAA) and NK 1-161 (No MAA), was initiated at 1×10^{-4} M Fe^{2+} . The overall magnitude of the response is greater if MAA is present in the polymer. The results obtained for Fe^{2+} were similar to those obtained for Pb^{2+} and the other transition metal ions investigated. Therefore, Fe^{2+} was judged to be an appropriate ion to use for further investigation into the role of carboxylic acids in the binding of transition metal ions by copolymers of NIPA and MAA.

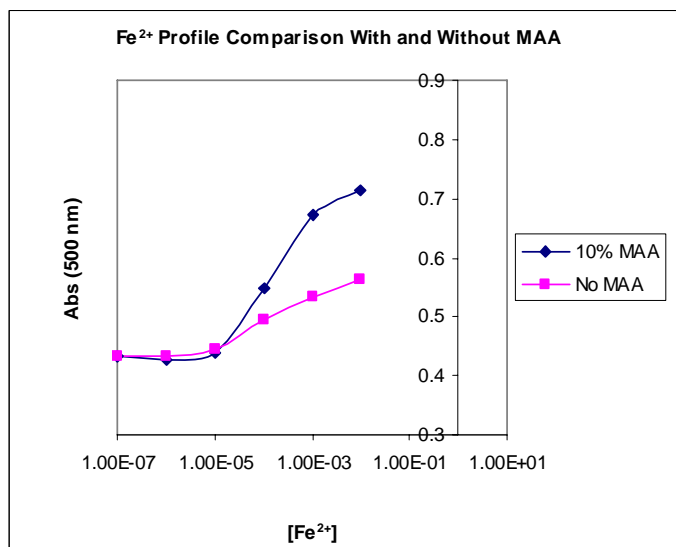


Figure 4.11: Fe²⁺ response profiles of NIPA-co-MAA (10%) and NK 1-161 (No MAA) in DI water.

Three buffer solutions (pH 3.75, pH 5.00, and pH 6.00) were prepared from 0.1 M sodium acetate and 0.1 M HCl. Iron (II) sulfate solutions were prepared to span the concentration range of 1.0×10^{-7} M to 1.0×10^{-2} M with the buffer solution used for serial dilution of the 0.10 M Fe²⁺ stock solution (prepared in deionized water). These solutions were prepared upon demand, as Fe²⁺ was not stable at room temperature and tended to form colloidal Fe³⁺ when left standing for extended periods of time. Otherwise, the procedure used to obtain the metal ion profiles is the same as previously discussed for Fe²⁺. (Protonated DI water baseline, 15 min equilibration time, and rinsing between each solution, Cary 6000i absorbance measurement at 500 nm.) Figure 4.12 shows the metal ion response profile for each pH investigated.

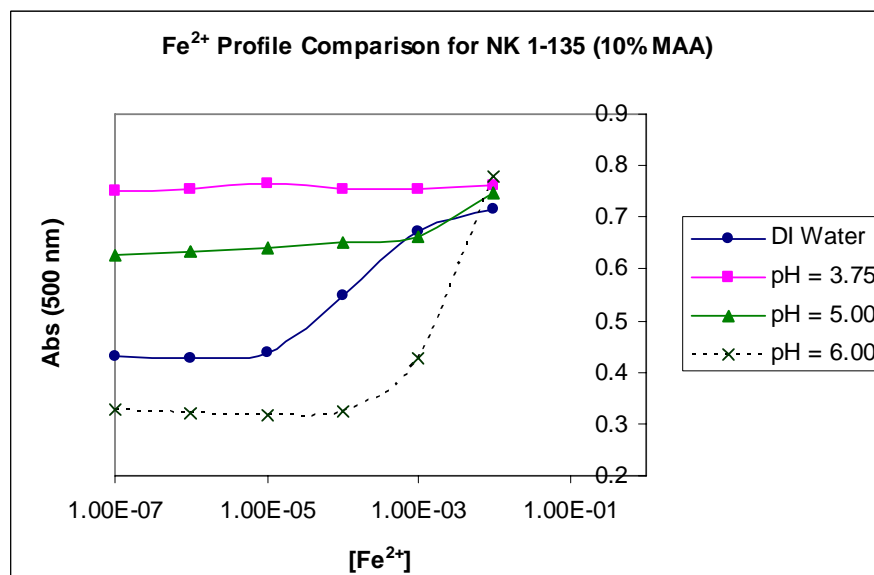


Figure 4.12: Comparison of Fe²⁺ responses for NK 1-135 (10% MAA) at pH = 3.75, 5.00, 6.00.

NK 1-135 did not swell or shrink when the NIPA-co-MAA (10%) polymer was challenged with Fe²⁺ in pH = 3.75 buffer. With the pH fixed at 3.75, the methacrylic acid groups are fully protonated, and the microspheres exist in a shrunken state over the entire metal ion concentration range investigated. The affinity of the carboxylic acid groups for H⁺ is greater than Fe²⁺. When the pH of the solutions containing Fe²⁺ is increased to 5.00, nearly half of the MAA groups on the polymer exist in a deprotonated state. Shrinking occurred at 1.0×10^{-2} M Fe²⁺, whereas in DI water it occurred at 1.0×10^{-4} M Fe²⁺. At pH 6.00, all of the MAA groups in the polymer exist in a deprotonated state. Shrinking occurred at 1.0×10^{-3} M Fe²⁺. Differences in the affinity of Fe²⁺ for the polymer in distilled water and in pH 6.00 buffer can be attributed to the presence of acetate, which forms a complex with Fe²⁺ in the buffered metal salt solutions. This competing equilibrium, which is occurring in solution, decreases the binding constant between Fe²⁺ and the NK 1-135 particles.

Figure 4.13 shows Fe^{2+} response profiles for NK 1-161 (0% MAA) and NK 1-135 (10% MAA) in a pH 3.75-buffered solution. For NK 1-161 (0% MAA), metal ion binding occurs in the absence of pH sensitive groups on the polymer backbone albeit at a lower level than in distilled water (see Figure 4.11), which can be attributed to the formation of a complex between acetic acid and Fe^{2+} in the buffer. For NK 1-135, the use of pH 3.75 buffer ensures that all of the carboxylic acids are in the protonated state. Therefore, these groups are not available to participate in metal ion binding. Since little or no change is observed with increasing metal ion concentration, one can conclude that carboxylic acids in NK 1-135 play a crucial role in metal ion binding.

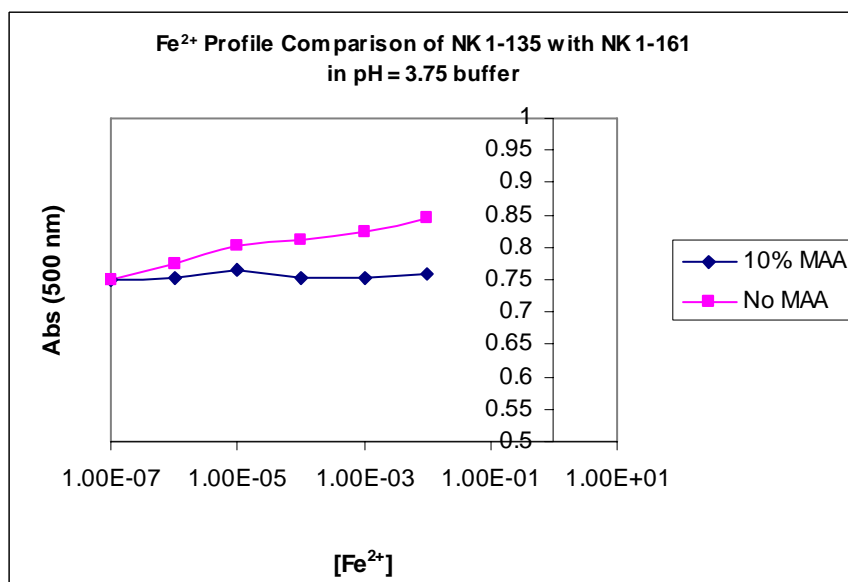


Figure 4.13: Fe^{2+} response profiles of NK 1-161 (No MAA) and NK 1-135 (10% MAA) in pH = 3.75 acetate buffer.

For NK 1-135, the response profiles obtained for the transition metal ions in distilled water and buffer can be attributed to Pb^{2+} , Cu^{2+} , Cd^{2+} , or Fe^{2+} being bound to both the carboxylic acid of the functional comonomer and to the amide on the polymer backbone. It is possible that a chelate is formed with the chelate acting as a crosslinker

reducing the particle diameter and lowering the affinity of the polymer for the solvent, which is water. Alternatively, the binding of the metal ions to the nitrogen atom of NIPA disrupts the hydrogen bonding that occurs between water and the NH_2 group on the polymer backbone reducing the affinity of the polymer for water. In either case, the refractive index of the polymer increases, because water is being expelled.

Two possible orientations have been proposed (64) for metal ion binding in polyNIPA and copolymers of NIPA and MAA (see Figure 4.14). Either orientation is at best an oversimplification of the actual binding mechanism for transition metal ions. Figure 4.14a depicts the formation of a chelate between two adjacent carboxylic acid groups and a metal ion. It is unlikely that chelation of the metal ion between two adjacent carboxylic acid groups on the polymer is the primary binding interaction as a decrease, not an increase in turbidity would occur as a result of metal ion binding (see Ca^{2+}). Figure 4.14b depicts the chelation of a metal ion by two adjacent amide groups on the polymer backbone. Although this scheme does provide a plausible explanation for the binding of transition metal ions by NK 1-161 (0% MAA), it does not explain metal ion binding by NK 1-135 as the carboxylic acid groups, which appear to play a role in metal ion binding, are not implicated in the proposed mechanism.

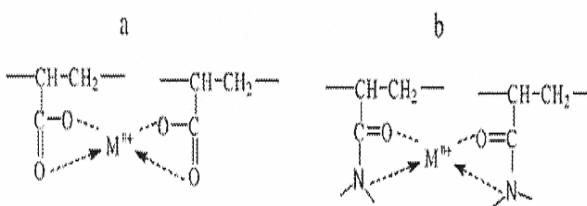


Figure 4.14. (a) Metal ion binding by adjacent carboxylic acid groups. (b) Metal ion binding by adjacent amide groups. (See reference 64).

Additional studies will be required to understand at a molecular level the binding of transition metal ions by polymers and copolymers of NIPA. In any study, complications will undoubtedly arise since the distribution of the functional monomer within the polymer is known only through statistical estimation based on hydrophobicity, relative abundance, and the relative reactivity of each monomer. Until the uncertainty in our knowledge about the structure of the polymer is eliminated or at least reduced, a clearer understanding of metal ion binding in these systems will remain elusive, as the approach that is currently being taken to solve this problem is from organic and inorganic chemistry, which requires a detailed knowledge of chemical structure.

Chapter 5

Conclusions

Lightly crosslinked copolymers of N-isopropylacrylamide were prepared for pH sensing using dispersion polymerization with acrylic acid, methacrylic acid, ethacrylic acid, or propacrylic acid used as functional comonomers. The diameter of the resulting microspheres was approximately 1 μ m. These microspheres were cast into hydrogel membranes for use as pH sensors. The membrane was turbid because the refractive index of the microspheres is higher than the refractive index of the hydrogel. As pH increases, the water content of the polymer particles also increases due to deprotonation of the pH sensitive monomer, which triggered a volume phase transition. The refractive index of the particles decreases and approaches that of the hydrogel, which is detected as a decrease in membrane turbidity.

The swelling behavior of these copolymers of NIPA in response to pH has been studied as a function of the ionic strength and temperature of the solution in contact with the membrane, the percentage of crosslinker used to synthesize the polymer, and the amount, pKa, and hydrophobicity of the pH sensitive co-monomers in the polymer formulation. The sensitivity of the pH response is greater than that predicted by the Henderson Hasselbalch equation since it occurs over a narrower pH range. Furthermore, polymer swelling is reversible and independent of ionic strength in low and moderate

ionic strength solutions (0.05M – 0.50M). Although higher temperature does not have an effect on the total swelling, it will occur over a narrower pH range.

The pH response of the membrane can also be increased by increasing the weight percent of polymer in the hydrogel. Furthermore, the pH response of the particles can be tuned by polymerizing NIPA using comonomers of differing pKa values such as ethacrylic acid and propacrylic acid. Thus, polymer materials capable of responding to the physiologically relevant pH values between 5.0 and 7.4 can be developed. One possible application of these pH sensitive polymer particles is monitoring the progress of open-heart surgery where pH serves as a measure of tissue ischemia. Gastric pH sensing is yet another possible application. A third potential application is bioconjugates for proteins since the carboxyl groups on these particles are isolated from each other.

The response time of the microspheres is rapid. For example, there is an immediate change in the turbidity of the membrane when the pH of the buffer is changed from 3 to 10. Furthermore, 90% of the full-scale response for swelling is achieved in less than two minutes. The rapid response of the membrane to the sample solution can be attributed to the porous nature of the immobilization membrane, the colloidal size and spherical shape of the NIPA particles, the presence of the pH sensitive comonomer at/near the particle's surface, and the thickness of the hydrogel membrane, which is approximately 127 μm . Submicron sized gel particles respond to external stimuli such as temperature or pH more quickly than bulk polymer films and as a result are more useful for chemical sensing.

The mechanism controlling metal ion adsorption by polyacrylamide hydrogels has also been investigated. Little is known about the adsorption of metal ions by polyNIPA.

Therefore, turbidity has been used to study noncompetitive metal ion binding by crosslinked polyNIPA-MAA particles. Solutions placed in contact with the polymer particles consisted of a metal salt dissolved in distilled water. Alkali metal ions cause a decrease in the refractive index of the particles as the presence of these cations in the solution causes the polymer to swell. In all likelihood, the monovalent cations displace protons from carboxylic acid groups of the polymer particles through an ion exchange mechanism. Deprotonation of the methacrylic acid groups in the copolymer structure increased the affinity of the polymer for water. The adsorbed ions act as fixed charges on the network chains raising the lower critical solution temperature of the polymer. The lack of selectivity exhibited by the polyNIPA-MAA particles towards the group I metal ions can be attributed to the low level of crosslinking used.

The swelling and shrinking behavior exhibited by polyNIPA-MAA particles in contact with solutions of Pb^{2+} or Cu^{2+} is more complex. At low concentrations of Pb^{2+} or Cu^{2+} (e.g., 10^{-7}M and 10^{-6}M), the decrease in refractive index is probably due to an increase in the transition temperature of the polymer, which can be attributed to deprotonation of the methacrylic acid groups by Pb^{2+} or Cu^{2+} via an ion exchange mechanism. At higher concentrations of Pb^{2+} or Cu^{2+} , the refractive index of the polymer particles increases suggesting that water is being squeezed out of the polymer. We attribute this to Pb^{2+} or Cu^{2+} being bound to both the carboxyl group by ion exchange and to the nitrogen atom of NIPA through coordination with its lone pair. In all likelihood, a five-member ring chelate is being formed. Pb^{2+} or Cu^{2+} via complexation through coordination and ion exchange is effectively acting as a crosslinker reducing the particle diameter and lowering the affinity of the polymer for the solvent, which is water.

Alternatively, the binding of Pb^{2+} or Cu^{2+} to the nitrogen atom of NIPA is disrupting the hydrogen bonds between the water molecules and the NH_2 group on the polymer backbone reducing the affinity of the polymer for water.

The hydrogel membranes are highly stable with respect to time and calibration, which is an important issue since one goal of this research is to improve stability of optical sensors based on indicator dyes. The membranes respond to multiple swelling and shrinking cycles. Furthermore, the approach reported here is not subject to the mechanical problems of delamination and/or cracking associated with polymer swelling. The microspheres swell freely in all three dimensions, increasing the volume change due to swelling and circumventing the problem of delamination that occurs when the swellable polymer is immobilized on a surface. The hydrogel not only serves as a flexible medium to hold the microspheres in place but also acts as a filter to protect the microspheres from sample components such as suspended particles that are too large to diffuse through the hydrogel. Membrane turbidity can be measured at any wavelength including near infrared wavelengths used for fiber optic telecommunications. Based on previous experience with other approaches to sensors that utilize swellable polymers, this approach may be the most practical for the preparation of chemical sensors that will find application to real world problems.

REFERENCES

1. Oh, K.S., Bae, Y. C. 1997. "Swelling Behavior of Submicron Gel Particles," *Journal of Applied Polymer Science*. 69: 109-114
2. Thomson, B., Rudin, A., Lajoie, G. 1995. "Dispersion Copolymerization of Styrene and Divinylbenzene: Synthesis of Monodisperse, Uniformly Crosslinked Particles," *J. Poly. Sci. Pt. A*. 33:345-357
3. Pelton, R. H. Chibante, P. 1986. "Preparation of Aqueous Lattices with N-isopropylacrylamide. *Colloid Surf.* 20: 247-256.
4. Snowden, M. J.; Vincent, B. J. 1992. "The Temperature-Controlled Flocculation of Crosslinked Latex Particles," *Chem. Soc., Chem. Commun.* 16, 1103-1105
5. McPhee, W.; Tam, K.C., Pelton, R. J. 1993. Poly(N-isopropylacrylamide) Latexes Prepared with Sodium Dodecyl Sulfate *J. Colloid Interface Sci.* 156(1): 24-30.
6. Pinkrah, V.T., Beezer, A.E., Chowdhry, B.Z., Gracia, L.H., Mitchell, J.C., Snowden, M.J. 2004. Thermodynamic Considerations of Microgel Swelling Behavior, *Langmuir*. 20: 8531-8536
7. Hirotsu, S., Hirokawa, Y., Tanaka, T. J. 1987. "Volume-phase transitions of Ionized N-isopropylacrylamide Gels," *Chem. Phys.* 87(2): 1392-1395.
8. Ilmain, F.; Tanaka, T.; Kokufuta, E. 1991. "Volume Transition in a Gel Driven by Hydrogen Bonding," *Nature*, 349: 400-401.
9. Hirokawa, Y.; Tanaka, T. J. 1984. "Volume Phase Transition in a Nonionic Gel," AIP Conference Proceedings, 107: 203-208.
10. Sierra-Martin, B., Choi, Y, Romero-Cano, M.S., Cosgrove, T. Vincent, B., Fernandez-Barbero, A. 2005. Microscopic Signature of a Microgel Volume Phase Transition," *Macromolecules*. 38: 10782-10787.
11. Fernandez-Nieves, A., Fernandez-Barbero, A., Vincent, B., Nieves, F.J. 2000. "Charge Controlled Swelling of Microgel Particles," *Macromolecules*. 33: 2114-2118

12. Liu, X., Wang, L., Wang, L., Huang, J., Chaobib, H. 2004. "The Effect of Salt and pH on the Phase-Transition Behavior of Temperature Sensitive Copolymers based on N-isopropylacrylamide," *Biomaterials*. 25:5659-5666
13. Hellweg, Thomas. 2003. "Properties of NIPAM based Intelligent Microgel Particles: Investigated Using Scattering Methods," *Nanoscale Materials*. 209-225.
14. Pelton, R. H. 2004. Macromolecular Symposia, "Unresolved Issues in the Preparation and Characterization of Thermoresponsive Microgels," 207: 57-65.
15. Seker, F; Ellis, A.B., J. 1998. "Correlation of Chemical Structure and Swelling Behavior in N-Alkylacrylamide Hydrogels," *Polym. Sci. Part A: Polym. Chem.*, 36:2095
16. Schild, H.G. 1992. "Poly(N-isopropylacrylamide): Experiment, Theory and Application," *Prog. Polym Sci.* 17:163-249.
17. Elaisarri, A. 2003. Colloidal Polymers: Synthesis and Characterization. Vol. 115 Surfactant Science Series.
18. Deshmukh, M. V., Vaidya, A.A, Kulkarni, M. G., Rajamohanam, P.R., Ganapathy, S. 2000. Development of New Class of Electronic Packaging Materials Based on Ternary Systems of Benzoxazine, Epoxy, and Phenolic Resins," *Polymer*. 41: 7951-7960
19. Oh, K.S, Bae, Y.C., 1999. "Volume Phase Transition of Submicron Sized Copolymer Gel Particles," *European Polymer Journal*. 35: 1653-1659
20. Siddhartha, M., Siegl, R. 2005. "Novel pH Sensitive N-Isopropylacrylamide Hydrogels for Pulsatile Drug Delivery," BMEI & BTI Graduate Student Poster/Gadget Session. University of Minnesota, MN
21. Dalkas, G., Pagonis, K., Bokias, G. 2006. "Control of the Lower Critical Solution Temperature-Type Cononsolvency Properties of Poly(N-isopropylacrylamide) in Water-Dioxane Mixtures through Copolymerization with Acrylamide," *Polymer*. 47:243-248
22. Elias, H.G. 1997 An Introduction to Polymer Science. 1st ed. VCH
23. Hang, X.; Colon, L.A. 2006 "Evaluation of Poly{N - isopropylacrylamide - co - [3-(methacryloylamino)propyl]- trimethylammonium} as a Stationary Phase for Capillary Electrochromatography," *Electrophoresis*, 27(5-6): 1060-1068.

24. Zhang, J. T.; Huang, S. W.; Zhuo, R. X. 2004 "Temperature-Sensitive Polyamidoamine Dendrimer/Poly (N - isopropylacrylamide) Hydrogels with Improved Responsive Properties," *Macromolecular Bioscience* 4(6): 575-578.
25. Fernandez-Barbero, A., Fernandez-Nieves, Grillo, I., and Lopez-Cabarcos, E. 2002. "Structural Modifications in the Swelling of Inhomogeneous Microgels by Light and Neutron Scattering," *Phys. Review E*, 66: 051803-(1-10).
26. Gan, D.; Lyon, A. L. 2001. "Tunable Swelling Kinetics in Core-Shell Hydrogel Nanoparticles," *J. Am. Chem. Soc.*, 123, 7511-7517.
27. Gan, D.; Lyon, A. L. 2001. "Interfacial Nonradiative Energy Transfer in Responsive Core-Shell Hydrogel Nanoparticles," *J. Am. Chem. Soc.*, 123, 8203-8209.
28. Debord, J. D., Lyon, A. L. 2000. "Thermoresponsive Photonic Crystals," *J. Phys. Chem. B.*, 104, 6327-6331.
29. Jones, C. D., Lyon, L. A. 2000. "Synthesis and Characterization of Multiresponsive Core-Shell Microgels," *Macromolecules* 33, 8301-8306.
30. Li, Y., and Tanaka, T. 1992. *Annu. Rev. Mater. Sci.* 22:243-77
31. Flory, P.J. Principles of Polymer Chemistry; Cornell University Press: New York 1953.
32. Lavine, B., Kaval, N., Westover, D., Oxenford, L. 2006, "New Approaches to Chemical Sensing - Sensors Based on Polymer Swelling," *Analytical Letters*. 39: 1-10.
33. Flory, P.J. and Rehner, J. 1943. "Statistical mechanics of cross-linked polymer networks. II. Swelling," *J. Chem. Physics*, 11: 521-526.
34. Pelton, R. 2000. "Temperature Sensitive Aqueous Microgels," *Adv. Colloid Interface Sci.*, 85:1-33
35. Saunders, B.R. and Vincent, B. 1997. "Osmotic De-swelling of Polystyrene Microgel Particles," *Colloid Polym. Sci.*, 275:9-17.
36. Sierra-Martin, B., Romero-Cano, M.S., Cosgrove, T., Vincent, B., Fernandez-Barbero, A. 2005. "Solvent Relaxation of Swelling PNIPAM Microgels by NMR," *Colloids and Surfaces A: Phys. Chem. Eng. Asp.* 270-271, 296-300.
37. Yuqing, M., Jianrong, C., Keming, F. 2005. "New technology for the Detection of pH," *J. Biochem. Biophys. Methods*. 63:1-9

38. Adhikari, B., Majumdar, S. 2004. "Polymers in Sensor Applications," *Prog. Poly Sci.* 29:699-766
39. Tokuyama, H., Yanagawa, K., Sakohara, S. 2006. "Temperature Swing Adsorption of Heavy Metals on Novel Phosphate-Type Adsorbents Using Thermosensitive Gels and/or Polymers," *Separation Purification Technology.* 50(1), 8-14.
40. Chabukswar, V., Pethkar, S., Athawale, A. 2001. "Acrylic Acid Doped Polyaniline as an Ammonia Sensor. 2001. *Sensors and Actuators B.* 77:657-663.
41. Huther, A., Xu, X., Maurer, G. 2006. "Swelling of Poly(N-isopropyl Acrylamide) Hydrogels in Aqueous Solutions of Sodium Chloride, *Fluid Phase Equilibrium.* 240: 186-196.
42. Ruel-Gariepy, E.; Leroux, J. C. 2004. "In Situ-Forming Hydrogels- Review of Temperature-Sensitive Systems," *European Journal of Pharmaceutics and Biopharmaceutics.* 58(2): 409-426.
43. Seitz, W. R., Rooney, M. T. V., Miele, E. W., Wang, H., Kaval, N., Zhang, L., Doherty, S.; Milde, S., Lenda, J. "Derivatized Swellable Polymer Microspheres for Chemical Transduction," 1999 *Anal. Chim. Acta.* 400, 55-64.
44. Motonaga, T., Shibayama, M., 2001. "Studies on pH and Temperature Dependence of the Dynamics and Heterogeneities in Poly(N-Isopropylacrylamide-Co-Sodium Acrylate) Gels," *Polymer*, 42: 8925-8934
45. Xue, W., Hamley, I. W. 2002. "Thermo-Reversible Swelling Behavior of Hydrogels Based on N-isopropylacrylamide with a Hydrophobic Comonomer" *Polymer.* 43: 3069-3077
46. Elliott, J.E., Macdonald, M., Nie, J., Bowman, C.N. 2003. "Structure and Swelling of Poly(acrylic acid) Hydrogels: Effect of pH, Ionic strength, and Dilution on the Crosslinked Polymer Structure," *Polymer*, 45: 1503-1510
47. Oktar, O., Caglar, P., Seitz, W.R. 2005. "Chemical Modulation of Thermosensitive Poly(N-isopropylacrylamide) Microsphere Swelling: A New Strategy for Chemical Sensing," *Sensors and Actuators B* 104: 179-185
48. Pohl, H.1978. *Dielectrophoresis.* Cambridge University Press, Cambridge.
49. Jones, T. B. 1995. *Electromechanics of Particles.* Cambridge University Press, New York
50. Stangroom, J. E. 1983. Electrorheological fluids. *Phys. in Technol.* **14**, 290-296); Halsey, T. C. & Toor, W.1990. Structure of Electrorheological Fluids. *Phys. Rev. Lett.* **65**, 2820-2823.

51. Inomata, H., Wada, N., Yagi, Y., Goto, G., Saito, S., 1994. "Swelling Behaviors of N-Alkylacrylamide Gels in Water: Effects of Copolymerization and Crosslinking Density," *Polymer*. 36: 875-877
52. Robert C. West (Editor) 1975. Handbook of Chemistry & Physics, 55th Edition. CRC Press, Cleveland, OH.
53. Tokuyama, H., Yanagawa, K., Sakohara, S. 2006 "Temperature Swing Adsorption of Heavy Metals on Novel Phosphate-Type Adsorbents Using Thermosensitive Gels and/or Polymers," *Separations and Purification Technology*, 50, 8-14.
54. Yamashita, K., Nishimura, T., Nango, M. 2003. "Preparation of IPN-type Stimuli-Responsive Heavy-Metal Ion Adsorbent Gel," *Polym. Adv. Technol.*, 14, 189-194.
55. Zhao, W. Li. H., Teasdale, P. R., John, R., Zhang, S. 2002. "Synthesis and Characterization of a Polyacrylamide-Polyacrylic Acid Copolymer Hydrogel for Environmental Analysis of Cu and Cd," *Reactive & Functional Polymers*, 52, 31-41.
56. Morris, G. E., Vincent, B., Snowden, M. J. 1997. "The Interaction of Thermosensitive Anionic Microgels with Metal Ion Solution Species," *J. Colloid Interface Science*, 190, 198-205
57. Fukushi, K., Hiro, K. 1990. "Use of Crown Ethers in the Iostachophoretic Determination of Metal Ions," *Journal of Chromatography*. 523: 281-292
58. Zhang, X., Zhang, J., Zhuo, R., Chu, C. 2002. "Synthesis and Properties of Thermosensitive, Crown Ether Incorporated Poly(N-isopropylacrylamide) Hydrogels," *Polymer*. 43: 4823-4827
59. Capitan-Vallvey, L., Fernandez-Ramos, M., Al-Natcheh, M. 2003. "A Disposable Single-Use Optical Sensor for Potassium Determination Based on Neutral Ionophore. *Sensors and Actuators B*. 88:217-222
60. Ganjali, M., Rouhollahi, A., Mardan, A., Hamzeloo, M., Mogimi. A., Shamsipur, M. 1998. Lead ion-selective electrode based on 4'-vinylbenzo-15-crown-5 Homopolymer," *Microchemical Journal* 60:122-133
61. Alexandratos, S., Stine, C. 2004. "Synthesis of Ion-Selective Polymer-Supported Crown Ethers," *Reactive and Functional Polymers*. 60:3-16
62. Harris, D. Quantitative Chemical Analysis. 5th ed. W. H Freeman and Co.1999
63. Hongming Wang, "Nitrated Poly(4-hydroxystyrene) Microspheres for Optical pH and Potassium Ion Sensing Based on Turbidity Changes Accompanying Polymer Swelling," PhD Thesis, University of New Hampshire, 2000.

64. Rivas, B.L et al. 2003." Water-Soluble Polymer-Metal Ion Interactions," *Prog. Polym. Sci.* 28: 173-208

APPENDIX I

BUFFER SOLUTION COMPOSITION

0.2 IS 0.05 M Citric Acid Buffer Calculations (500mL)

pH of each buffer solution was adjusted to its final value using 4M NaOH
Prepared buffers also contain 0.5% paraformaldehyde as a preservative.

pH	CA ⁻		IS Contr.	NaCl (g)	Citric Acid (g)
3.0	0.0213		0.0112	5.4760	4.8033
3.2	0.0271		0.0138	5.3984	4.8033
3.4	0.0326		0.0165	5.3218	4.8033
3.6	0.0374		0.0188	5.2542	4.8033
3.8	0.0412		0.0207	5.1999	4.8033
pH	CA ²⁻	CA ⁻	IS Contr.	NaCl (g)	Citric Acid (g)
4.0	0.0074	0.0426	0.0361	4.7522	4.8033
4.2	0.0108	0.0392	0.0412	4.6052	4.8033
4.4	0.0152	0.0348	0.0478	4.4146	4.8033
4.6	0.0204	0.0296	0.0556	4.1864	4.8033
4.8	0.0261	0.0239	0.0642	3.9385	4.8033
5.0	0.0317	0.0183	0.0726	3.6954	4.8033
5.2	0.0367	0.0133	0.0800	3.4802	4.8033
5.4	0.0407	0.0093	0.0860	3.3061	4.8033
5.6	0.0437	0.0063	0.0905	3.1752	4.8033
pH	CA ³⁻	CA ²⁻	IS Contr.	NaCl (g)	Citric Acid (g)
5.8	0.0101	0.0399	0.1253	2.1669	4.8033
6.0	0.0143	0.0357	0.1358	1.8610	4.8033
6.2	0.0195	0.0305	0.1486	1.4897	4.8033
6.4	0.0251	0.0249	0.1628	1.0791	4.8033
6.6	0.0308	0.0192	0.1769	0.6695	4.8033
6.8	0.0359	0.0141	0.1896	0.3004	4.8033
7.0	0.0400	0.0100	0.2001	-0.0026	4.8033

Preparation of 1.0 IS buffer Solutions from 0.2 IS Solutions by NaCl Adjustment

1.0 IS Buffer prepared by adding the appropriate amount of NaCl to 100ml of the 0.2 IS buffer solution. pH of 1.0 IS buffer is adjusted to final value using 4M NaOH

0.20 IS Buffers (500mL)			1.0 IS Buffers (100mL)		
pH	NaCl (g)	0.2 IS Buffer [NaCl] (g/mL)	1.0 IS Buffer [NaCl] (g/mL)	Δ [NaCl] (g/mL)	NaCl (g)
3.00	5.4760	1.10E-02	5.48E-02	4.38E-02	4.3808
3.20	5.3984	1.08E-02	5.40E-02	4.32E-02	4.3187
3.40	5.3218	1.06E-02	5.32E-02	4.26E-02	4.2574
3.60	5.2542	1.05E-02	5.25E-02	4.20E-02	4.2034
3.80	5.1999	1.04E-02	5.20E-02	4.16E-02	4.1599
4.00	4.7522	9.50E-03	4.75E-02	3.80E-02	3.8017
4.20	4.6052	9.21E-03	4.61E-02	3.68E-02	3.6842
4.40	4.4146	8.83E-03	4.41E-02	3.53E-02	3.5316
4.60	4.1864	8.37E-03	4.19E-02	3.35E-02	3.3491
4.80	3.9385	7.88E-03	3.94E-02	3.15E-02	3.1508
5.00	3.6954	7.39E-03	3.70E-02	2.96E-02	2.9564
5.20	3.4802	6.96E-03	3.48E-02	2.78E-02	2.7842
5.40	3.3061	6.61E-03	3.31E-02	2.64E-02	2.6449
5.60	3.1752	6.35E-03	3.18E-02	2.54E-02	2.5402
5.80	2.1669	4.33E-03	2.17E-02	1.73E-02	1.7335
6.00	1.8610	3.72E-03	1.86E-02	1.49E-02	1.4888
6.20	1.4897	2.98E-03	1.49E-02	1.19E-02	1.1917
6.40	1.0791	2.16E-03	1.08E-02	8.63E-03	0.8633
6.60	0.6695	1.34E-03	6.69E-03	5.36E-03	0.5356

Phosphate Buffer Calculations

pH	HA ²⁻	HA ²⁻ IS Contribution	NaCl (g)	NaH ₂ PO ₄ mass (g)
7.0	0.0194	0.0387	0.3553	5.998
7.2	0.0250	0.0501	0.2897	5.998
7.4	0.0307	0.0614	0.2241	5.998
7.6	0.0358	0.0716	0.1649	5.998
7.8	0.0400	0.0800	0.1162	5.998
8.0	0.0432	0.0863	0.0792	5.998
8.2	0.0455	0.0909	0.0526	5.998
8.4	0.0470	0.0941	0.0343	5.998
8.6	0.0481	0.0962	0.0222	5.998
9.0	0.0493	0.0985	0.0086	5.998
9.5	0.0499	0.0997	0.0016	5.998
10.0	0.0503	0.1005	-0.0032	5.998

The pH of each buffer solution was measured at room temperature (23° C) with a calibrated pH meter. The ionic strength of each buffer solution was adjusted with NaCl for all ionic strength adjustments. The pH of the 1.0 ionic strength buffer was adjusted to its proscribed value after addition of NaCl using a few drops of 4M NaOH. pH values of each buffer was confirmed prior to use.

APPENDIX II

POLYMER COMPOSITIONAL TABLES

	NAME	DATE	mmol	mmol	mmol	mmol	mmol	g	ml
			NIPA	MAA	NTBA	MBA	Total		
			MON1	MON2	MON3	XLINK	MON	INIT	SOLV1
001	1NK07	01/22/05	17	1.0		1	19	0.100	100
002	1NK11	02/09/05	25	3.0		2	30	0.100	100
003	1NK15	02/17/05	17	2.0		1	20	0.150	100
004	1NK18	02/20/05	17	2.0		2	21	0.150	100
005	1NK22	02/23/05	17	2.0		1	20	0.130	100
006	1NK24	03/01/05	17	3.0	3	1	24	0.150	100
007	1NK26	03/03/05	17	2.0		1	20	0.130	100
008	1NK28	03/08/05	17	2.0		1	20	0.150	100
009	1NK30	03/11/05	16	2.0	1	1	20	0.150	100
010	1NK32	03/19/05	15	2.0	2	1	20	0.150	100
011	1NK34	03/19/05	15	2.0	2	1	20	0.150	100
012	1NK36	04/07/05	17	2.0		1	20	0.100	100
013	1NK37	04/07/05	17	2.0		1	20	0.150	100
014	1NK39	04/12/05	17	2.0		1	20	0.153	100
015	1NK41	04/12/05	13	2.0	4	1	20	0.150	105
016	1NK43	04/17/05	13	2.0	4	1	20	0.152	100
017	1NK45	04/17/05	13	2.0	4	1	20	0.150	100
018	1NK50	04/21/05	14	1.0	4	1	20	0.150	100
019	1NK51	04/21/05	15	2.0	2	1	20	0.150	100
019	1NK52	04/24/05	14	1.0	4	1	20	0.150	100
020	1NK54	04/25/05	14	1.0	4	1	20	0.150	100
021	1NK56	04/27/05	15	1.0	3	1	20	0.150	105
022	1NK59	05/07/05	18	1.0		1	20	0.150	105
023	1NK60	05/09/05	14	2.0	2	2	20	0.150	100
024	1NK63	05/15/05	15	1.0	3	1	20	0.100	100
025	1NK64	05/17/05	15	1.0	2	2	20	0.150	100
026	1NK67	05/21/05	19	0.0	0	1	20	0.150	100
027	1NK69	05/30/05	15	1.0	2	2	20	0.150	100
028	1NK71	06/01/05	18	1.0	0	1	20	0.150	100
029	1NK72	06/03/05	18	1.0	0	1	20	0.150	100
030	1NK74	06/05/05	15	2.0	2	1	20	0.150	100
031	1NK77	06/11/05	16	1.0	2	1	20	0.150	100
032	1NK78	06/16/05	17	2.0	0	1	20	0.150	100
033	1NK79	05/17/05	14	2.0	2	2	20	0.150	100
034	1NK80	05/21/05	14	2.0	2	2	20	0.150	100
035	1NK81	06/29/05	14	2.0	2	2	20	0.100	100
036	1NK82	06/30/05	14	2.0	2	2	20	0.200	50

	NAME	DATE	mmol NIPA MON1	mmol MAA MON2	mmol NTBA MON3	mmol MBA XLINK	mmol Total MON	g INIT	ml SOLV1
037	1NK83	06/30/05	14	2.0	2	2	20	0.100	100
038	1NK84	07/03/05	14	2.0	2	2	20	0.150	100
039	1NK85	07/01/05	14	2.0	2	2	20	0.150	100
040	1NK86	07/05/05	14	2.0	2	2	20	0.150	90
041	1NK87	07/09/05	13	2.0	3	2	20	0.200	90
042	1NK88	07/10/05	13	2.0	3	2	20	0.200	50
045	1NK91	07/22/05	14	2.0	2	2	20	0.150	90
046	1NK93	08/01/05	14	2.0	2	2	20	0.200	50
047	1NK94	08/04/05	15	2.0	2	1	20	1.500	100
048	1NK95	08/05/05	14	2.0	2	2	20	0.200	100
049	1NK96	07/14/05	14	2.0	2	2	20	0.200	95
050	1NK97	08/08/05	15	1.0	3	1	20	0.200	105
051	1NK98	08/10/05	14	2.0	2	2	20	0.200	100
052	1NK99	08/16/05	15	2.0	2	1	20	0.200	100
053	1NK100	08/17/05	14	2.0	2	2	20	0.200	80
054	1NK101	08/16/05	14	2.0	2	2	20	0.200	50
055	1NK103	09/05/05	13	6.0	0	1	20	0.200	100
056	1NK104	09/06/05	11	6.0	2	1	20	0.200	100
057	1NK105	09/07/05	5	0.0	2	1	8	0.200	50
			6	6.0		0.5	12.5	0.100	100
058	1NK107	09/09/05	17	2.0	0	1	20	0.150	0.6465g
059	1NK108	09/09/05	14	2.0	2	2	20	0.200	100
060	1NK109	09/10/05	7	1.0	1.5	0.5	10	0.200	0.83g
061	1NK110	09/12/05	15	4.0	0	1	20	0.200	100
062	1NK112	09/18/05	14	2.0	2	2	20	0.200	100
063	1NK113	09/18/05	15	1.0	3	1	20	0.200	100
064	1NK115	09/27/05	11	6.0	2	1	20	0.200	100
065	1NK116	09/28/05	14	3.0	2	1	20	0.200	100
066	1NK117	09/29/05	12	4.0	0	4	20	0.200	100
067	1NK119	10/02/05	12	4.0	2	2	20	0.200	100
068	1NK121	10/04/05	15	4.0	0	1	20	0.200	100
069	1NK123	10/04/05	13	3.0	2	2	20	0.200	100
070	1NK124	10/08/05	13	3.0	2	2	20	0.200	100
071	1NK125	10/08/05	15	5.0	5	1	26	0.200	100
072	1NK127	10/17/05	11	5.0	2	2	20	0.200	100
073	1NK128	10/18/05	15	4.0	0	1	20	0.200	100
074	1NK129	10/21/05	15	4.0	0	1	20	0.200	100
075	1NK130	10/21/05	15	4.0	0	1	20	0.200	100
076	1NK131	10/24/05	17	2.0	0	1	20	0.200	100
077	1NK132	10/24/05	17	2.0	0	1	20	0.200	100
078	1NK133	10/26/05	17	2.0	0	1	20	0.200	100
079	1NK134	10/28/05	17	2.0	0	1	20	0.200	100
080	1NK135	10/28/05	14	2.0	2	2	20	0.200	100
081	1NK136	10/28/05	14	2.0	2	2	20	0.200	100
082	1NK137	10/30/05	14	2.0	2	2	20	0.200	100
083	1NK138	10/30/05	14	2.0	2	2	20	0.200	100

			mmol	mmol	mmol	mmol	mmol	g	ml
	NAME	DATE	NIPA	MAA	NTBA	MBA	XLINK	Total	
			MON1	MON2	MON3			MON	INIT SOLV1
084	1NK139	11/03/05	12	2.0	2	4		20	0.200 100
085	1NK140	11/03/05	12	2.0	2	4		20	0.200 100
086	1NK141	11/07/05	12	2.0	2	4		20	0.200 100
087	1NK142	11/08/05	13	2.0	2	3		20	0.200 100
088	1NK143	11/08/05	13	2.0	2	3		20	0.200 100
089	1NK144	11/10/05	2	2.0	14	2		20	0.200 100
090	1NK145	11/10/05	2	2.0	14	2		20	0.200 100
091	1NK146	11/13/05	14	2.0	2	2		20	0.200 100
092	1NK147	11/13/05	14	2.0	2	2		20	0.200 100
093	1NK148	11/16/05	13	2.0	2	3		20	0.200 100
094	1NK149	11/18/05	14	4.0	0	2		20	0.200 100
095	1NK150	11/19/05	12	4.0	2	2		20	0.200 100
096	1NK151	11/20/05	12	4.0	2	2		20	0.200 100
097	1NK152	11/21/05	12	2.0	2	4		20	0.200 100
098	1NK155	11/13/05	14	2.0	2	2		20	0.200 100
099	1NK156	11/27/05	14	2.0	2	2		20	0.200 100
100	1NK157	11/29/05	15	2.0	2	1		20	0.200 100
101	1NK158	11/29/05	15	2.0	2	1		20	0.200 100
102	1NK159	12/02/05	14	2.0	2	2		20	0.200 100
103	1NK160	12/02/05	14	2.0	2	2		20	0.200 100
104	1NK161	12/06/05	16	0.0	2	2		20	0.200 100
105	1NK162	12/06/05	16	0.0	2	2		20	0.200 100
106	2NK003	12/13/05	14	4.0	0	2		20	0.200 100
107	2NK004	12/13/05	14	4.0	0	2		20	0.200 100
108	2NK005	05/09/05	14	2.0	2	2		20	0.150 100
109	2NK007	01/09/06	10	9.0	0	5		24	0.100 6.5
110	2NK009	01/14/06	14	2.0	2	2		20	0.100 6.5
111	2NK010	01/15/06	16	2.0	0	2		20	0.100 7.5
112	2NK012	01/18/06	12	6.0	0	2		20	0.100 7.5
113	2NK013	01/18/06	12	6.0	0	2		20	0.100 7.5
114	2NK014	01/19/06	14	2.0	0	4		20	0.100 7.5
115	2NK016	01/21/06	16	2.0	0	2		20	0.100 7.5
116	2NK017	01/21/06	14	4.0	0	2		20	0.100 7.5
117	2NK019	01/25/06	14	2.0	2.0	2		20	0.100 7.5
118	2NK020	01/29/06	16	2.0	0	2		20	0.100 7.5
119	2NK021	01/29/06	16	2.0	0	2		20	0.100 7.5
120	2NK022	01/30/06	14	2.0	2.0	2		20	0.100 7.5
121	2NK023	01/30/06	17	1.0	0	2		20	0.100 7.5
122	2NK024	01/31/06	14	2.0	2	2		20	0.100 50.0
123	2NK025	12/02/05	16	2.0		2		20	0.200 100
124	2NK026	02/06/06	15	1.0	1.0	1		18	0.100 30.0
125	2NK027	02/07/06	14	2.0	2	2		20	0.100 30.0
126	2NK029	02/08/06	14	2.0	2	2		20	0.100 30.0
127	2NK030	02/09/06	14	2.0	2.0	2		20	0.100 60.0
128	2NK031	02/12/06	14	2.0	2	2		20	0.100 50.0
129	2NK032	02/12/06	14	2.0	2	2		20	0.200 50.0
130	2NK033	02/14/06	14	2.0	2.0	2		20	0.100 60.0

			mmol NIPA MON1	mmol MAA MON2	mmol NTBA MON3	mmol MBA XLINK	mmol Total MON	g INIT	ml SOLV1
131	2NK034	02/14/06	16	2.0	0	2	20	0.100	50.0
132	2NK035	02/15/06	14	2.0	2.0	2	20	0.100	60.0
133	2NK036	02/16/06	14	3.0	2.0	2	21	0.100	60.0
134	2NK037	02/16/06	14	2.0	2.0	2	20	0.100	60.0
135	2NK038	02/16/06	14	2.0	2.0	2	20	0.200	60.0
136	2NK039	02/19/06	15	2.0	1.0	2	20	0.150	60.0
137	2NK040	02/19/06	15	2.0	1.0	2	20	0.100	60.0
138	2NK042	05/22/05	16	0.0	2	2	20	0.200	100
139	2NK043	05/22/05	16	0.0	2	2	20	0.200	100

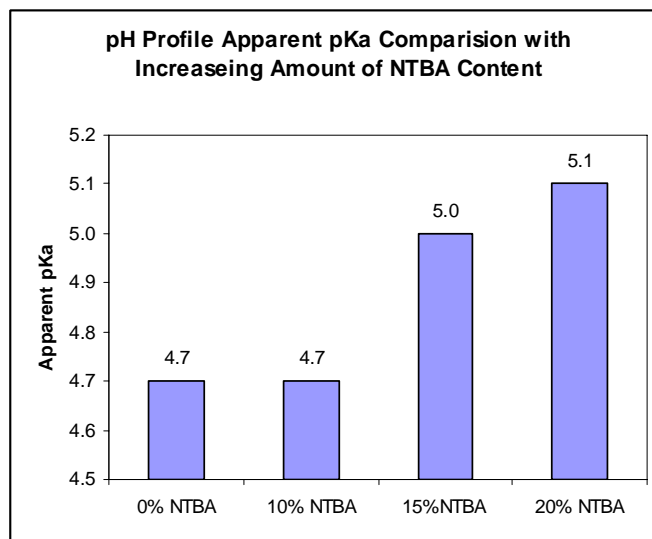
KEY

NIPA	N-Isopropylacrylamide	: Temperature sensitive hydrophilic monomer
MAA	Methacrylic acid	: Functional monomer (Recognition monomer)
NTBA	N-Tert-butyl acrylamide	: Monomer which decreases the LCST of NIPA
MBA	N,N-methylenebisacrylamide	: Crosslinking monomer
INIT	Initiator	: AIBN for thermal rxn, DMPA for photo rxn
AIBN	2,2"-Azobis(isobutyronitrile)	
DMPA	Dimethoxy phenyl-acetophenone	

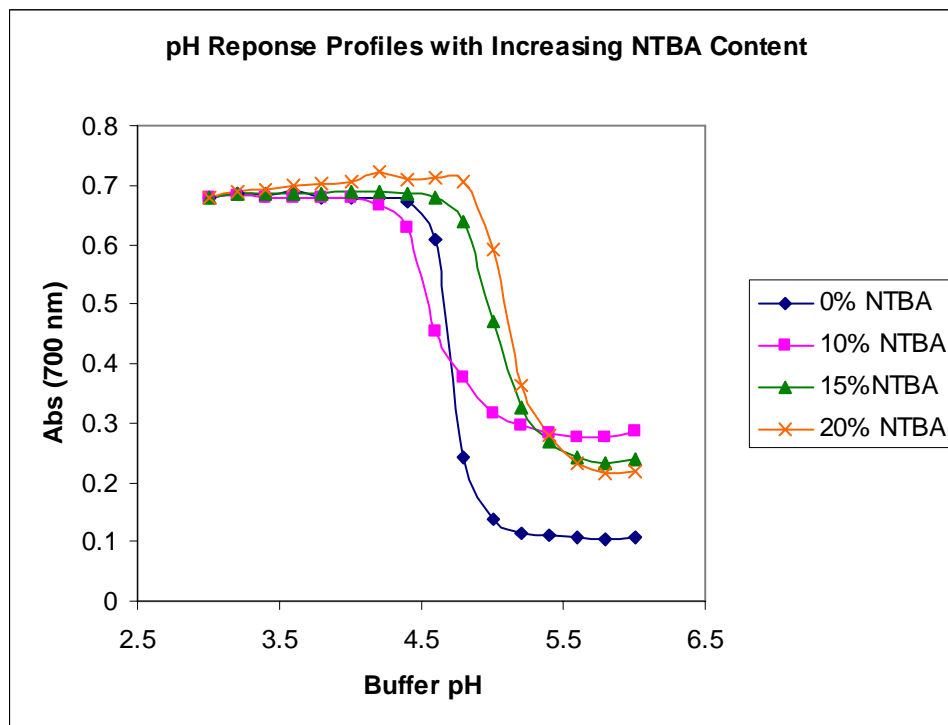
APPENDIX III

EFFECT OF NTBA ON pH SWELLING

NTBA (N-t-butylacrylamide) is a hydrophobic co-monomer used to make small adjustments in the phase transition temperature of NIPA co-polymers. This led to the idea that increasing the amount of NTBA in the polymer microspheres could have an impact on the apparent pKa of the polymer. The percent composition of NTBA was increased from 0% to 20% at 5% increments to determine its effect on the apparent pKa. At low % NTBA composition, there was not a significant impact on the apparent pKa of the pH induced volume phase transition.



Apparent pKa values determined from the pH response profiles of polymers containing increasing amounts of NTBA.



pH response profiles for polymers containing increasing amounts of NTBA.

VITA

Leah Oxenford

Candidate for the Degree of

Master of Science

Thesis: CHARACTERIZATION OF N-ISOPROPYL ACRYLAMIDE-CO-METHACRYLIC ACID POLYMERS FOR PH AND METAL ION BINDING

Major Field: Chemistry

Biographical:

Personal Data: Born in Grand Junction, Colorado on September 27, 1980.
Married October 20, 2002 to Jeremy Oxenford

Education: Oklahoma State University (2006)
MS Degree in Analytical Chemistry

University of Northern Colorado (2004)
BS Degree in Chemistry: ACS Certified
BS Degree in Biology: Cellular Biology

Professional: Oklahoma State University: Teaching/Research Assistant
(2004-2006)

The Hach Company: Assistant Application Chemist
(2000-2004).

University of Northern Colorado Chemistry Stockroom:
Attendant, (2000-2002)